

SCALE UP OF BENZOXAZINONE DERIVATIVE SYNTHESIS IN BATCH REACTOR



A Dissertation Submitted in Partial Fulfillment of the Requirements
for the Degree of Doctor of Engineering in Chemical Engineering

Department of Chemical Engineering

FACULTY OF ENGINEERING

Chulalongkorn University

Academic Year 2022

Copyright of Chulalongkorn University

การขยายขนาดการสังเคราะห์อนุพันธ์เบนซอกซาซิโนนในเครื่องปฏิกรณ์แบบกะ



วิทยานิพนธ์นี้เป็นส่วนหนึ่งของการศึกษาตามหลักสูตรปริญญาวิศวกรรมศาสตรดุษฎีบัณฑิต

สาขาวิชาวิศวกรรมเคมี ภาควิชาวิศวกรรมเคมี

คณะวิศวกรรมศาสตร์ จุฬาลงกรณ์มหาวิทยาลัย

ปีการศึกษา 2565

ลิขสิทธิ์ของจุฬาลงกรณ์มหาวิทยาลัย

สุเมธ บุญเกิด : การขยายขนาดการสังเคราะห์อนุพันธ์เบนซอกซาซิโนนในเครื่องปฏิกรณ์แบบกะ. (

SCALE UP OF BENZOXAZINONE DERIVATIVE SYNTHESIS IN BATCH REACTOR)

อ.ที่ปรึกษาหลัก : ผศ. ดร.อภิวัฒน์ สุทธิธารวัช, อ.ที่ปรึกษาร่วม : ดร.ภญ.อรศิริ ศรีคุณ

อนุพันธ์เบนซอกซาซิโนนเป็นสารตั้งต้นในการสังเคราะห์วัตถุดื้อยา Deferasirox ซึ่งเป็นยาสำหรับจับไอออนเหล็กในผู้ป่วยธาลัสซีเมีย ตัวแปรในการสังเคราะห์อนุพันธ์เบนซอกซาซิโนนศึกษาจากปฏิกิริยาควบแน่นระหว่างกรดซาลิไซลิก ซาลิไซลาไมด์ ไซยานูริกคลอไรด์ และไตรเอทิลลามีน โดยใช้โทลูอีนเป็นตัวทำละลาย อัตราส่วนโมลสมมูลระหว่างกรดซาลิไซลิก ซาลิไซลาไมด์ ไซยานูริกคลอไรด์ และ ไตรเอทิลลามีน ที่ 1:1:0.67:1 ให้อัตราผลผลิตขั้นต้นของอนุพันธ์เบนซอกซาซิโนน 46.77% ในการสังเคราะห์ระดับปฏิบัติการ โดยมีการค้นพบสาร 4-chloro-2-(2-hydroxyphenyl)-4H-benzo[e][1,3]oxazine-4-ol ในระหว่างการสังเคราะห์อนุพันธ์เบนซอกซาซิโนน นอกจากนี้ปฏิกิริยาการสังเคราะห์อนุพันธ์เบนซอกซาซิโนนได้นำเสนอในรูปแบบจำลองเพื่อใช้ในการศึกษาการหาค่าคงที่ทางจลนศาสตร์เคมี ในการศึกษาการขยายขนาดการสังเคราะห์อนุพันธ์เบนซอกซาซิโนน จากระดับปฏิบัติการสู่ขนาดเครื่องปฏิกรณ์ 1 ลิตรและ 10 ลิตร โดยใช้อัตราส่วนโมลสมมูลระหว่างกรดซาลิไซลิก ซาลิไซลาไมด์ ไซยานูริกคลอไรด์ และ ไตรเอทิลลามีน ที่ 1:1:0.67:1 พบว่าความเร็วรอบในการกวนที่ 200 รอบต่อนาทีในเครื่องปฏิกรณ์ขนาด 10 ลิตร ให้อัตราผลผลิตขั้นต้นของ Benzoxazinone derivative ที่ 43.18% ซึ่งพบว่า การขยายขนาดของกระบวนการจะเป็นการขยายขนาดโดยที่ความเร็วปลายใบกวนมีค่าคงที่ เนื่องจากในระบบมีอนุภาคของแข็งเกิดขึ้นในระหว่างการเกิดปฏิกิริยา แรงเฉือนที่เท่ากันจะทำให้ขนาดของอนุภาคของแข็งมีขนาดใกล้เคียงกัน และส่งผลต่อการเกิดปฏิกิริยาที่อนุภาคของแข็งนั้นละลายกลับเปลี่ยนเป็นผลิตภัณฑ์อีกครั้ง

สาขาวิชา วิศวกรรมเคมี

ปีการศึกษา 2565

ลายมือชื่อนิสิต

ลายมือชื่อ อ.ที่ปรึกษาหลัก

ลายมือชื่อ อ.ที่ปรึกษาร่วม

5771441821 : MAJOR CHEMICAL ENGINEERING

KEYWORD: scale up, 4-chloro-2-(2-hydroxyphenyl)-4H-benzo[e][1,3]oxazine-4-ol

Sumate Boonkird :

SCALE UP OF BENZOXAZINONE DERIVATIVE SYNTHESIS IN BATCH REACTOR.

Advisor: Asst. Prof. APINAN SOOTTITANTAWAT, D.Eng. Co-advisor: Onsiri Srikun, Ph.D.

Benzoxazinone derivative is one of starting materials in the synthesis of Deferasirox (a Chelating iron for thalassemia patient). The parameters of Benzoxazinone derivative synthesis were investigated from the condensation of salicylic acid, salicylamide, cyanuric chloride, and triethylamine using toluene as solvent. The mole equivalent ratio of salicylic acid: salicylamide:cyanuric chloride:triethylamine at 1:1:0.67:1 provided the 46.77% yield of Benzoxazinone derivative in laboratory scale. Surprisingly, 4-chloro-2-(2-hydroxyphenyl)-4H-benzo[e][1,3]oxazine-4-ol was observed in the synthesis of Benzoxazinone derivative. In addition, the reaction scheme of Benzoxazinone derivative synthesis was proposed as a model for the study of the chemical kinetic constant. Furthermore, the scale up of Benzoxazinone derivative synthesis was studied from laboratory scale to 1-L reactor and 10-L reactor using the mole equivalent ratio from laboratory scale. The result revealed that the mixing speed at 200 rpm of 10-L reactor gave 43.18 % yield. It was found that the scale-up process involved using a constant tip speed, as the solid was formed in the reaction system. As a result, the same shear force would produce the same size of the solid. Consequently, the solid in the reaction mixture could dissolve and be transformed into the product.

Field of Study: Chemical Engineering

Student's Signature

Academic Year: 2022

Advisor's Signature

Co-advisor's Signature

ACKNOWLEDGEMENTS

I would like to thank my committee members for their guidance to fulfil my dissertation.

Above all, I would like to thank my family for supporting, love, and always be my side.

My deepest appreciation goes to Asst. prof. Apinan suitithantawat, my advisor for his precious guidance from the first time. He provides the inspiration to conduct this dissertation and and Prof. dr. Blaž Likozar for his support in Slovenia.

A special thank goes to Dr. Komkrit Hasitapan for his suggestion in organic chemistry.

Thanks to my friends and Mr. Wasan Kongnaikhaw.

Finally, I would like to thank the scholarship support from Research and Development Institute, The Government Pharmaceutical Organization, Thailand. and support from Laboratory of Catalysis and Chemical Reaction Engineering, National Institute of Chemistry, Slovenia.



จุฬาลงกรณ์มหาวิทยาลัย
CHULALONGKORN UNIVERSITY

Sumate Boonkird

TABLE OF CONTENTS

	Page
.....	iii
ABSTRACT (THAI).....	iii
.....	iv
ABSTRACT (ENGLISH).....	iv
ACKNOWLEDGEMENTS.....	v
TABLE OF CONTENTS.....	vi
LIST OF TABLES.....	x
LIST OF FIGURES.....	xiii
CHAPTER I.....	1
GENERAL BACKGROUND.....	1
1.1 Introduction.....	1
1.2 Objectives.....	2
1.3 Scope of this work.....	2
1.4 Advantage.....	3
CHAPTER II.....	4
THEORY AND LITERATURE REVIEWS.....	4
2.1 Benzoxazine.....	4
2.2 Thalassemia.....	5
2.3 Synthesis of Benzoxazinone derivative.....	6
2.4 Reaction Mechanism and Pathway.....	9
2.5 Chemical kinetics.....	13

2.6 Reaction calorimetry for determining thermodynamic and chemical kinetic parameters.....	16
2.7 Reactor and process scale-up.....	21
2.8 Scale-up process.....	22
CHAPTER III.....	39
EXPERIMENT.....	39
3.1 Materials and reagents.....	39
3.2 Synthesis of benzoxazinone derivative (8).....	40
3.3 Determination of the chemicals concentration in the reaction.....	41
3.4 Synthesis of tris-quaternary ammonium salt (10).....	41
3.5 Isolation of 4-chloro-2-(2-hydroxyphenyl)-4H-benzo[e][1,3]oxazine-4-ol (9) from the reaction.....	42
3.6 Determination of heat of reaction using reaction calorimeter (RC1e, Mettler Toledo).....	42
3.4 1-L Reactor for synthesis.....	43
3.5 10-L Reactor for synthesis.....	44
3.6 Analytical procedure.....	44
CHAPTER IV.....	47
THE REACTION SCHEME OF BENZOXAZINONE DERIVATIVE.....	47
4.1 Structural elucidation of unknown compounds.....	47
4.2 The reaction scheme for benzoxazinone derivative (8) synthesis.....	48
4.3 The conversion profile of the reactant and yield profile of the product....	50
4.4 Effect of salicylic acid (1): salicylamide (6) ratio.....	53
4.5 Effect of triethylamine concentration.....	53
4.6 The effect of the reaction temperature.....	54

4.7 The overall heat of the reaction	56
CHAPTER V	58
THE KINETIC STUDY OF BENZOXAZINONE DERIVATIVE SYNTHESIS	58
5.1 The kinetic study of Benzoxazinone derivative synthesis	58
5.2 The results from the kinetic study	60
5.2.1 the effect of starting materials concentration on kinetic parameter	62
5.2.2 the effect of triethylamine on kinetic parameter	67
5.2.3 the kinetics parameter from the effect of temperature the experiment entry 2,6-7	68
5.3 The usage of kinetic parameters from optimization.....	69
CHAPTER VI	72
THE SCALE-UP OF BENZOXAZINONE DERIVATIVE SYNTHESIS	72
6.1 The Scale-up of Benzoxazinone derivative synthesis in a 1-L reactor	72
6.1.1 The effect of mixing speed on the %yield of Benzoxazinone derivative.	72
6.1.2 The result of the synthesis of Benzoxazinone derivative in a 1-L reactor	73
6.2 The Scale-up of Benzoxazinone derivative synthesis in a 10-L reactor	77
6.2.1 The correlation between 1-L and 10-L reactor.....	77
6.2.2 The result from the scale-up of Benzoxazinone derivative synthesis in a 10-L reactor	79
CHAPTER VII.....	83
CONCLUSION AND RECOMMENDATION	83
7.1 Conclusion.....	83

7.2 Recommendation.....	85
REFERENCES	86
Appendix	94
1 HPLC calculation	94
1.1 concentration calculation	94
1.2 %conversion of salicylic acid/salicylamide calculation	94
1.3 %yield of Benzoxazinone derivative/compound (7) calculation	94
1.4 The purity of Benzoxazinone derivative using the parameters in entry 3... ..	97
2 kinetic parameters experiment.....	98
2.1 program for kinetic study	98
2.2 The results from program optimization	104
VITA.....	132

LIST OF TABLES

	Page
Table 1 Iron chelator properties [21, 25-27].....	6
Table 2 Variables in the synthesis of Benzoxazinone derivative.	9
Table 3 The Table shows the empirical (n) of stirrer speed and tank diameter at any objective.....	38
Table 4 Chemicals and reagents.....	39
Table 5 Summary of the standard calibration curve point.....	45
Table 6 The conversion of reactants and yield of products profile during the reaction at 110 °C (Reflux) and mole ratios of salicylic acid (1), cyanuric chloride (2), salicylamide (6), and triethylamine at 1:0.67:1:1	51
Table 7 Effect of reaction parameters on the conversion of reactant and yield of the product after 1320 min (22 h) reaction time.....	55
Table 8 Summary of 7 conditions for kinetics modelling optimization.....	59
Table 9 The equilibrium constants using various ratios of salicylic acid: salicylamide from 1:0.75, 1:0.85, and 1:1 (conditions in Table 8 from entry 1-3)	62
Table 10 Kinetic constant for salicylic acid:salicylamide ratio (1:1 equivalent), triethylamine (1 equivalent), and refluxing toluene (entry 3).....	64
Table 11 The equilibrium constants using conditions in Table 8 from entries 2,4-5.	67
Table 12 The equilibrium constants using conditions in Table 8 from entries 2,6-7.	68
Table 13 The relations between conversion of salicylic acid and rate of disappear of salicylic acid in the experiment entry 3.	71
Table 14 The difference in %yield of Benzoxazinone derivative between laboratory scale (round-bottom flask) and 1-L reactor.....	74

Table 15 The relation of mixing speed between 1-L and 10-L in the standard reactor	78
Table 16 The difference in yield of Benzoxazinone derivative between 1-L reactor 400 rpm (as a reference, Rt) and 10-L reactor (as Testing, Tt).....	80
Table 17 Molecular weight of selected components	95
Table 18 the concentration and area of Benzoxazinone derivative working standard for the calibration curve.....	95
Table 19 The example calculation of Benzoxazinone derivative in the section “The effect of the ratio of salicylic acid and salicylamide with 1:0.85 salicylic acid : salicylamide ratio”	97
Table 20 The example for conversion/yield (%) of 4 species in the experiment and model calculation from program optimization in entry 2.	103
Table 21 Kinetic constant for salicylic acid:salicylamide ratio (1:0.75 equivalent), triethylamine (1 equivalent), and refluxing toluene (entry 1).....	104
Table 22 Kinetic constant for salicylic acid:salicylamide ratio (1:0.85 equivalent), triethylamine (1 equivalent), and refluxing toluene (entry 2).....	106
Table 24 Kinetic constant for salicylic acid:salicylamide ratio (1:0.85 equivalent), triethylamine (0.1 equivalent), and refluxing toluene (entry 4).....	108
Table 25 Kinetic constant for salicylic acid:salicylamide ratio (1:0.85 equivalent), triethylamine (2 equivalent), and refluxing toluene (entry 5).....	110
Table 26 Kinetic constant for salicylic acid:salicylamide ratio (1:0.85 equivalent), triethylamine (1 equivalent), and 80 °C reaction temperature (entry 6)	112
Table 27 Kinetic constant for salicylic acid:salicylamide ratio (1:0.85 equivalent), triethylamine (1 equivalent), and 100 °C reaction temperature (entry 7).....	114
Table 28 ¹ H-NMR and ¹³ C-NMR spectroscopic data of 4-chloro-2-(2-hydroxyphenyl)-4H-benzo[e] [1,3] oxazine-4-ol, compound (9) in CDCl ₃	123

Table 29 ^{13}C -NMR and DEPT spectroscopic data of 4-chloro-2-(2-hydroxyphenyl)-4H-benzo[e] [1,3] oxazine-4-ol, compound (9) in CDCl_3 124

Table 30 ^1H -detected heteronuclear multiple quantum correlations (HMQC) spectroscopic data of 4-chloro-2-(2-hydroxyphenyl)-4H-benzo[e] [1,3] oxazine-4-ol, compound (9) in CDCl_3 125

Table 31 ^1H -detected heteronuclear multiple bond correlations (HMBC) spectroscopic data of 4-chloro-2-(2-hydroxyphenyl)-4H-benzo[e] [1,3] oxazine-4-ol, compound (9) in CDCl_3 125



LIST OF FIGURES

	Page
Figure 1 The example of Benzoxazine: 2 <i>H</i> -benzo[e]1,3-oxazine.	4
Figure 2 The general route of Benzoxazinone derivative synthesis.	8
Figure 3 The methodology scheme in chemical kinetic development [58].....	13
Figure 4 Reaction calorimetry: On the left, heat-flow, heat balance, and power-compensation calorimeter, On the right, Peltier calorimeter.	16
Figure 5 heat-flow, heat balance, and power-compensation calorimeter.....	17
Figure 6 Batch reactor (Saeki and Emura, [70])	21
Figure 7 Standard tank reactor with dimension (Hugh Stitt and Simmons, [72]).....	23
Figure 8 Correlation between P_0 , Reynolds number, and stirrer type (Hemrajani and Tatterson, [73]).....	25
Figure 9 Turbulent power number of blade retreat curve impeller (RCI) (Hugh Stitt และ Simmons, [72])	26
Figure 10 Standard stirrer tank for scale up.....	28
Figure 11 The relationship between $((P/V)_2 / (P/V)_1) = (V)_2 / (V)_1$	31
Figure 12 The experiment in round bottom flask.	40
Figure 13 Automatic reaction calorimeter (RC1e, Mettler Toledo).....	43
Figure 14 1-L double jacket reactor.	43
Figure 15 10-L double wall reactor, Büchiglasuster®	44
Figure 16 Chemical structure of 4-Chloro-2-(2-hydroxyphenyl)-4 <i>H</i> -benzo[e][1,3]oxazine-4-ol (9).....	47
Figure 17 The reaction scheme for Benzoxazinone derivative (8) synthesis from salicylic acid (1) and salicylamide (6) using cyanuric chloride (2) as a chlorinating agent under the base condition of triethylamine.	49

Figure 18 Reaction picture of Benzoxazinone derivative synthesis (8).....	52
Figure 19 The reaction heat flow for the Benzoxazinone derivative (8) formation from salicylic acid (1) and salicylamide (6) using cyanuric chloride (2) as a chlorinating agent at 80 °C.....	57
Figure 20 Chemical structures in kinetic study	58
Figure 22 The graphical results from fitting in entry 3.....	65
Figure 21 R ² -value from fitted model conversion and experimental conversion (%) of salicylic acid, model yield experimental yield (%) of compound (8, 9 and 10) with 95% confidential band for salicylic acid:salicylamide:cyanuric chloride:triethylamine mole ratio of 1:1:0.67:1 at refluxing toluene.....	66
Figure 23 The effect of mixing speed on the %yield of Benzoxazinone derivative....	73
Figure 24 the liquid level in the benzoxazinone derivative in the 1-L reactor in the same quantity of materials a) at a mixing speed of 100 rpm, b) at a mixing speed of 400 rpm, c) at a mixing speed of 600 rpm with a high level of liquid vortex effect. ..	76
Figure 25 The comparison of %yield of Benzoxazinone derivative profile in a 10-L reactor with various speeds.	81
Figure 26 The components concentration of 1-L 400 rpm, 10-L 200, and 250 rpm at 6 hours of reaction time.....	81
Figure 27 Calibration curve of Benzoxazinone derivative in the experiment of “The effect of the ratio of salicylic acid and salicylamide with 1:0.85 salicylic acid : salicylamide ratio”.....	96
Figure 28 The HPLC chromatogram show the peak of Benzoxazinone derivative	98
Figure 29 The first page of CERRES (Chemical Reaction and Reactor Engineering Simulations).	100
Figure 30 The 3 parameters of Experimental data, Chemistry data, and mode of Operation.....	101
Figure 31 Chemical species in the synthesis.	101

Figure 32 The experimental data set.....	102
Figure 33 R ² -value from fitted model conversion and experimental conversion (%) of salicylic acid, model yield experimental yield (%) of compound (8, 9 and 10) with 95% confidential band for salicylic acid:salicylamide ratio (1:0.75 equivalent), triethylamine (1 equivalent), and refluxing toluene.	104
Figure 34 The graphical results from fitting in entry 1.....	105
Figure 35 R ² -value from fitted model conversion and experimental conversion (%) of salicylic acid, model yield experimental yield (%) of compound (8, 9 and 10) with 95% confidential band for salicylic acid:salicylamide ratio (1:0.85 equivalent), triethylamine (1 equivalent), and refluxing toluene.	106
Figure 36 The graphical results from fitting in entry 2.....	107
Figure 39 R ² -value from fitted model conversion and experimental conversion (%) of salicylic acid, model yield experimental yield (%) of compound (8, 9 and 10) with 95% confidential band salicylic acid:salicylamide ratio (1:0.85 equivalent), triethylamine (0.1 equivalent), and refluxing toluene	108
Figure 40 The graphical results from fitting in entry 4.....	109
Figure 41 R ² -value from fitted model conversion and experimental conversion (%) of salicylic acid, model yield experimental yield (%) of compound (8, 9 and 10) with 95% confidential band salicylic acid:salicylamide ratio (1:0.85 equivalent), triethylamine (2 equivalent), and refluxing toluene	110
Figure 42 The graphical results from fitting in entry 5.....	111
Figure 43 R ² -value from fitted model conversion and experimental conversion (%) of salicylic acid, model yield experimental yield (%) of compound (8, 9 and 10) with 95% confidential band salicylic acid:salicylamide ratio (1:0.85 equivalent), triethylamine (1 equivalent), and 80 °C reaction temperature.....	112
Figure 44 The graphical results from fitting in entry 6.....	113

Figure 45 R ² -value from fitted model conversion and experimental conversion (%) of salicylic acid, model yield experimental yield (%) of compound (8, 9 and 10) with 95% confidential band salicylic acid:salicylamide ratio (1:0.85 equivalent), triethylamine (1 equivalent), and 100 °C reaction temperature.....	114
Figure 46 The graphical results from fitting in entry 6.....	115
Figure 47 ¹ H NMR spectrum of 4-chloro-2-(2-hydroxyphenyl)-4 <i>H</i> -benzo[e] [1,3] oxazine-4-ol, compound (9) in CDCl ₃	116
Figure 48 ¹ H NMR spectrum of 4-chloro-2-(2-hydroxyphenyl)-4 <i>H</i> -benzo[e] [1,3] oxazine-4-ol, compound (9) in CDCl ₃	117
Figure 49 ¹ H NMR spectrum of 4-chloro-2-(2-hydroxyphenyl)-4 <i>H</i> -benzo[e] [1,3] oxazine-4-ol, compound (9) in CDCl ₃	118
Figure 50 ¹³ C NMR spectrum of 4-chloro-2-(2-hydroxyphenyl)-4 <i>H</i> -benzo[e] [1,3] oxazine-4-ol, compound (9) in CDCl ₃	119
Figure 51 ¹³ C NMR (Dept-135) spectrum of 4-chloro-2-(2-hydroxyphenyl)-4 <i>H</i> -benzo[e] [1,3] oxazine-4-ol, compound (9) in CDCl ₃	120
Figure 52 ¹³ C NMR HMBC spectrum of 4-chloro-2-(2-hydroxyphenyl)-4 <i>H</i> -benzo[e] [1,3] oxazine-4-ol, compound (9) in CDCl ₃	121
Figure 53 ¹³ C NMR HMQC spectrum of 4-chloro-2-(2-hydroxyphenyl)-4 <i>H</i> -benzo[e] [1,3] oxazine-4-ol, compound (9) in CDCl ₃	122
Figure 54 The position in structure of 4-chloro-2-(2-hydroxyphenyl)-4 <i>H</i> -benzo[e] [1,3] oxazine-4-ol	123
Figure 55 HSMS spectrum of 4-chloro-2-(2-hydroxyphenyl)-4 <i>H</i> -benzo[e] [1,3] oxazine-4-ol, compound (9)	126
Figure 56 FT-IR spectrum of 4-chloro-2-(2-hydroxyphenyl)-4 <i>H</i> -benzo[e] [1,3] oxazine-4-ol, compound (9).....	127
Figure 57 HPLC chromatogram of 4-chloro-2-(2-hydroxyphenyl)-4 <i>H</i> -benzo[e] [1,3] oxazine-4-ol, compound (9).....	128

Figure 58 ^1H NMR spectrum of Tri-quaternary salt (compound 10) in DMSO- d_6	129
Figure 59 HPLC chromatogram of Tri-quaternary salt compound 10.	130
Figure 60 HPLC chromatogram of solid compositions after 6 hours of Benzoxazinone synthesis using 20%DMSO/Acetonitrile as dilution medium.	131



CHAPTER I

GENERAL BACKGROUND

1.1 Introduction

At present, Thalassemia patients are treated in the chelating iron program with three drugs: Deferoxamine (DFO), Deferiprone (L1), and Deferasirox (DFX). The Government Pharmaceutical Organization (GPO) successfully researched and developed Deferiprone's synthesis process and formulation for the oral dosage form. This process has been proven and monitored by Thai Food and Drug Ministry of Public Health. The patients treated with Deferiprone course will closely monitor by a specialist doctor. For the nation's security, The Government Pharmaceutical Organization has researched and developed the synthesis process and formulation of Deferasirox to promote the alternate treatment choice. Due to the price of Deferasirox, the synthesis process should reduce the cost of raw materials such as Benzoxazinone derivative imported from China or India. Moreover, the synthetic process of Benzoxazinone using thionyl chloride (chlorinating agent) is at risk of exploding when inappropriate handling. This process causes the price of Benzoxazinone derivative more expensive. To aim for national drug support, the Government Pharmaceutical Organization cooperated with the national nanotechnology to develop a new process for synthesizing Benzoxazinone derivative. To reduce the price of raw materials and increase the possibility of industrial production of Benzoxazinone derivative is the target research of the cooperation. In this study, the scale up process of Benzoxazinone derivative is researched from the reaction kinetic investigation from the laboratory to develop the parameters to 250 L reactor with equivalent yield in the laboratory.

1.2 Objectives

1.2.1 To investigate the reaction mechanism in the synthesis of Benzoxazinone intermediate on the laboratory scale.

1.2.2 To study the chemical kinetic and thermodynamic parameters in synthesizing Benzoxazinone intermediate, such as rate of reaction, rate constant, and heat of reaction.

1.2.3 To investigate the effect of parameters on the scale up of Benzoxazinone intermediate in laboratory scale to 1, 10 L reactor, with the target of the equivalent of yield/purity.

1.3 Scope of this work

1.3.1 From the synthesis process of Benzoxazinone intermediate developed by National Nanotechnology Center, NSTDA and the Government Pharmaceutical Organization's grant, the investigation of the reaction mechanism of Benzoxazinone derivative and by-products affected the yield of the main product is conducted. After the synthesis of Benzoxazinone derivative, the unknown substances are purified using column chromatography, and the structure elucidation of the purified unknown substance is performed using NMR, HRSMS, LC-MS, HPLC, FT-IR, etc.

1.3.2 The reaction kinetic model and experiment comparison must be performed using regression analysis.

1.3.3 In the study, the parameters such as rate of reaction, rate constant, chemical kinetic, thermodynamic, and heat of reaction are conducted using Calorimetry Reaction (RC1e)

1.3.4 The scale up of 10-L reactor should perform after the optimum parameters were investigated to evaluate the yield and purity between laboratory and a 10-L reactor.

1.4 Advantage

To have the parameters to produce Benzoxazinone derivative in a 10 L reactor with equivalent yield and purity of laboratory.



CHAPTER II

THEORY AND LITERATURE REVIEWS

2.1 Benzoxazine

Benzoxazine and its derivatives, composed of a benzene ring and a six-membered ring with hetero atoms such as oxygen and nitrogen, are known for heterocyclic compounds shown in Figure 1. These compounds play a vital role in the industry, such as monomers in thermosetting plastic processing [1-3]. Furthermore, benzoxazine molecule containing carbonyl group widely found in agricultural chemicals such as herbicides [4] (flumioxazin and thidiazimin containing the core 4H-1,4-benzoxazin-3-one structure) [5] and pharmaceutical area which shown its properties in pharmacological and bioactive activities [6, 7], for example, anticancer activities [8-10], antiobesity [11, 12], antimicrobial activity [13, 14], antimycobacterial activity [13], antiplatelet aggregation activity [15], antidiabetic [16], and antidepressant activity [17, 18]. Moreover, they can be used as a starting material (or intermediate) for the synthesis of active pharmaceutical ingredients [19, 20].

จุฬาลงกรณ์มหาวิทยาลัย
CHULALONGKORN UNIVERSITY

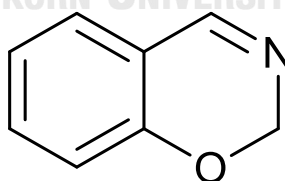


Figure 1 The example of Benzoxazine: 2H-benzo[e]1,3-oxazine.

2.2 Thalassemia

Thalassemia is an inherited autosomal recessive hemoglobin disorder, typically found in tropical countries in various population regions of sub-Saharan Africa, the Mediterranean region, the Middle East to South and Southeast Asia [21]. In Thailand, the spread of Thalassemia was found in 1 percent of the population (0.6 million), and 30 to 40% (18-24 million) of the population are carriers [22]. Thalassemia can be divided into two groups of genotypic diagnosis (α and β thalassemia) [23]. In general, the treatment of thalassemia patient focuses on the phenotype of diagnosis depending on the severity of the disease from normal (silent carrier) to major [24]. The transfusion is one of the treatments for the patient to improve the anemia and relieve the ineffective erythropoiesis (the gastro-intestine absorbs erythrocyte's inability back into the body), but simultaneously induces the overloaded iron accumulated within organelles, especially in the liver and heart. The mechanism to excrete the overloaded iron in the human body is low efficiency. Using a chelating agent provided good efficiency in the elimination of overloaded iron. In general, patients who receive 10-12 transfusions or ferritin over 1,000 mg/L will start a chelation therapy program [25].

2.2 Chelating iron

Deferasirox (known for Exjade, ICL-67A, Novartis Switzerland) is one of the orphan drugs (Deferoxamine, Deferiprone, Deferasirox) to treat the patient who suffer from beta-thalassemia and chorionic anemia to reduce the iron accumulation during long-term blood transfusion and the patient with Non-Transfusion-Dependent Thalassemia [24]. The tridentate molecule of Deferasirox binds ferric iron with 2:1 (2 molecules of Deferasirox bind with one molecule of ferric iron), and it has low specific with biological metal forms such as copper and zinc [26]. The administration of Deferasirox, an oral dosage form, was approved by US and EU in 2005 and 2006, respectively, for once-daily usage. The properties of iron chelator are shown in Table 1

Table 1 Iron chelator properties [21, 25-27].

Properties	Deferoxamine	Deferasirox	Deferiprone
Route of administration	Intravenous or subcutaneous	oral	oral
Half-life (hour)	0.5	12-16	2-3
administration	8 – 24 hours/day 5 – 7 days/week	Once daily	Three times per day
Mode of excretion	Urinary and fecal	Urinary	Fecal
Side effect and toxicity	Dermatological, ocular, auditory	Gastrointestinal, renal, hepatic	Hematological (neutropenia, agranulocytosis), arthropathic
Iron binding efficiency	1:1 (hexadentate)	2:1 (tridentate)	3:1 (bidentate)
Iron selectivity	High selective	High selective	Zinc is excreted

2.3 Synthesis of Benzoxazinone derivative

The synthesis of Deferasirox was mainly found using Benzoxazinone derivative and 4-hydrazinone benzoic acid as starting material. Benzoxazinone

derivative is the key intermediate to synthesis Deferasirox because it is found in the first step in the synthesis of Deferasirox. The synthesis of Deferasirox has been developed and reported using a two-step procedure by several researchers, according to Table 2. The first step uses chemicals as such, salicylic acid and salicylamide with thionyl chloride and pyridine at reflux in xylene to produce the solid product of 50-55% of the molecule called Benzoxazinone intermediate [2-(2-hydroxyphenyl)benz[e] [1,3]oxazin-4one] through the condensation. In the second step, Benzoxazinone intermediate reacted with 4-hydrazinonebenzoic acid in the presence of absolute ethanol at reflux to give 80% of deferasirox yield. In the synthesis process of Benzoxazinone derivative, it is substantially required chlorinating agents to convert salicylic acid to salicyloyl chloride. The most common use chlorinating agent is thionyl chloride. It provides a higher yield than other chlorinating agents. According to Jarassopon [20], they investigated the new chemical to replace thionyl chloride due to its hazardous property at high temperature and difficulty while handling on the production scale.

Moreover, the process using thionyl chloride as a chlorinating solvent in Table 2 showed the yield of benzoxazinone derivative over 50% using salicylic acid and salicylamide as starting materials. But the usage of thionyl chloride in Thailand is infringed against Thai law because thionyl chloride is classified as a reagent in the synthesis of methamphetamine and under the law in Hazardous Substance Act B.E. 2535

Cyanuric chloride (2,4,6-trichloro-1,3,5-triazine) is a prominent chlorinating agent instead of thionyl chloride because it offers a highly effective chlorinating agent used in many reactions. In addition, its appearance in solid provides good handling even in the production scale and is inexpensive compared to thionyl chloride and other chlorinating agents such as cyanuric fluoride.

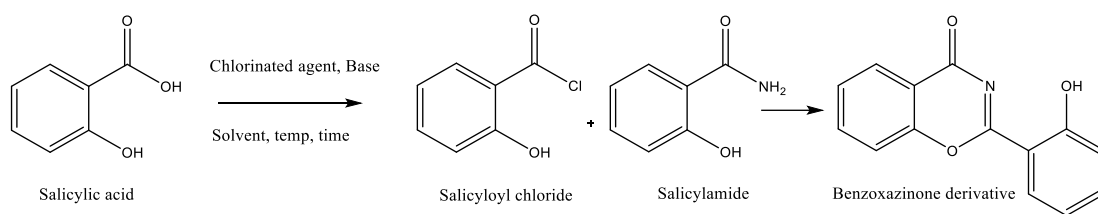


Figure 2 The general route of Benzoxazinone derivative synthesis.



Table 2 Variables in the synthesis of Benzoxazinone derivative.

No.	Starting material		Chlorinated agent	Base	Temp. (°C)	Hours	Solvent	Yield (%)	references
1.	Salicylic acid	Salicylamide	SOCl ₂	-	120	2	xylene	95	[28]
2.	Salicylic acid	Salicylamide	SOCl ₂	pyridine	reflux	16	xylene	76	[29]
3.	Salicylic acid	Salicylamide	SOCl ₂	-	180	3	xylene	-	[30]
4.	Salicyloyl chloride	Salicylamide	SOCl ₂	tetra butyl ammonium bromide	110	4	toluene	-	[31]
5.	Salicylic acid	Salicylamide	SOCl ₂	-	126	2	xylene	-	[32]
6.	Salicylic acid	salicylamide	SOCl ₂	-	140-160	3-5	xylene	52 g	[33]
	Salicylic acid 0.362	Salicylamide 0.255	SOCl ₂ 0.3981	-	140-180	3-5	anisole	52 g	[33]
7.	Salicylic acid	salicylamide	SOCl ₂	pyridine	140-145	2	o-xylene	15	[34]
8.	Salicylic acid	salicylamide	Cyanuric acid	Triethyl amine	reflux	16	toluene	53	[20]

2.4 Reaction Mechanism and Pathway

According to Miller [35], the chemical reaction mechanism is the chemical reaction consisting of all substances from starting material and by-product to the product. The chemical reaction mechanism related to chemical kinetic modeling, as seen in 2.5, Howell [36] stated that chemical kinetic investigation is pivotal to the chemical kinetic mechanism. Moreover, chemical reaction mechanism depends on knowledge of chemical analysis, organic chemistry, physical chemistry, thermodynamic, statistical thermodynamics, and quantum mechanics. The reaction mechanism has been investigated in various studies, especially to analyze kinetic modeling. In contrast, a chemical kinetics study is helpful in investigating the reaction mechanism. Santacesaria [37], Oliveira, Hudebine, Guillaume, and Verstraete [38] explained that the purpose of chemical kinetic is to investigate the reaction mechanism and to study the reaction rate with related parameters.

Kinetic modeling analysis related to various fields, for example, the study of the detailed chemical kinetic reaction mechanism for combustion of hydrocarbon [39], Detailed kinetic modeling in the process of coal pyrolysis [40], the kinetics and deactivation of catalytic acetylation of glycerol—A by-product of biodiesel [41], Modelling chemical kinetics of a complex reaction network of active pharmaceutical ingredient (API) synthesis [42]. In these studies, the modeling process related to chemical change of starting material, intermediate, by-products, and conditions in the synthesis.

To set up chemical kinetic modeling based on the hypothesis, the indicated data from the experiment used the change from starting material to product. Hill and Root [43] stated that reaction mechanisms correspond to the experimental data. Gargurevich [44] stated that chemical reaction kinetic knowledge covers various fields such as chemistry, reaction chemistry, chemical thermodynamics, statistical mechanics, chemical kinetics principles, and quantum chemistry. To investigate the reaction mechanism with systematical methodology, Wang [45] studies the kinetic using a differential equation without a chemical mechanism. Fan, Bertók, and Friedler [46] studied the graph-theoretical method,

Szalkai [47] studied the general algorithmic method in reaction syntheses using linear algebra, and Bentley [48] explained the method to investigate the reaction mechanisms by-product studies.

Vertis, Oliveira, and Bernard [49] proposed a methodology to study the systematic development of kinetic models for systems described by linear reaction schemes in accordance with the study of Blackmond [50] in a robust methodology for mechanistic studies of complex catalytic reactions using data from the experiment. From Carolina experiment, there are five steps to be performed.

1. Identify the reaction of each chemical species in the system that corresponds to stoichiometry. Moreover, the thermodynamic data should be considered, such as the study of Fishtik, Alexander, and Datta [51] to investigate methanol synthesis using copper catalysts. They specify the chemical species in the system. Toch, Thybaut, and Marin [52] set the methodology in the chemical kinetic modeling using n-Hexane Hydroisomerization. In the first step, they collect important data.
2. Set up the chemical network consisting of species in the system using a circle line or arrow to present the chemical reaction between species. The other chemical network can be organized to give the same result, such as a graphical method [47], [53], incremental identification [54]
3. Consider the data from the experiment based on the relationship with concentration and time in differential equation $(d(C)/dt)$ to calculate the polynomial coefficient. Tirronen and Salmi [53] stated that the system with short-time intermediate or fast reaction should consider a quasi-steady state method to estimate the concentration. Then, the reaction rate can be estimated to 0 and with a low concentration of intermediate as a result, $r_i = \sum_{j=i}^n v_{ij}R_j = 0$. this method will eliminate the concentration of the intermediate from chemical rate equation.
4. In the model-based experiment, the result of concentration change with time will be investigated with the experiment compared to the proposed modeling as in the study of Flores-Sánchez, Flores-Tlacuahuac, and Pedraza-Segura [55];

Grom [42]; Grénman [56]. They choose the possible reaction from the chemical reaction network. Jin, X. et al. [57] investigated the kinetic modeling of the carboxylation of propylene oxide to propylene carbonate using an ion-exchange resin catalyst in a semi-batch slurry reactor. They conducted the experiment to compare the result from the kinetic modeling with the concentration profile, and precise kinetic modeling will correspond with data from the experiment.

5. Perform regress analysis in each reaction step. The good correlation between reaction rate, starting material, and products showed the same result with the chemical reaction network. Therefore, the model can predict/estimate the chemical kinetic parameters. In contrast, the experiment and data collection should be studied in more detail. In the first and second experiments of Toch, Thybaut, and Marin [52], they stated that regression analysis required a good initial guess to compute the parameters close to an actual parameter. The initial guess can be calculated using linearization of the model or more literature review.

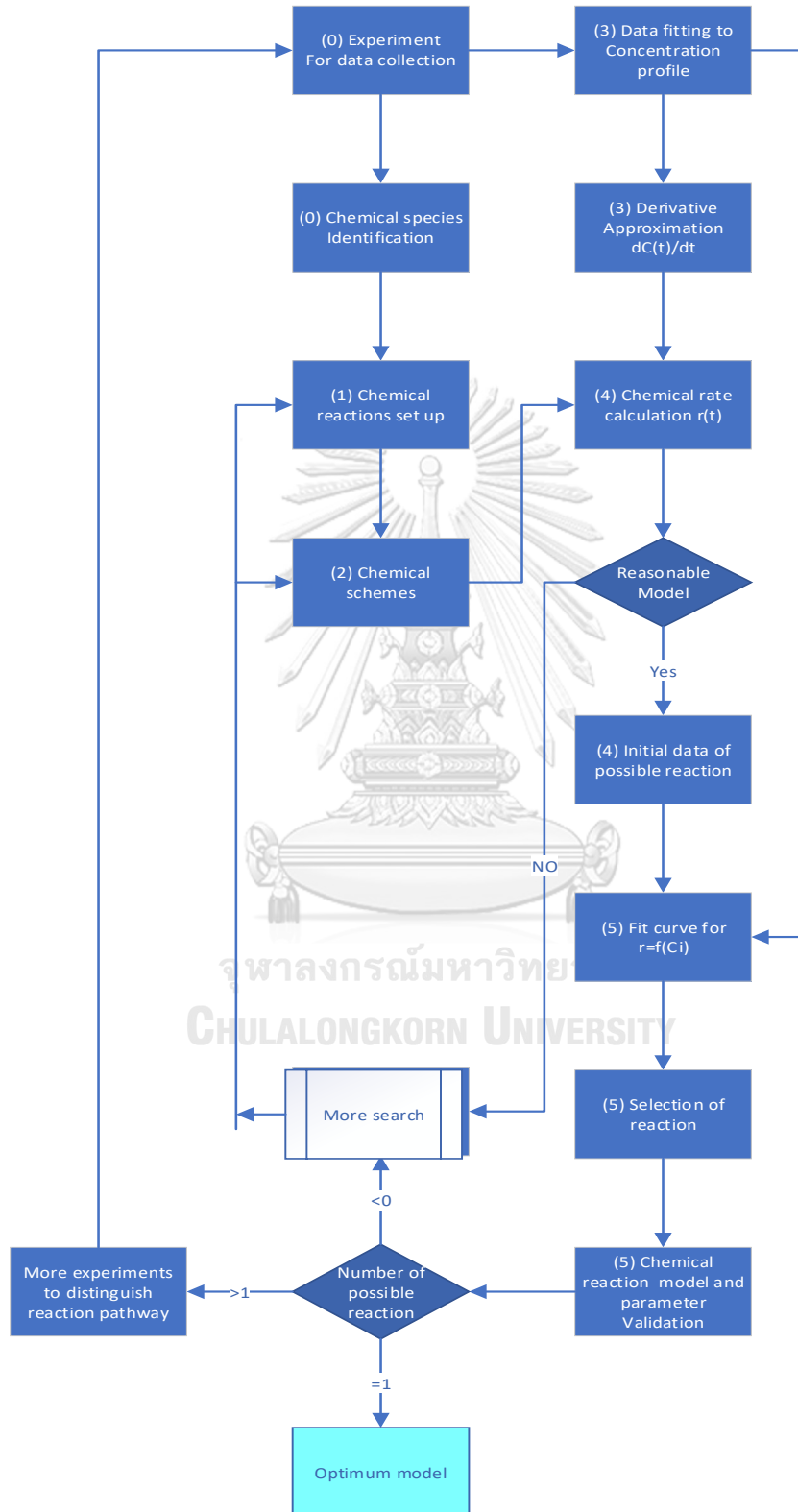


Figure 3 The methodology scheme in chemical kinetic development [58]

At present, the investigation of chemical kinetic widely uses the computerized program to reduce time-consuming as in the study of rate-based construction of kinetic models for complex systems of Sunsnow et al. [59]; Automatic generation of microkinetic mechanisms for heterogeneous catalysis of Goldsmith and West [60]; Katare et al. [61].

The chemical pathway and reaction mechanism plays a crucial role in the development of the chemical and pharmaceutical industry. The sample of chemical pathway and reaction mechanism study is used to evaluate the process optimization, process safety evaluation, and scale sensitivity understanding. Singh [62] stated that understanding the rate-limiting step will help the pharmaceutical industry to research for laboratory scale until industry scale and to succeed in product quality control.

2.5 Chemical kinetics

Chemical kinetics plays a pivotal role in the research and development of chemical synthesis. Chemical kinetics is the study of the rate of change from substances (starting material) to other substances (intermediates, by-products, products) with the defined unit as lost mass/mole of starting material or mass/mole of producing material per time scale.

The rate of reaction can be defined as

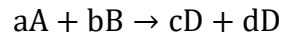
$$r_i = \frac{1}{\nu} \frac{dn_i}{dt} = \frac{dC_i}{dt}$$

i = specie in reaction

n_i = mole of specie i

C_i = concentration of specie i

For homogeneous reaction



With the basis of using species A for calculation, the rate of A is defined as the lost mass of A per volume and time, r_A . At the same time, the other species are defined as r_B , r_C , and r_D . Species A and B are starting materials (decreasing with time). Then, the reaction rate may rewrite as $-r_A$ and $-r_B$.

Divided by the coefficient of A, we can write the arbitrary reaction rate (r) with the same number.

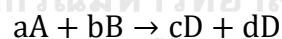
$$r = \frac{-r_A}{a} = \frac{-r_B}{b} = \frac{r_C}{c} = \frac{r_D}{d}$$

or

$$r = \frac{-1}{a} \frac{d[A]}{dt} = \frac{-1}{b} \frac{d[B]}{dt} = \frac{1}{c} \frac{d[C]}{dt} = \frac{1}{d} \frac{d[D]}{dt}$$

Consider the elementary reaction or the order of reaction equal to the coefficient in stoichiometry

And



then, the rate of reaction is

$$-r_A = kC_A^a C_B^b$$

a is reaction order of substance A

b is reaction order of substance B

n is total reaction order, ($n = a+b$)

k is chemical equilibrium

For any temperature, k can be defined as the Arrhenius constant,

$$k = Ae^{-E/RT}$$

A = frequency factor

E = Activation energy, J/mol

R = Ideal gas constant, 8.314, J/(mol K)

T = temperature, K

Rearranged to

$$-r_A = -\frac{dC_A}{dt} = Ae^{-E/RT}C_A^aC_B^b$$

This rate equation is satisfied with elementary chemical reaction. For another reaction, the reaction mechanism should be studied in detail, consisting of what elementary chemical reaction is. Moreover, the rate-limiting step should be classified.

Determination of chemical kinetic parameters

Fogler [63] explains four methods for the determination of chemical kinetic parameters from the rate of reaction using the analytical data from the experiment to calculate the concentration change from time to time.

1. Differential and integral method
2. Method of initial rates
3. Method of half-life
4. Regression analysis

Moreover, Singh [62] explained the method of measuring rate constant using the calorimetry technique. This technique was applied in the synthesis of Sodium benzoate. Pecar, Gorsek, [64] and Triaryl phosphates (Carlos and João [65])

2.6 Reaction calorimetry for determining thermodynamic and chemical kinetic parameters

The reaction calorimetry is widely applicable in the thermodynamic and chemical kinetic analysis to develop the production process and evaluate thermal process safety in those processes. The relation between the chemical reaction rate and the heat-flow rate was defined according to Zogg et al. [66].

$$\dot{q}_{\text{react}}(t) \sim r(t)V_r$$

Whereas,

$\dot{q}_{\text{react}}(t)$ = heat flow rate by chemical reaction, (W)

$r(t)$ = chemical reaction rate, (mol/m³/s)

V_r = reaction volume

Those three variables change with time. Therefore, the appropriate monitoring with online spectroscopy (mid-IR, FTIR, or NIR Raman) or Off-line (HPLC) will represent thermodynamic and chemical kinetic data.

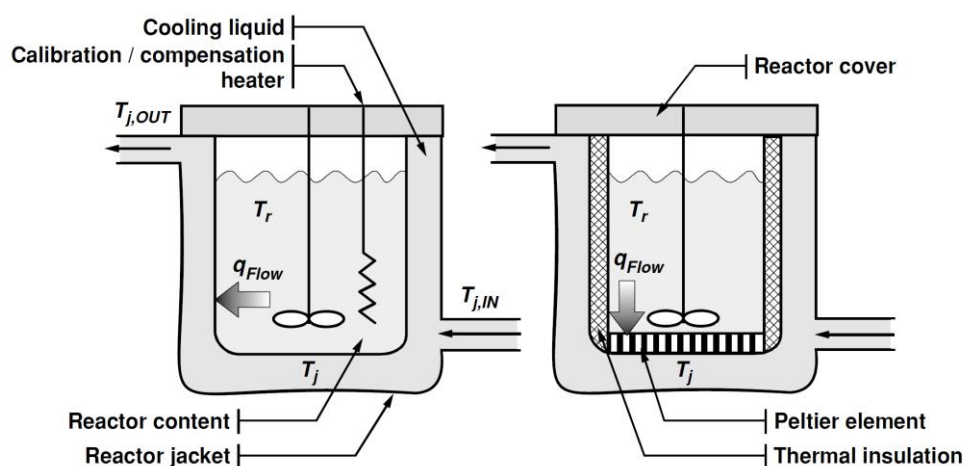


Figure 4 Reaction calorimetry: On the left, heat-flow, heat balance, and power-compensation calorimeter, On the right, Peltier calorimeter.

In general, reaction calorimetry consists of the reactor surrounded by thermal fluid, as shown in Figure 4

At present, heat-flow type reaction calorimeter is produced by various brands such as RC1 (Mettler Toledo), SynCalo (Systag), and Simular (HEL). The temperature within the reactor (T_r) is controlled using thermal fluid in the jacket (T_j). The heat flow in the reactor is sent through thermal fluid in the jacket (q_{flow}), and the difference between both temperatures is calculated using the heat transfer coefficient from the calibration heater.

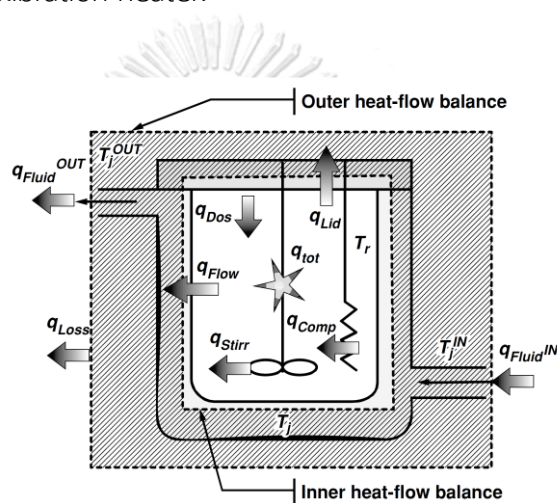


Figure 5 heat-flow, heat balance, and power-compensation calorimeter.

For steady-state isothermal heat flow in Figure 5, the system comprises various heat-flow. Therefore, the total heat flow (q_{tot}) in calorimetry can be found in the equation.

$$q_{tot} = q_{React} + q_{Mix} + q_{Phase}$$

Whereas,

q_{React} = reaction heat-flow rate

q_{Mix} = heat-flow rate from mixing

q_{Phase} = heat-flow rate from phase change

and

$$q_{\text{React}} = -\sum_{j=1 \dots N_R} \Delta_r H_j r_j V_r$$

$\Delta_r H_j r_j$ = enthalpy of reaction

V_r = reaction volume

r_j = reaction rate

N_R = number of reactions

Heat generated by mixing was calculated by

$$q_{\text{Stirr}} = Ne \rho_r n_s^3 A = \pi r^2 d_R^5$$

Which,

Ne = Newton number

ρ_r = density of the substance in the calorimeter

n_s = mixing speed

d_R = stirrer diameter

Heat by dosing (adding substance)

$$q_{\text{Dos}} = f c_{p, \text{Dos}} (T_{\text{Dos}} - T_r)$$

Which,

F =flow rate

$c_{p, \text{Dos}}$ =heat capacity of dosing substance

T_{Dos} =temperature of dosing substance (K)

Heat flow

$$q_{\text{Flow}} = UA(T_r - T_j)$$

Where,

U = Overall heat transfer coefficient

A = heat transfer area

The overall heat transfer coefficient (U) can be calculated from

$$\frac{1}{U} = \frac{1}{h_r} + \frac{1}{\phi}$$

h_r = heat transfer coefficient of reactor side

ϕ = heat transfer coefficient of the instrument

The heat transfer coefficient of the instrument can be calculated from

$$\frac{1}{\phi} = \frac{L}{\lambda_w} + \frac{1}{h_j}$$

Where,

λ_w = heat conductivity of the reactor

h_j = heat transfer coefficient of the jacket

L = reactor thickness

However, the overall heat transfer coefficient (U) and heat transfer area (A) usually change with the reaction. Therefore, the calibration must be performed using a calibration heater before and after the experiment.

The application of reaction calorimetry

The primary purpose of reaction calorimetry is to investigate reaction enthalpy and chemical kinetic parameters; rate constant, reaction order, activation energy (various temperature changes in the reaction)

Reaction enthalpy calculation from the heat flow rate

In the experiment, reaction enthalpy is the summation of overall heat in the system.

$$Q_{\text{tot}} = \int_{t=0}^{t=t_f} q_{\text{tot}} dt$$

$$Q_{\text{tot}} = - \sum_{j=1 \dots N_R} \Delta_r H_j n_i + Q_{\text{mix}} + Q_{\text{Phase}} + Q_{\text{Error}}$$

Which,

t_f = time

Q_{tot} = overall heat in the system

n_i = mole in the reaction

Q_{mix} = heat of mixing

Q_{Phase} = heat of phase change

Q_{Error} = heat of measurement error

If the heat of mixing, heat of phase change, and heat of measurement error are neglected, the total enthalpy can be reduced to $-\Delta_r H \approx \Delta H = \frac{Q_{\text{tot}}}{n}$, whereas ΔH is total enthalpy change. In general, the other heats cannot be neglected. The total enthalpy change can be found using thermal conversion

$$X_{\text{thermal}}(t) = \frac{\int_{\tau=0}^{\tau=t_f} q_{\text{tot}} dt}{Q_{\text{tot}}}$$

The chemical kinetic parameters calculation in the batch reactor

Consider the reaction with n-order in the constant batch reactor



$$r_A(t) = -kC_A(t)^n$$

The heat of reaction, when neglecting the heat of mixing, heat of phase change, and heat of measurement error, is

$$q_{\text{React}}(t) = -\Delta_r H r_A(t) V_r$$

$$r_A(t) = \frac{q_{\text{tot}}(t)}{V_r \Delta_r H} = -kC_{A,0}^n (1 - X_{\text{thermal}}(t))^n$$

The order of the reaction can be calculated for the relation between $\log r_A(t)$ and $\log (1 - X_{\text{thermal}}(t))$, kinetic constant from non-linear least square

There are some publications using a Reaction Calorimeter to determine chemical kinetic constant; Crevatin et al. [67] investigate the kinetic of ketonization reaction using reaction calorimetry, and Pinto Machado e Silva and Cajaiba da Silva [65] evaluate kinetic parameters from the synthesis of triaryl phosphates using reaction calorimetry; Pečar, Darja, and Andreja Goršek [64] study the kinetic modeling of ethylene glycol monoesterification using Reaction Calorimeter; Kartnaller, Vinicius, et al. [68] evaluate the kinetics of the esterification of oleic acid.

2.7 Reactor and process scale-up

The batch reactor is commonly found in active pharmaceutical ingredients and products because it can produce high-value products, small quantities, and various products (Ehly et al. [69]). The structure of this reactor consists of a vessel with a stirrer, baffle, and heating/cooling system in Figure 6. Generally, the standard size of the tank or vessel of the reactor provides the dimension as shown in Figure 7, 10 for a reference value to calculate the dimension when scaled up.

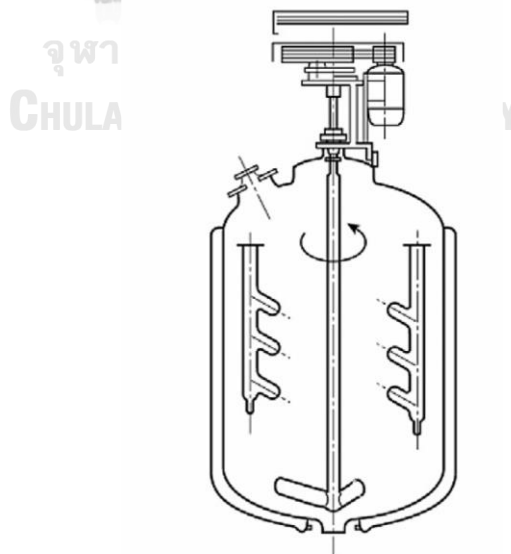


Figure 6 Batch reactor (Saeki and Emura, [70])

2.8 Scale-up process

The laboratory experiment generally provides that the synthetic process can be produced. Moreover, all parameters should be investigated for the process scale up. With small size and well mixing, the thermodynamic and chemical kinetic can be neglected in the synthesis process. Therefore, the scale-up process uses the knowledge from the laboratory scale to the production scale (industrial scale) by performing the experiment on a pilot scale. Additional conditions for the production scale will be added, such as synthesis time, instrument types, product purity, etc. The different sizes of the reactor can provide different product yields because of the flow pattern within the reactor. The purpose of process scale up is to justify the criteria for the production from the laboratory to industrial production. According to Monsalve-Bravo, Moscoso-Vasquez, and Alvarez [71], they classified three methods in the scale-up.

1. Physical approach

1.1 similarity criteria

1.1.1 geometrical similarity

1.1.2 mechanical similarity

1.1.3 thermal similarity

1.1.4 chemical similarity

1.2 Dimensional analysis

1.2.1 Buckingham π -theorem

1.2.2 Inspection analysis

2. Experimental approach

2.1 Trial and error

2.2 Rule of thumb

3. Fundamental approach

3.1 Simulation

3.2 Dynamic hierarchy (Hankel matrix)

The similarity criteria, particularly the geometrical similarity between the different sizes, is commonly used because of simplicity. Consider the geometry of the reactor in different sizes in Figure 7

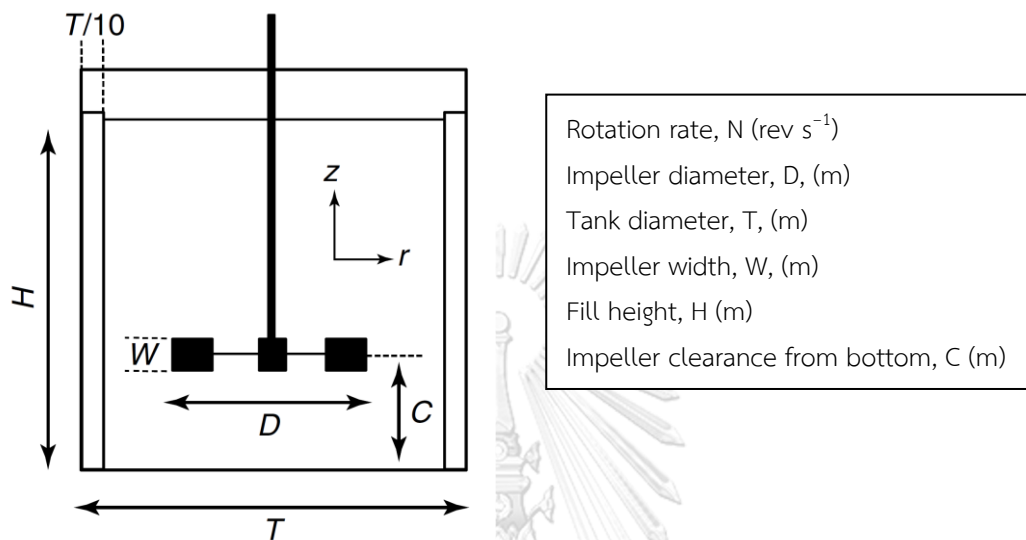


Figure 7 Standard tank reactor with dimension (Hugh Stitt and Simmons, [72])

The general criteria to construct the reactor vessel/tank are classified by standard geometry with specified size.

$$\frac{\text{impeller diameter}}{\text{tank diameter}} = \frac{D}{T} = \frac{1}{3}$$

$$\frac{\text{fill height}}{\text{tank diameter}} = \frac{H}{T} = \frac{1}{1}$$

$$\frac{\text{baffle width}}{\text{tank diameter}} = \frac{W}{D} = \frac{1}{8} \text{ to } \frac{1}{5}$$

$$\frac{\text{fill height}}{\text{tank diameter}} = \frac{H}{T} = \frac{1}{1}$$

$$\frac{\text{Baffle width}}{\text{tank diameter}} = \frac{B}{T} = \frac{1}{10}$$

$$\frac{\text{impeller clearance}}{\text{tank diameter}} = \frac{C}{T} = \frac{1}{3}$$

The objective of the process should be specified before the scale-up process. The process understanding is required to know what controlling mechanism affects the process to provide the ratio between the controlling mechanism (worker) over the job.

$$\frac{\text{size of worker}}{\text{size of job}} = \text{constant}$$

The effect of parameters on the pattern flow in the reactor should be performed on a laboratory scale, such as the power of mixing, stirrer type, temperature, etc., before conducting the process scale-up.

When considering the parameters effect of power (P),

$$P = f(\rho, \mu, N, g, \frac{D}{T}, \frac{H}{T}, \frac{C}{T}, \text{geometric ratio, etc.})$$

For the geometry similarity (the similar size; $\frac{D}{T}, \frac{H}{T}, \frac{C}{T}$ are constant)

$$P_0 = \frac{P}{\rho N^3 D^5} = f(\text{Re})$$

With the empirical experiment in glassed steel 3-blade retreat, the relationship between P_0 , Re (Reynolds number), and stirrer type is shown in Figure 8

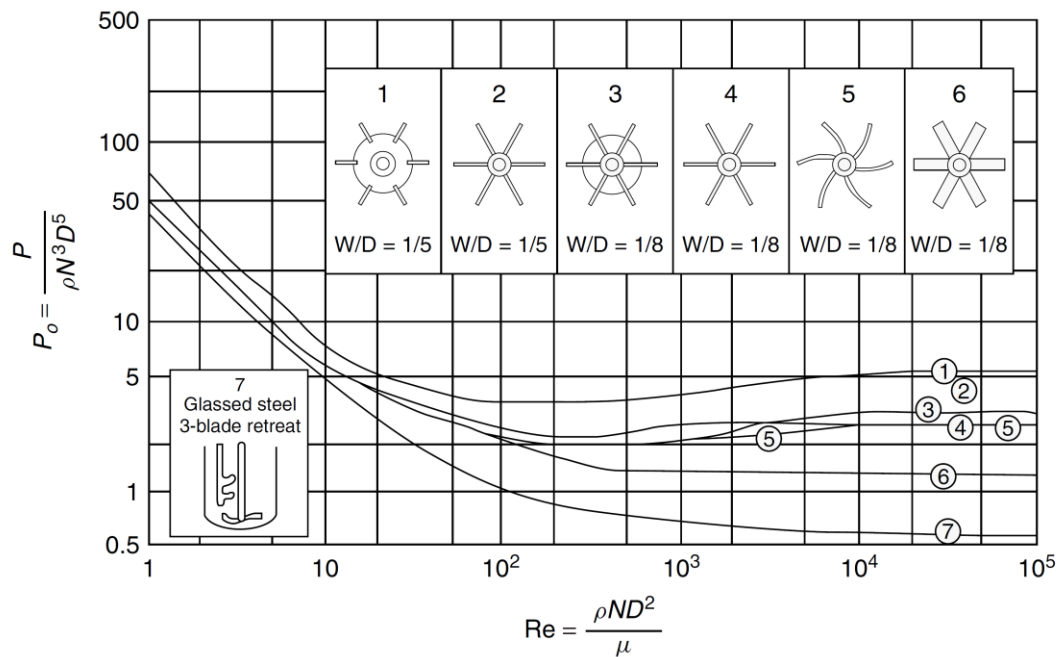


Figure 8 Correlation between P_0 , Reynolds number, and stirrer type (Hemrajani and Tatterson, [73])

In general, the stirrer type in industrial applications is widely used depending on the process, i.e., Rushton disk turbine, pitched blade turbine, marine propeller. The glass-lined reactors in the Government Pharmaceutical Organization are constructed with a 3-blade retreat curve impeller (RCI) which P_0 is provided according to Figure 9


Impeller		Po (turbulent)				
	Three-blade retreat curve impeller (RCI) glass-coated steel	C/T (tank base)	0.16 flat	0.16 conical	0.31 flat	0.31 conical
		Four wall baffles	0.99 ^b	0.87 ^b	0.93 ^b	0.89 ^b
		One wall baffle	0.56 ^b	0.51 ^b	0.56 ^b	0.43 ^b
		Beaver tail	0.46 ^b	0.41 ^b	0.42 ^b	0.33 ^b

Figure 9 Turbulent power number of blade retreat curve impeller (RCI) (Hugh Stitt and Simmons, [72])

Hannon, J. [74], Atherton, J., Houson, I., and Talford, M [75] explained that the intrinsic rate of reaction does not depend on the size of the reactor, small and large reactors followed by the same rate of reaction. In case the rate of reaction is more significant than the physical rate process during the synthesis, such as rate of mass transfer, mixing, solubility, heat transfer (heat transfer area per volume), and addition rate of the substance. The physical rate process in the synthesis is not dominated over the system. Then, chemical kinetic is the process control parameter in the system. Consequently, the scale-up process will follow the optimum experiment.

In addition, the mixing effect dominated over the rate of reaction. The scale-up process will not follow the result of the experiment. It is necessary to conduct the effect of mixing in each synthesis. Bourne, J.R. [76] investigate the mixing effect on the laboratory scale. In general, the study of the mixing effect considers the geometrical similarity between each reactor scale. To simplify this procedure, the standard tank will be specified. In laboratory scale synthesis, it is obvious that a round-bottomed flask is commonly used for the study, and another reason is that the mixing in a round-bottomed flask is well-mixed equipment. For the scale up

process, the geometrical structure of the reactor differs from the laboratory scale. This difference will decrease when using a standard tank such as a dished-bottom glass vessel in the study of mixing effect on product distribution.

To investigate the scale-up process, Keng et al. [77] studied the palm ester from the alcoholysis of palm oil with oleyl alcohol in n-hexane using a lipase catalyst. The optimum process parameters were chosen from the experiment on the laboratory scale. The effect of agitator type (6-blade disc Rushton turbine (RT), AL-hydrofoil turbine (AL-H), and 2-bladed elephant ear turbine (EE)) and mixing speed on %yield of palm ester was investigated using a 2-L reactor with the speed of 50, 150, 250, and 350 rpm. The result showed that the yield of palm ester increased when the agitation speed increased because the substrate and catalyst surface area increased. Moreover, the agitation speed of the 6-blade disc Rushton turbine (RT) at 250 rpm provided the maximum %yield of 95.8% of palm ester synthesis. The scale-up process from the 2-L reactor to the 75-L reactor was conducted using a 6-blade disc Rushton turbine (RT) at 250 rpm as a basis. With a constant tip speed approach in the 75-L reactor, the result showed that %yield of palm ester in the 75-L reactor (50-L working volume) provided a yield of 97.2% after 5 hours of reaction time in comparison with the 2-L reactor, but the rate of palm ester production is higher because the 75-L reactor consisted of more number of turbines.

Imamoglu, E. and F.V. Sukan [78] investigated the scale up process of bioethanol production from 2, 5, and 10 L reactors. The optimum parameters were investigated on a laboratory scale. Phase number was used to characterize the phase of the solution in bioethanol production. Moreover, microorganism as a catalyst in bioethanol production was sensitive to the environment, such as pH, mixing speed, temperature etc. Therefore, the constant agitation speed was used to conduct the scale-up process.

For the scale-up of the laboratory tank reactor to the pilot or industrial tank reactor, the calculation first considers the standard geometry, and the liquid height equals tank diameter ($H=T$).

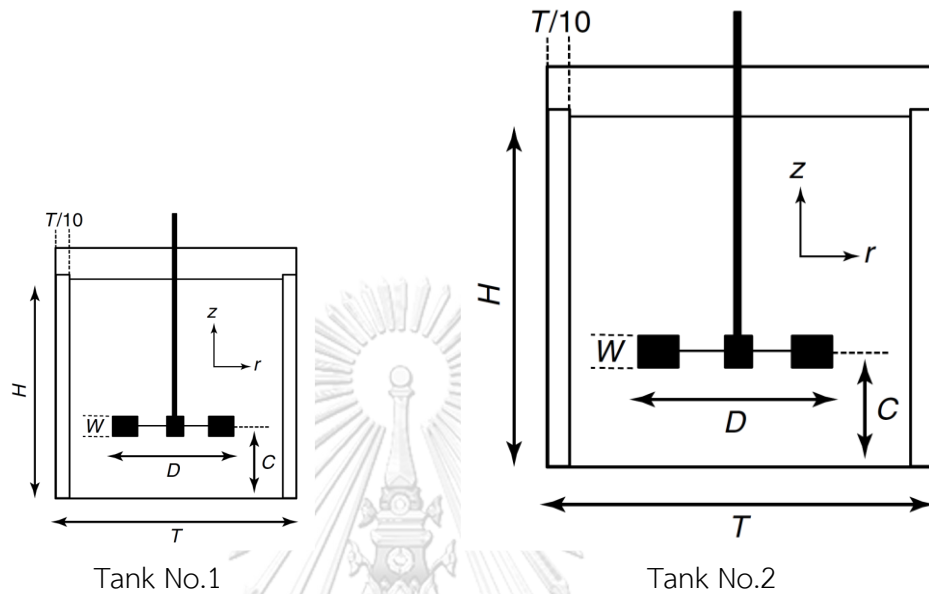


Figure 10 Standard stirrer tank for scale up.

The tank volume in the first tank

$$V_1 = \left(\frac{\pi D_1^2}{4}\right) H_1 = \left(\frac{\pi D_1^3}{4}\right)$$

Whereas,

V_1 = tank volume no.1

D_1 = tank diameter no.1

H_1 = Liquid height in tank no.1

The tank volume in the second tank

$$V_2 = \left(\frac{\pi D_2^2}{4}\right) H_2 = \left(\frac{\pi D_2^3}{4}\right)$$

Whereas,

V_2 = tank volume no.2

D_2 = tank diameter no.2

H_2 = Liquid height in tank no.2

Then,

$$\frac{V_2}{V_1} = \frac{\left(\frac{\pi D_2^2}{4}\right) H_2}{\left(\frac{\pi D_1^2}{4}\right) H_1} = \left(\frac{D_2^3}{D_1^3}\right)$$

The scale-up ratio (R) is defined as the ratio between the dimension of tank 1 divided by the dimension of tank 2. The volume varies with the tank diameter over 3, ($V \propto D^3$)

$$\left(\frac{V_2}{V_1}\right)^{1/3} = \left(\frac{D_2}{D_1}\right)$$

The result of the process when keeping geometrical similarity (R) can be defined in terms of stirrer speed (N), stirrer diameter (D)

$$R \propto N^c D^d$$

The relationship between power, stirrer speed (N), and stirrer diameter (D, $V \propto D^3$).

$$\frac{P}{V} \propto N^a D^b$$

Then,

$$N \propto \left(\frac{P}{V}\right)^{\frac{1}{a}} / D^{\frac{b}{a}}$$

$$R \propto \left(\frac{P}{V}\right)^{\frac{c}{a}} / D^{\frac{b-ad}{c}}$$

$$R \propto \left(\frac{P}{V}\right)^{\frac{c}{a}} / V^{\frac{b-ad}{3}}$$

$$\frac{(P/V)_2}{(P/V)_1} = \left(\frac{V_2}{V_1}\right)^{\frac{b-ad}{3}}$$

This equation represents the relationship between $\frac{(P/V)_2}{(P/V)_1} = \frac{(V)_2}{(V)_1}$, and shown in the Figure 11



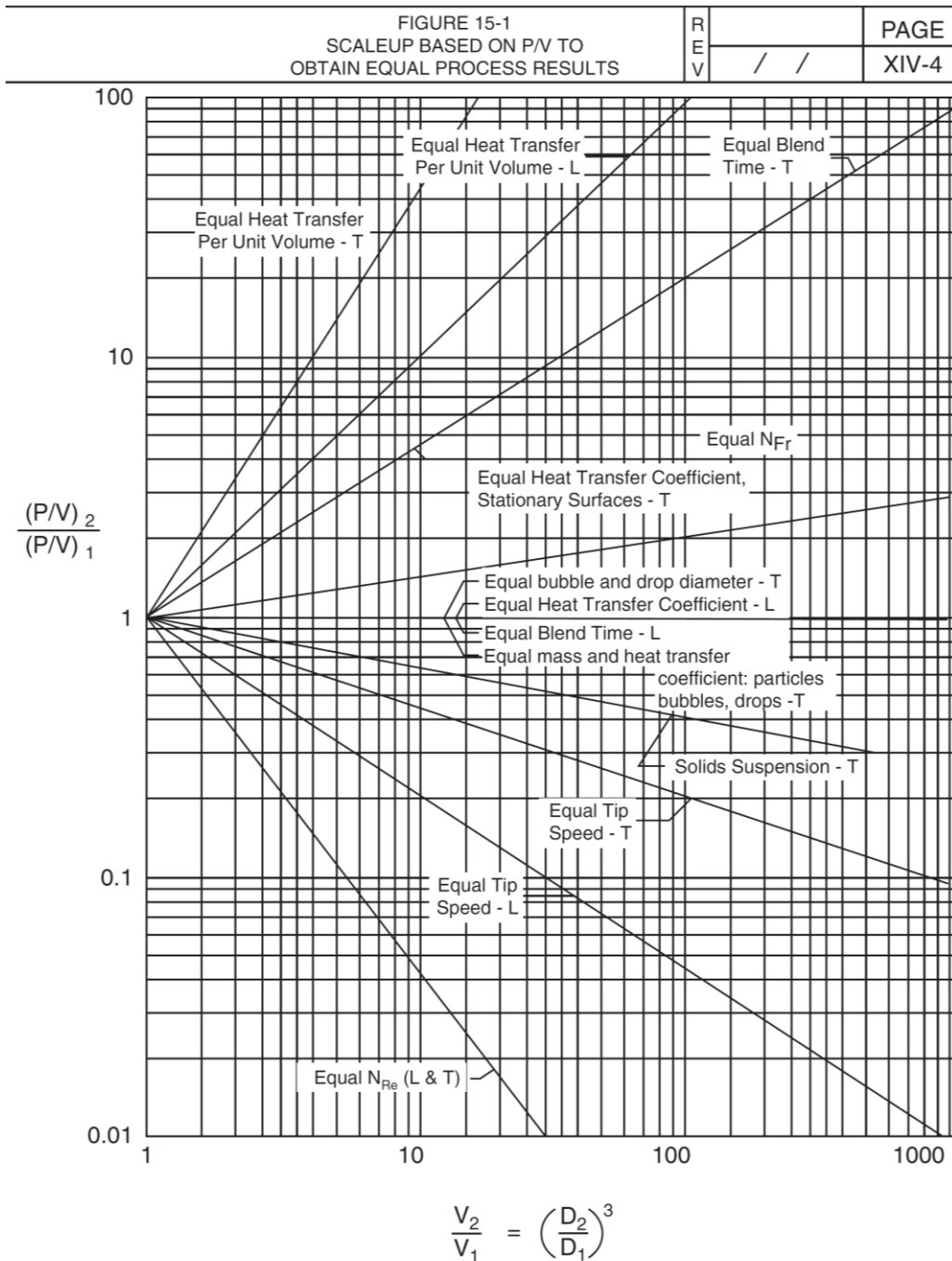


Figure 11 The relationship between $((P/V)_2 / (P/V)_1) = (V_2)/(V_1)$

With the selected objects from the picture, the power can be calculated in tank 2 using data from tank 1.

The 13 equal physical processes from tank 1 to tank 2 are classified.

1. Equal heat transfer per unit volume, Turbulent
2. Equal heat transfer per unit volume, Laminar
3. Equal blend time, Turbulent
4. Equal blend time, Laminar
5. Equal Froude Number (N_{fr})
6. Equal heat transfer coefficient, Turbulent
7. Equal heat transfer coefficient, Laminar
8. Equal bubble and drop diameter, Turbulent
9. Equal mass and heat transfer coefficient, Turbulent
10. Equal solid suspension, Turbulent
11. Equal tip speed, Turbulent
12. Equal tip speed, Laminar
13. Equal Reynold Number (N_{re}), Turbulent, Laminar

For the general relationship of tank scale-up, the target can be described below

1. Equal Reynold number

Reynold number is a dimensionless number defined as the ratio of inertial forces to viscous forces within a fluid and describes the flow pattern of liquid and depends on various parameters

$$N_{re} = \frac{\rho v D_p}{\mu} = \frac{\rho D^2 N}{\mu}$$

Whereas,

N_{re} = Reynold number

ρ = fluid density (kg/m^3)

μ = fluid viscosity (kg/m^s)

v = fluid velocity (m/s)

D_p = tank diameter (m)

D = stirrer diameter (m)

N = stirrer speed (rpm)

$$N_{re1} = N_{re2}$$

$$\frac{\rho_1 D_1^2 N_1}{\mu_1} = \frac{\rho_2 D_2^2 N_2}{\mu_2}$$

The substance in tank 1 and tank 2 are the same properties.

$$\rho_1 = \rho_2$$

$$\mu_1 = \mu_2$$

$$D_1^2 N_1 = D_2^2 N_2$$

$$N_2 = N_1 \frac{D_1^2}{D_2^2} = N_1 \left(\frac{D_1}{D_2} \right)^2$$

2. Equal Froude number

Froude number is a dimensionless number defined as the ratio of the flow inertia to the external field (gravity)

$$N_{fr} = \frac{DN^2}{g}$$

Whereas,

N_{fr} = Froude number

D = stirrer diameter (m)

N = stirrer speed (rpm)

g = gravity (m/s^2)

$$N_{fr1} = N_{fr1}$$

$$\frac{D_1 N_1^2}{g} = \frac{D_2 N_2^2}{g}$$

$$N_2 = N_1 \left(\frac{D_1}{D_2} \right)^{1/2}$$

3. Equal stirrer tip speed

Stirrer tip speed can be calculated from

$$v = \omega R = \omega \frac{D}{2}$$

Whereas,

v = stirrer tip speed, (m/s)

ω = tangential velocity (rad/s)

R = stirrer radius (m)

D = stirred diameter (m)

$$v_1 = v_2$$

$$\omega_1 \frac{D_1}{2} = \omega_2 \frac{D_2}{2}$$

With $\omega = 2\pi N$, N is the stirrer speed (rpm)

$$2\pi N_1 \frac{D_1}{2} = 2\pi N_2 \frac{D_2}{2}$$

$$N_1 D_1 = N_2 D_2$$

$$N_2 = N_1 \left(\frac{D_1}{D_2} \right)^1$$

4. Equal mixing time

Mixing time corresponds to mixing speed to complete mixing in the tank

$$F_t = NT_m$$

Whereas,

F_t = mixing time factor, (round)

N = stirrer speed (rpm)

T_m = mixing time (s)

D = stirred diameter (m)

$$F_{t1} = F_{t2}$$

$$N_1 T_{m1} = N_2 T_{m2}$$

$$N_1 = N_2$$

5. Equal heat transfer coefficient/volume

Consider heat transfer in the reactor through convection, then

$$Q = hA\Delta T$$

Whereas,

Q = heat transfer, (m/s)

h = heat transfer coefficient, (rad/s)

A = transfer area (m^2)

ΔT = temperature difference ($^{\circ}C$)

Nusselt Number is a dimensionless parameter used in calculations of heat transfer between a moving fluid and a solid body. It represents the relationship between Reynold number and Prandtl number.

$$Nu = f(N_{re}, N_{pr})$$

The relationship between heat transfer coefficient, stirrer speed, and tank diameter is shown below.

$$h \propto N^x D^{x/2}$$

from

$$\frac{Q_1}{V_1} = \frac{Q_2}{V_2}$$

$$\frac{h_1 A_1 \Delta T}{V_1} = \frac{h_2 A_2 \Delta T}{V_2}$$

The heated area and volume calculated from $A = \pi D_t^2$, and $V = \pi \frac{D_t^2}{4} H$, respectively.

$$\frac{h_1 A_1 \Delta T}{\pi \frac{D_1^2}{4}} = \frac{h_2 A_2 \Delta T}{\pi \frac{D_2^2}{4}}$$

$$\frac{h_1}{D_1} = \frac{h_2}{D_2}$$

And

$$h \propto N^x D^{x/2}$$

Then,

$$\frac{N_1^x D_1^{x/2}}{D_1} = \frac{N_2^x D_2^{x/2}}{D_2}$$

$$\left(\frac{D_1}{D_2}\right)^{\frac{x}{2}-1} = \left(\frac{N_2}{N_1}\right)^x$$

$$\left(\frac{D_1}{D_2}\right)^{-x} = \left(\frac{N_2}{N_1}\right)^x$$

$$N_2 = N_1 \left(\frac{D_2}{D_1}\right)^x$$

6. Equal heat transfer coefficient

For equal heat transfer coefficient,

$$h_1 = h_2$$

From

$$h \propto N^x D^{x/2}$$

$$N_1^x D_1^{x/2} = N_2^x D_2^{x/2}$$

$$N_1^x \left(\frac{D_1}{D_2}\right)^{x/2} = N_2^x$$

$$N_2 = N_1 \left(\frac{D_1}{D_2}\right)^{1/2}$$

7. Equal power per unit volume

Power number is a dimensionless parameter used for estimating the power consumed by the agitating impeller.

$$N_p = \frac{P}{\rho N^3 D^5}$$

Whereas,

N_p = power number, (m/s)

P = power, (watt)

ρ = fluid density (kg/m³)

N = stirred speed (rpm)

D = tank diameter (m)

When,

$$N_{p1} = N_{p2}$$

$$\frac{P_1}{\rho N_1^3 D_1^5} = \frac{P_2}{\rho N_2^3 D_2^5}$$

The fluid in Tank 1 and 2 are the same properties.

And

$$V \propto D^3$$

$$\frac{P_2}{P_1} = \left(\frac{N_2}{N_1}\right)^3 = \left(\frac{D_2}{D_1}\right)^5$$

$$\frac{P_2/V_2}{P_1/V_1} = \left(\frac{N_2}{N_1}\right)^3 = \left(\frac{D_2}{D_1}\right)^2$$

When,

$$\frac{P_1}{V_1} = \frac{P_2}{V_2}$$

Then,

$$\left(\frac{N_2}{N_1}\right)^3 = \left(\frac{D_2}{D_1}\right)^2$$

$$N_2 = N_1 \left(\frac{D_1}{D_2}\right)^{2/3}$$

Table 3 The Table shows the empirical (n) of stirrer speed and tank diameter at any objective.

CHULALONGKORN UNIVERSITY

Objective	Empirical (n)
1. Equal Reynold number	2
2. Equal Froude number	1/2
3. Equal stirrer tip speed	1
4. Equal mixing time	0
5. Equal heat transfer coefficient per volume	-1
6. Equal heat transfer coefficient	1/2
7. Equal power per volume	2/3

CHAPTER III

EXPERIMENT

3.1 Materials and reagents

The materials and reagents used in this research without further purification were shown in the Table below

Table 4 Chemicals and reagents

Chemicals and reagents	sources
Salicylic acid	Sigma-Aldrich
Salicylamide	Sigma-Aldrich
Cyanuric chloride	Acros organics
Salicyloyl chloride as a working standard	Pharmaffiliates
Benzoxazinone derivative as working standard	TRC (Toronto Research Chemicals)
Bis-salimide as working standard (%Area)	The Government Pharmaceutical Organization.
Triethylamine	Aldrich-chemie
Toluene	Emparta [®] ACS, labscan (Thailand)

3.2 Synthesis of benzoxazinone derivative (8)

According to Jarussopon [20], to synthesize 2-(2-Hydroxyphenyl)-4*H*-1,3-benzoxazin-4-one or benzoxazinone derivative (8), A mixture of salicylic acid (1) (13.8 g, 0.1 mol), salicylamide (6) (11.65 g, 0.085 mol) and 2,4,6-trichloro-1,3,5-triazine or cyanuric chloride (2) (12.3g, 0.067 mol) was added to 500-ml two round-bottom neck flask and equipped with a condenser and a Dean-stark trap. Three hundred milliliters of toluene were added to a mixture. Then, the suspension was heated up to 80 °C and stirred at this temperature for 30 minutes. Next, Triethylamine (13.9 mL, 0.1 mol) was slowly added to the reaction mixture. After that, the reaction mixture was heated to 110 °C and refluxed. The chemicals from the mixture were investigated at each time of reaction. The mole ratios of salicylic acid (1), cyanuric chloride (2), and salicylamide (6) were varied at 1:0.67:0.75, 1:0.67:0.85, 1:0.67:1.

The mole ratios of salicylic acid (1) to triethylamine were also studied at 1:0.1, 1:1 and 1:2. The TLC technique was also used to monitor the reaction progression with 40% ethyl acetate/hexane as a mobile phase. After the completion of the reaction, the reaction mixture was cooled down to 80 °C, and the reaction mixture was filtered to remove the solid substances. The precipitation of the solid was observed during the reaction. The solid and filtrate were further analyzed using HPLC to determine the chemicals and their amount. The experiments were done in triplicate to determine the concentration profile in each condition, and the average values were reported.

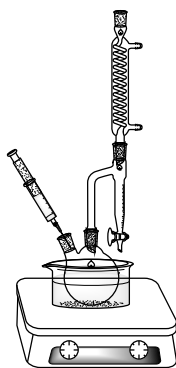


Figure 12 The experiment in round bottom flask.

3.3 Determination of the chemicals concentration in the reaction

To determine the reaction scheme, the HPLC technique was used to analyze the chemical reaction. Liquid chromatography (HPLC) (Agilent, 1100 series) equipped with an Inertsil ODS-3V column and photodiode array detector (PDA). The filtrated reaction product was diluted with acetonitrile before analyses. The injection volume was 10 μ L. Mobile phase A consisted of 0.01 M potassium dihydrogen phosphate adjusted pH to 3.0 \pm 0.05 with phosphoric acid, and mobile phase B consisted of acetonitrile and methanol in the ratio of 90:10 v/v in isocratic mode (mobile phase A: mobile phase B, 50:50). The flowrate was 1 ml/min with 25 minutes for runtime. The HPLC chromatogram showed the known and unknown peaks of products. Two major unknown peaks were further investigated. The relative response factor was used to quantify all known chemicals to Benzoxaxinone derivative standard. The results were shown in the form of conversion and yield, which were defined as

$$\text{Conversion } x_i = \frac{\text{Initial concentration of i} - \text{Concentration of i (mol/l)}}{\text{Initial concentration i (mol/l)}}$$

$$\text{Yield } y_j = \frac{\text{Concentration of j (mol/l)}}{\text{Initial Concentration salicylic acid (mol/l)}}$$

3.4 Synthesis of tris-quaternary ammonium salt (10)

According to Somnath Gholap, and Navanath Gunjal [79], the reaction of 2,4,6-trichloro-1,3,5-triazine or cyanuric chloride (**2**) in the presence of triethylamine gives the tris-quaternary ammonium salt as a product. Therefore, the reaction of cyanuric chloride (**2**) in the presence of triethylamine with refluxing toluene was studied. After the completion of the reaction, the reaction mixture was purified using column chromatography to provide the white solid as a product. The white solid was dissolved in the acetonitrile and then characterized by HPLC. The chromatogram showed the peak at the same retention time of the unknown peak from

benzoxazinone derivative synthesis reaction product. Therefore, it was postulated that the chemical structure of the other unknown peak was tris-quaternary ammonium salt (10).

3.5 Isolation of 4-chloro-2-(2-hydroxyphenyl)-4H-benzo[e][1,3]oxazine-4-ol (9) from the reaction

To elucidate the chemical structure of the unknown compounds, the filtrate of the product mixture was then evaporated under reduced pressure to provide a crude product as a sticky matter for the chemical structure elucidation of unknown compounds. The sticky matter was purified by preparative column chromatography using silica gel (F256) as the stationary phase and ethyl acetate: hexane (10:90) as the mobile phase. The fraction was collected and analyzed by TLC and HPLC. All fractions with the same spot on TLC were combined and concentrated under reduced pressure to provide a white solid. The chemical structure of the solid product was elucidated, which was 4-Chloro-2-(2-hydroxyphenyl)-4H-benzo[e][1,3]oxazine-4-ol (9).

3.6 Determination of heat of reaction using reaction calorimeter (RC1e, Mettler Toledo)

The overall heat of the reaction of the Benzoxazinone derivative (8) synthesis was measured using a reaction calorimeter (RC1e, Mettler Toledo) with a 500 mL vessel with UA 4.83 W/K. 18.40 g of salicylic acid (1) was added to 400 mL toluene. The cyanuric chloride (2) and salicylamide (6) were added to the solution at 1 mole equivalent to salicylic acid. After that, one mole equivalent of triethylamine was slowly added to the reaction mixture for 3 hrs. The coolant temperature was measured and then used to calculate the removal heat rate to keep a constant reaction temperature at 80 °C. The reaction time of 250 minutes was used, and the remaining salicylic acid was measured. The overall heat of the reaction was

calculated from the peak area of removal heat rate based on one mole reacted of salicylic acid (1).



Figure 13 Automatic reaction calorimeter (RC1e, Mettler Toledo)

3.4 1-L Reactor for synthesis

Reactor diameter = 0.1 m

Stirrer diameter = 0.06 m



Figure 14 1-L double jacket reactor.

3.5 10-L Reactor for synthesis

Reactor diameter = 0.2 m

Stirrer diameter = 0.12 m



Figure 15 10-L double wall reactor, Büchiglasuster®.

3.6 Analytical procedure

The HPLC technique was used to analyze the chemical reaction. Liquid chromatography (HPLC) (Agilent, 1100 series) equipped with an Inertsil ODS-3V column and photodiode array detector (PDA). The filtrated reaction product was diluted with acetonitrile before being analyzed. The injection volume was 10 μL . Mobile phase A consisted of 0.01 M potassium dihydrogen phosphate adjusted pH to 3.0 ± 0.05 with phosphoric acid, and mobile phase B consisted of acetonitrile and methanol in the ratio of 90:10 v/v in isocratic mode (mobile phase A: mobile phase B, 50:50). The flowrate was 1 ml/min with 25 minutes for runtime.

Standard preparation for HPLC for profile experiment

Accurately weigh about 12.5 mg of 2-Hydroxyphenyl-4*H*-1-3-Benzoxazin-4-one into a 25-mL volumetric flask. Add about 15 ml of HPLC-grade acetonitrile and sonicate until a clear solution was obtained. Adjust to volume with HPLC grade acetonitrile (standard stock solution 1).

For calibration curve preparation, Pipet 1 ml of the standard stock solution into a 25-ml volumetric flask. Adjust to volume with HPLC-grade acetonitrile. Filter the solution through a 0.45 μm porosity nylon membrane filter and use the filtrate (standard stock solution 2). Pipet 10 ml of standard stock solution 2 into a 25-ml volumetric flask. Adjust to volume with HPLC grade acetonitrile (standard stock solution 3) and Pipet 1 ml of standard stock solution 2 into a 10-ml volumetric flask. Adjust to volume with HPLC grade acetonitrile (standard stock solution 4). Filter the solution through a 0.45 μm porosity nylon membrane filter and use the filtrate. The last point, pipet 1 ml of standard stock solution 4 into a 10-ml volumetric flask. Adjust to volume with HPLC grade acetonitrile (standard stock solution 5). Filter the solution through a 0.45 μm porosity nylon membrane filter and use the filtrate.

Table 5 Summary of the standard calibration curve point

No.	procedure	Concentration (mg/ml)
1.	$\frac{12.5 \text{ ml}}{25 \text{ ml}}$	0.5
2.	$\frac{12.5 \text{ ml}}{25 \text{ ml}} \times \frac{1 \text{ ml}}{25 \text{ ml}}$	0.02
3.	$\frac{12.5 \text{ ml}}{25 \text{ ml}} \times \frac{1 \text{ ml}}{25 \text{ ml}} \times \frac{10 \text{ ml}}{25 \text{ ml}}$	0.008
4.	$\frac{12.5 \text{ ml}}{25 \text{ ml}} \times \frac{1 \text{ ml}}{25 \text{ ml}} \times \frac{1 \text{ ml}}{10 \text{ ml}}$	0.002
5.	$\frac{12.5 \text{ ml}}{25 \text{ ml}} \times \frac{1 \text{ ml}}{25 \text{ ml}} \times \frac{1 \text{ ml}}{10 \text{ ml}} \times \frac{1 \text{ ml}}{10 \text{ ml}}$	0.0002

Preparation of sample solution

Pipet 10 μL of sample into a 10-mL volumetric flask. Dilute with HPLC-grade acetonitrile. Filter the solution through a 0.45 μm porosity nylon membrane filter and use the filtrate.

chemical structure elucidation

The ^1H and ^{13}C NMR spectra were structurally studied for identification and characterization using Bruker Avance-500 (500 MHz). The chemical shifts were given in parts per million (δ ppm). The high-resolution mass spectra (HSMS) were obtained on a Bruker micro TOF spectrometer in the ESI mode. The infrared spectrum was determined by Attenuated Total Reflection (ATR) technique. The IR spectra was recorded on Perkin Elmer Spectrum Two FT-IR Spectrometer in the range of 4000 cm^{-1} to 650 cm^{-1} .

CHAPTER IV

THE REACTION SCHEME OF BENZOXAZINONE DERIVATIVE

In this chapter, the intensive study of Benzoxazinone derivative synthesis from salicylic acid and salicylamide using cyanuric chloride as a chlorinating agent was conducted. The reaction scheme was investigated using the concentration profile of chemicals in the reaction mixture. The chemical structure elucidation was used to identify the chemical structure of unknown compounds. The heat of the reaction and effect of reaction parameters: reaction time, temperature, the concentration ratio of each reactant, and the concentration of triethylamine (Et₃N) were studied.

4.1 Structural elucidation of unknown compounds

The white powder compounds was confirm structure as the 4-Chloro-2-(2-hydroxyphenyl)-4*H*-benzo[e][1,3]oxazine-4-ol (**7**) as shown in Figure 16 by melting point, m.p.: 95-98 °C, FT-IR: 3243, 3110, 1680, 1616, 1583, 1246, 754 cm⁻¹; ¹H-NMR (500 MHz, CDCl₃, δ (ppm)) and ¹³C-NMR (500 MHz, CDCl₃, δ (ppm)) spectra were ¹H-NMR (CDCl₃): δ 7.01 (ddd, *J* = 7.2, 7.2, 1.0 Hz, ¹H), 7.06 (dd, *J* = 8.4, 0.9 Hz, ¹H), 7.42 (td, *J* = 7.6, 1.0, ¹H), 7.47 (dd, *J* = 8.3, 0.7 Hz, ¹H), 7.58 (ddd, *J* = 7.3, 7.3, 1.7 Hz, ¹H), 7.71 (ddd, *J* = 7.7, 7.6, 1.6 Hz, ¹H), 7.75 (dd, *J* = 7.7, 1.6 Hz, ¹H), 8.15 (dd, *J* = 8.0, 1.7 Hz, ¹H), 10.13 (s, OH); ¹³C NMR (CDCl₃): δ 107.2, 110.9, 114.8, 117.9, 119.9, 123.2, 126.7, 130.6, 133.5, 134.1, 137.2, 151.7, 162.4, 167.6; HRMS: Calcd for C₁₄H₁₀ClNO₃Na (M+Na⁺-HCl) 262.0480. Found: 262.0470.

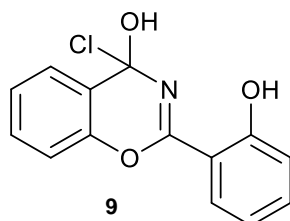


Figure 16 Chemical structure of 4-Chloro-2-(2-hydroxyphenyl)-4*H*-benzo[e][1,3]oxazine-4-ol (**9**).

4.2 The reaction scheme for benzoxazinone derivative (8) synthesis.

According to Jarassopon et al. [20], the reaction scheme of benzoxazinone derivative synthesis was proposed. First, the salicylic acid (1) reacted with cyanuric chloride (2) to form salicyloyl chloride (3) as Rxn 1 in Figure 17. The condensation between salicyloyl chloride (3) and salicylamide (6) then occurred to form an intermediate bis-salimide (7) as Rxn 3. After that, cyclization of bis-salimide (7) provides a six-membered ring of benzoxazinone derivative (8) as Rxn 4. However, from the chemical structure elucidation of the solid product, as mentioned before, the hydrochloric acid reacted with benzoxazinone derivative (8) to yield compound 4-chloro-2-(2-hydroxyphenyl)-4*H*-benzo[e][1,3]oxazine-4-ol (8) which was a new reported compound from this synthesis route as Rxn 5.

Furthermore, because of the unknown peak from HPLC, the reaction of cyanuric chloride (2) in the presence of triethylamine was studied. The tris-quaternary ammonium salt was found as a product of this reaction. This product indicates that in the Benzoxazinone derivative (8) synthesis route using a chlorinating reagent of cyanuric chloride (2) under a base condition of triethylamine will give a by-product of tris-quaternary ammonium salt (10) as in Rxn 6

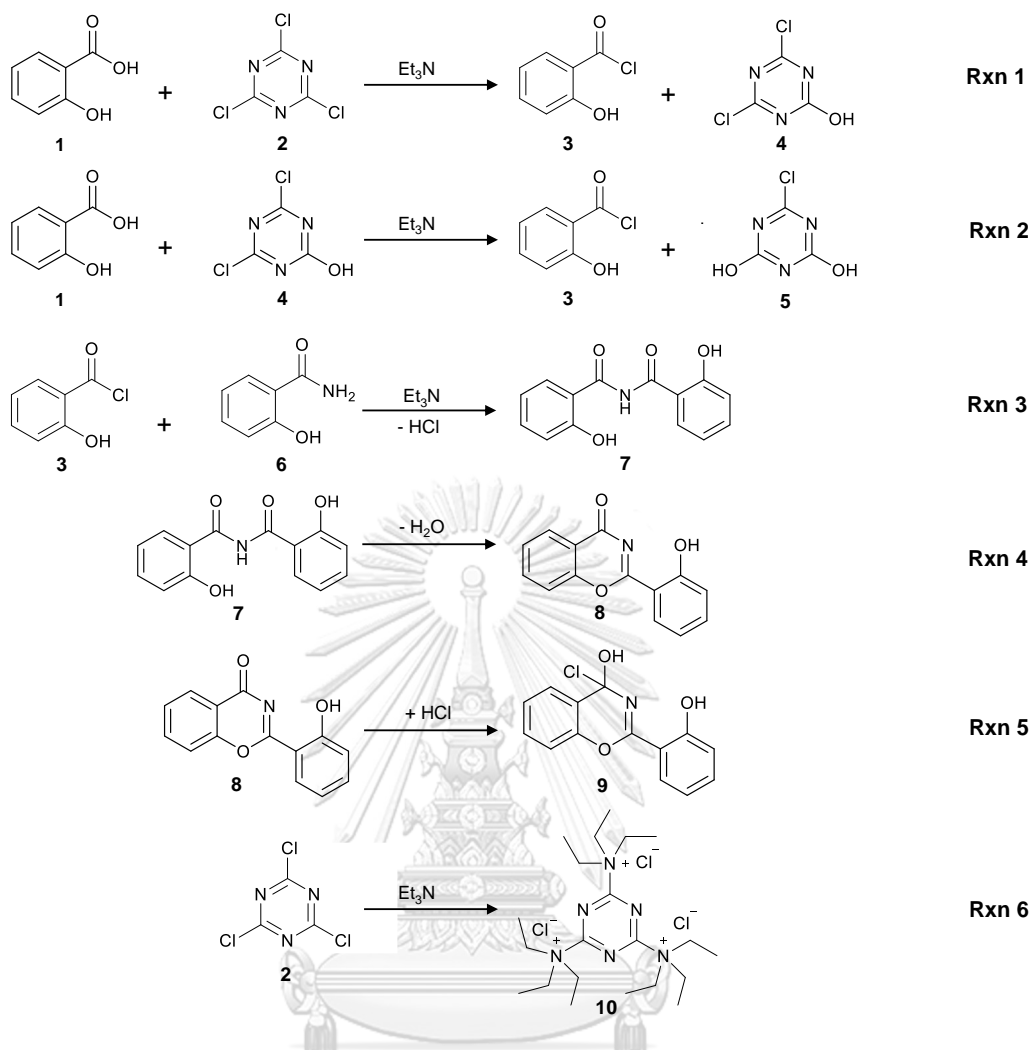


Figure 17 The reaction scheme for Benzoxazinone derivative (**8**) synthesis from salicylic acid (**1**) and salicylamide (**6**) using cyanuric chloride (**2**) as a chlorinating agent under the base condition of triethylamine.

4.3 The conversion profile of the reactant and yield profile of the product

To understand the reaction better, the reactant's conversion profile and the product's yield profile in the filtrate product were studied, as shown in Table 6. The ratio of each starting chemical salicylic acid (**1**), cyanuric chloride (**2**), salicylamide (**6**), and triethylamine was 1:0.67:1:1. The reaction temperature was 110 °C (reflux temperature). At prescribed time intervals, the amount of each chemical was measured unless a reactive cyanuric chloride (**2**), 2,6-dichloro-1,3,5-triazine (**4**), and 2-monochloro-1,3,5-triazine (**5**). Considering the reactant, salicylic acid (**1**) and salicylamide (**6**) conversion increases dramatically even in the early 5 minutes of the reaction and slowly increases until constant after 120 minutes. In contrast, the product yield of compounds **3**, **7**, **8**, and **9** were not in balance with the reacted reactant **1** and **6**. According to the experiment, solid precipitation was observed during the reaction. To characterize the compositions of the solid, HPLC was performed. The results showed that the main component of the solid consisted of bis-salimide (**7**) and salicylamide (**6**). That means salicyloyl chloride (**3**) and salicylamide (**6**) were immediately converted to bis-salimide (**7**) as a solid product during the reaction. The solid was formed at the beginning of the reaction and trapped all components, especially bis-salimide (**7**) and salicylamide (**6**). As a result, the conversion of **6** was not equal to the summation of the yield of **7**, **8**, and **9**. Therefore, the conversion of salicylamide (**6**) should be lower, and the yield of bis-salimide (**7**) should be higher than the value in Table 6 because only the concentration in the filtrate was shown. Furthermore, the incomplete conversion of salicylic acid (**1**) agrees with the Rxn 6, in which a yield of **10** was observed.

Table 6 The conversion of reactants and yield of products profile during the reaction at 110 °C (Reflux) and mole ratios of salicylic acid (1), cyanuric chloride (2), salicylamide (6), and triethylamine at 1:0.67:1:1

Reaction time (min)	% Conversion (n=3)			% Yield (n=3)						
	x ₁	x ₆	x ₃	y ₇	y ₈	y ₉	y ₁₀	y ₉	y ₁₀	
0	0	0	0	0	0	0	0	0	0	
5	80.02±1.16	66.40±1.25	0.85±0.38	4.87±2.82	2.51±1.17	0	0	0	0	
10	82.78±0.80	70.61±1.40	1.07±0.33	5.63±3.26	4.96±1.71	0	0	0	0.88±0.5	
15	84.46±0.87	71.57±2.00	1.37±0.30	5.17±2.99	9.79±2.03	0.24±0.09	1.66±0.61	0.24±0.09	1.66±0.61	
20	87.78±0.79	75.65±1.18	1.57±0.15	3.48±2.02	14.95±1.90	0.42±0.97	2.62±0.97	0.42±0.97	2.62±0.97	
30	90.55±1.10	78.27±0.40	2.04±0.16	1.37±1.17	23.37±2.43	1.07±1.11	3.77±1.47	1.07±1.11	3.77±1.47	
45	93.54±1.93	81.15±1.32	2.36±0.17	1.11±0.54	28.72±3.69	1.62±0.78	5.34±2.18	1.62±0.78	5.34±2.18	
60	95.54±1.91	83.17±3.04	2.43±0.52	0.72±0.42	29.30±7.56	2.15±0.90	5.71±1.69	2.15±0.90	5.71±1.69	
120	96.42±2.77	79.43±0.32	2.84±0.68	0.35±0.19	37.04±6.20	4.19±1.02	8.93±2.07	4.19±1.02	8.93±2.07	
180	96.13±3.74	77.38±3.21	2.71±0.90	0.19±0.19	40.68±5.86	5.93±1.01	10.55±0.58	5.93±1.01	10.55±0.58	
240	96.49±3.74	78.40±0.76	2.71±1.04	0.18±0.10	40.15±8.47	6.39±1.46	10.46±1.91	6.39±1.46	10.46±1.91	
300	96.42±3.86	77.18±1.38	2.73±0.98	0.15±0.17	42.95±7.52	7.93±1.50	11.46±1.51	7.93±1.50	11.46±1.51	
360	96.70±4.26	77.63±0.54	2.71±1.14	0.15±0.17	42.91±10.94	7.65±2.74	11.61±2.92	7.65±2.74	11.61±2.92	
1320	93.59±2.10	76.24±2.72	2.24±0.0.69	0.00±0.0	46.77±10.12	9.14±4.21	11.90±1.2	9.14±4.21	11.90±1.2	

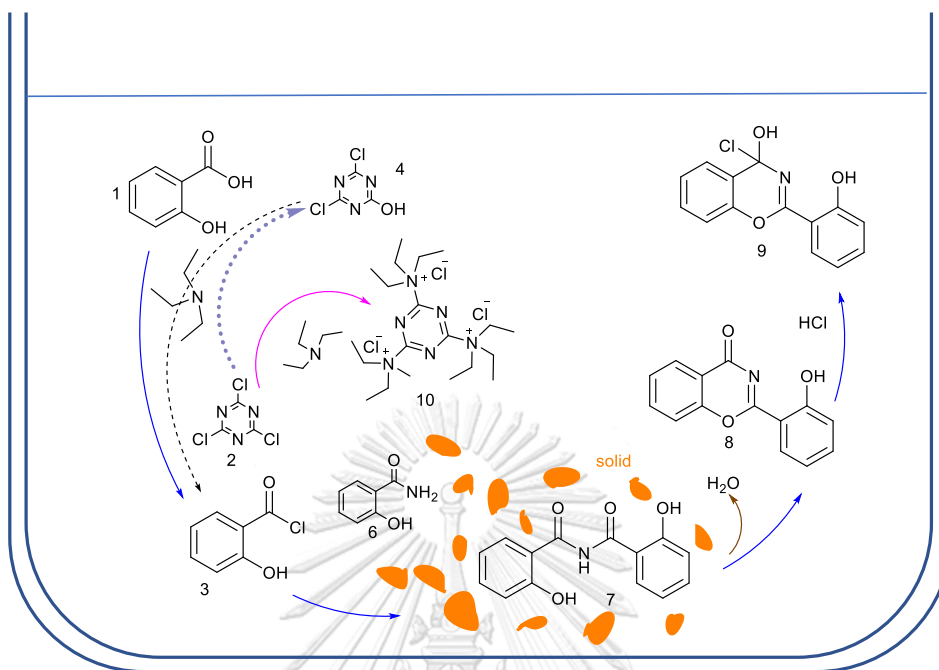


Figure 18 Reaction picture of Benzoxazinone derivative synthesis (8)

To summarize the reaction from the reaction picture of Benzoxazinone derivative synthesis, salicylic acid (1), cyanuric chloride (2), and triethylamine rapidly convert to salicyloyl chloride (3). At the same time, salicylamide (6) immediately reacts with salicyloyl chloride (3) to form bis-salimide (7). The solid is formed at the beginning of the reaction and trapped inside bis-salimide (7) and salicylamide (6). Bis-salimide in the solution mixture converted to Benzoxazinone derivative (8). In the presence of HCl, Benzoxazinone derivative converts to a compound (9). In addition, cyanuric chloride reacts with triethylamine to form a compound (10).

4.4 Effect of salicylic acid (1): salicylamide (6) ratio

The effect of the molar ratio of salicylic acid (1) to salicylamide (6) on the product yield was studied in Entries 1-3 of Table 2. The amount of salicylamide (6) varied from 0.75, 0.85, and 1.0, equivalent to salicylic acid (1). The yield of benzoxazinone derivative (8) significantly increased when salicylamide increased. This higher yield is due to the high salicylamide concentration surrounding the salicylic acid molecule. It enhanced the possibility of the two species of molecules to react. Not only did the highest equivalent of salicylamide give the highest amount of Benzoxazinone derivative, but it also left unreacted molecules more than the low equivalent of salicylamide. Furthermore, the yield of compound (9) tends to increase with the decrease of salicylamide (6). The yield of compound (10) is reported to be around 11 % for all ratios.

The purity of the Benzoxazinone derivative from entry 3 was determined after the reaction was completed in 22 hours. The reaction mixture was cooled to 80°C and filtered to remove the solid. The solvent was then removed under reduced pressure. Next, ethanol was added to the flask containing the yellow solid and cooled to 0°C. the mixture was filtered and then, the solid was dry in vacuum oven for 5 hours. The purity was determined using HPLC, and the relative area of the peak in the chromatogram indicated that the purity of the Benzoxazinone derivative from the parameters in entry 3 was 98.64% (see Appendix 1.4). As a result, the by-product, compound 9, can be removed from the product through crystallization in ethanol.

4.5 Effect of triethylamine concentration

The effect of triethylamine was studied in Entries 2, 4, and 5 of Table 7. Triethylamine was used as a catalyst in this reaction. Moreover, the amount of triethylamine could control the pH of the reaction mixture. The acidic mixture will be neutralized by triethylamine. The effects of the catalyst were studied using 0.1, 1,

and 2 triethylamine equivalent to salicylic acid. The results showed that the optimal yield of Benzoxazinone derivative (**6**) was observed at 1 equivalent of triethylamine. The lower yield of **6** may be due to lower salicylamide (**6**) conversion at the higher triethylamine. Furthermore, increasing triethylamine lowers the yield of compound (**7**) because HCl in the mixture was neutralized by triethylamine which the Rxn 4 in Figure 17 required HCl to change the structure. The higher yield of compound (**8**) surprisingly increases with the decrease of triethylamine.

4.6 The effect of the reaction temperature

Temperature is an essential parameter in chemical synthesis. This study will use 80, 100 °C and refluxing temperatures (110 °C), as shown in Entries 6, 7, and 2. The lower temperatures, the lower the maximum conversion of 1 and 4 were observed. However, the benzoxazinone derivative (**6**) yield is not much different, but the reflux temperature gave the highest yield. Moreover, the higher the reaction temperature, the more yield of the compound (**7**).

When the temperature rose from 80 °C to refluxing temperature of toluene (110 °C), the effect of temperature on the amount of benzoxazinone derivative trended to increase benzoxazinone derivative. Then, the experiment using xylene, which has a boiling point of 138.4 °C, seemed to produce more benzoxazinone derivative. Although both toluene and xylene were classified in class 2 of “International Council For Harmonisation Of Technical Requirements For Pharmaceuticals For Human Use”. However, the energy consumption during the synthesis process over 6 hours was one of the essential parameters, including purity and yield, to consider in the production scale. Therefore, the process with a lower temperature was more suitable to operate in the industrial section than the process with a higher temperature.

Table 7 Effect of reaction parameters on the conversion of reactant and yield of the product after 1320 min (22 h) reaction time

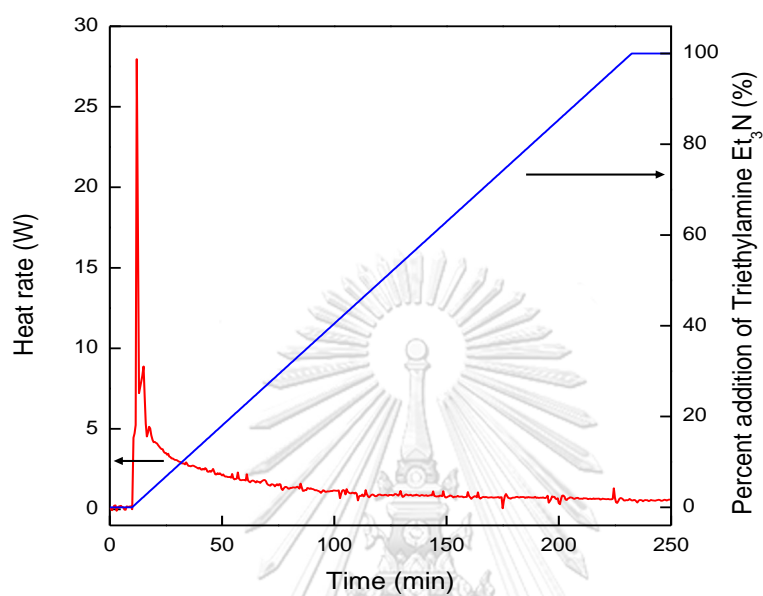
Entry	1 (equiv.)	2 (equiv.)	6 (equiv.)	Et ₃ N (equiv.)	Temperature (°C)	% Conversion (n=3)			% Yield (n=3)					
						x ₁	x ₆	y ₃	y ₇	y ₈	y ₉	y ₁₀		
1	1	0.67	0.75	1	Reflux 110 °C	99.24±0.24	83.02±0.24	0.34±0.25	0.71±0.06	33.12±0.92	14.04±0.96	11.69±2.97		
2	1	0.67	0.85	1	Reflux 110 °C	96.36±2.46	84.75±1.21	2.19±1.64	0	40.02±3.26	15.74±0.41	10.58±2.15		
3	1	0.67	1	1	Reflux 110 °C	93.59±2.10	76.24±2.72	2.24±0.69	0	46.77±10.12	9.14±4.21	11.90±1.21		
4	1	0.67	0.85	0.1	Reflux 110 °C	100.00±0.00	82.69±0.36	0	0	13.48±0.92	36.57±4.00	17.62±0.32		
5	1	0.67	0.85	2	Reflux 110 °C	95.26±0.18	62.25±1.88	0.82±0.07	0.00	25.44±0.54	4.27±0.59	8.46±5.45		
6	1	0.67	0.85	1	80 °C	87.85±0.96	84.93±0.73	3.87±0.29	1.46±0.85	36.19±1.92	4.77±1.17	4.25±2.30		
7	1	0.67	0.85	1	100 °C	92.30±1.13	90.00±1.58	2.58±2.14	0.75±0.07	34.76±6.17	10.55±3.14	8.74±3.14		

4.7 The overall heat of the reaction

The overall heat of the reaction of the Benzoxazinone derivative (**8**) synthesis was measured using a reaction calorimeter (RC1e, Mettler Toledo) with a 500 mL vessel with UA 4.83 W/K. 18.40 g of salicylic acid (**1**) was added to 400 mL toluene. The cyanuric chloride (**2**) and salicylamide (**6**) were added to the solution at 1 mole equivalent to salicylic acid. After that, one mole equivalent of triethylamine was slowly added to the reaction mixture for 3 hrs. The coolant temperature was measured and then used to calculate the removal heat rate to keep a constant reaction temperature at 80 °C. The reaction time of 250 minutes was used, and the remaining salicylic acid was measured. The overall heat of the reaction was calculated from the peak area of removal heat rate based on one mole reacted of salicylic acid (**1**).

The reaction calorimeter was used to measure the overall heat of the reaction. The salicylic acid (**1**, 0.133 mol), salicylamide (**6**, 0.133 mol), cyanuric chloride (**2**, 0.089 mol), and triethylamine (0.133 mol) in 400 mL of toluene were used to perform the data measurement at 80 °C. The triethylamine was added to the reaction mixture for 3 hours. The overall heat transfer coefficients were measured before and after the reaction for heat flow calculation. The heat flow of the reaction was automatically measured by controlling the reaction temperature at 80 °C, as shown in Figure 19. After 250 min, the conversion of salicylic acid (**1**) at 0.89 was measured. Therefore, the apparent heat of the reaction, which was calculated from the peak area, was about -177 kJ/mol salicylic (**1**) at 80 °C. The reaction is quite highly exothermic.

Figure 19 The reaction heat flow for the Benzoxazinone derivative (**8**) formation from salicylic acid (**1**) and salicylamide (**6**) using cyanuric chloride (**2**) as a chlorinating agent at 80 °C



CHAPTER V

THE KINETIC STUDY OF BENZOXAZINONE DERIVATIVE SYNTHESIS

5.1 The kinetic study of Benzoxazinone derivative synthesis

In this study, the concentration profiles during the synthesis of each condition in experiments 4.4 to 4.6 were used to evaluate the kinetic parameters. The route of Benzoxazinone derivative synthesis (Figure 17) was rearranged to write the chemical equation in the program.

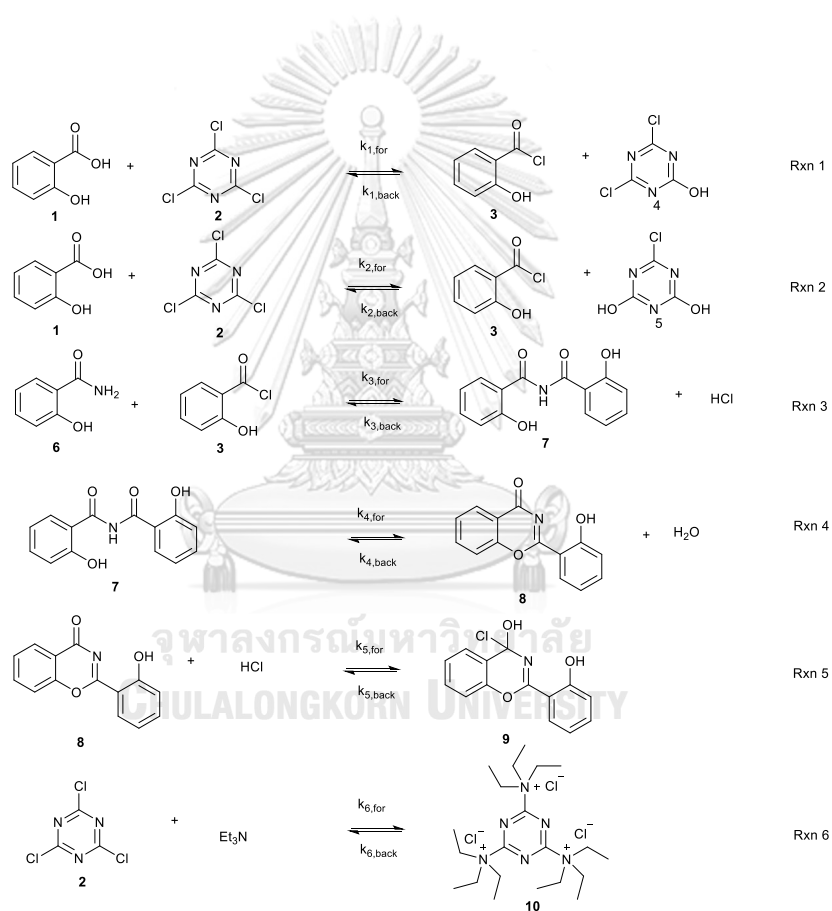


Figure 20 Chemical structures in kinetic study

The sets of chemical data, experimental data, and the optimization mode of operation were assigned to the program CERRES (Chemical Reaction and Reactor Engineering Simulations, <https://www.cerres.org>). The operation setting method was shown in Appendix 2. The optimization mode of the program was performed to calculate the kinetics constant from 7 experiments. Those parameters were shown in the Table below. For the kinetic constant, the direct constant (k_{forward} and k_{backward}) was chosen in order to fit the experimental data with model concentration using optimization mode. Moreover, R^2 value from linear regression of parity plot of salicylic acid, salicylamide, Benzoxazinone derivative and compound (9) between experimental yield/conversion and model yield/conversion were shown in each of 7 experiments.

Table 8 Summary of 7 conditions for kinetics modelling optimization

Entry	Salicylic acid:Salicylamide (equiv.)	Triethylamine (equiv.)	Temperature (°C)
1	1:0.75	1	110*
2	1:0.85	1	110*
3	1:1	1	110*
4	1:0.85	0.1	110*
5	1:0.85	2	110*
6	1:0.85	1	80**
7	1:0.85	1	100**

* Dropping triethylamine at 80 °C and heated up to refluxing toluene

** Dropping triethylamine at observed temperature

5.2 The results from the kinetic study

In this experiment, the outcome of kinetic constants was calculated using CERRES (Chemical Reaction and Reactor Engineering Simulations) invented by the National Institute of Chemistry - Kemijski inštitut. Slovenia.

From the definition of reaction rate;

$$R = k_{for} C_{reacg,1}^{order_{reacg,1}} C_{reacg,2}^{order_{reacg,2}} \dots - k_{back} C_{prod,1}^{order_{prod,1}} C_{prod,2}^{order_{prod,2}} \dots$$

Where k_{for} and k_{back} are the rate constants of the forward and backward reaction, $C_{reacg,i}$ and $C_{prod,i}$ are the concentrations of reagent,*i* and product,*i*, and $order_{reacg,i}$, and $order_{prod,i}$ are the orders for each species, which by default equals the stoichiometric amount of species *i* in the reaction. For the liquid phase species, *C* is concentrations (mol/L).

In this study, the assumption of an elementary reaction in the network reaction was proposed. The stoichiometric number of the species related to the order of concentration in the rate equation.

The experiments were conducted using sampling times of 5, 10, 15, 20, 30, 45, 60, 120, 180, 240, 300, 360, and 1,320 minutes. The fitting time in the program was used from 0 to 360 minutes in order to investigate the parameters in the scale-up process described in Chapter VI. The components of the reaction solution were analyzed using HPLC. The detectable components included salicylic acid, salicylamide, salicyloyl chloride, bis-salimide **7**, a benzoxazinone derivative **8**, compound **9**, and compound **10**.

The model conversion/yield and kinetic constants were calculated based on the experimental concentrations of four species: salicylic acid, benzoxazinone derivative **8**, compound **9**, and compound **10**. Salicylic acid and bis-salimide **7** formed solids in the reaction, so their concentrations as measured by HPLC were lower than the actual concentrations. In addition, salicyloyl chloride **3** was an

intermediate that immediately reacted with the substrate, so its concentration was also lower than the actual concentration.



5.2.1 the effect of starting materials concentration on kinetic parameter

In this study, the concentration of starting material (salicylamide) was changed from the 0.75, 0.85 and 1.0 mole ratio using the same ratio of 1:0.67:1 mole equivalent of salicylic acid, cyanuric chloride and triethylamine. The equilibrium constant depends on the reaction temperature. At entries 1-3, the reaction was conducted at a constant temperature at refluxing toluene. The equilibrium constant should have the same value for each reaction. (Parity plot and graphical results from fitting were shown in the appendix) From the equilibrium constant in Table 9, if k_{for}/k_{back} in each equation is more than 1,000, k_{back} in that equation could be neglected. In contrast, if k_{for}/k_{back} is less than 0.001, k_{for} in the equation could be neglected. Then, the k-value in Table 9 could not be neglected.

Table 9 The equilibrium constants using various ratios of salicylic acid: salicylamide from 1:0.75, 1:0.85, and 1:1 (conditions in Table 8 from entry 1-3)

Equation no.	Entry 1			Entry 2			Entry 3		
	k_{for}	k_{back}	k_{for}/k_{back}	k_{for}	k_{back}	k_{for}/k_{back}	k_{for}	k_{back}	k_{for}/k_{back}
1	1.57E+00	8.18E-01	1.923	2.41E+00	1.55E+00	1.555	1.15E+00	2.00E+00	0.571
2	8.58E-01	1.32E+00	0.653	7.49E-03	4.29E-03	1.745	1.87E-01	5.95E+00	0.031
3	4.16E-01	1.38E+00	0.301	7.19E-04	2.17E-04	3.311	9.76E-01	6.08E-01	1.606
4	2.26E+00	1.19E+00	1.901	2.33E+00	1.15E+00	2.017	5.15E-03	1.08E-03	4.787
5	1.42E+00	1.86E+00	0.761	9.00E-01	1.94E+00	0.464	6.41E-02	2.54E-01	0.253
6	2.33E-02	6.25E-01	0.037	2.61E-02	1.81E+00	0.014	8.81E-02	2.22E+00	0.040

From the results of experiments, the entry 3 provided the highest yield in the synthesis of Benzoxazinone derivative. The equilibrium constants from the optimization, the k -values were chosen to conduct because this condition provided the highest yield of benzoxazinone derivative. Therefore, a detailed explanation of each step was performed. In the first equation, the k -value represented the conversion of salicylic acid into an intermediate substance, salicyloyl chloride. The k_{for} and k_{back} are quite similar and the value of k -values in this step was more than the other steps. It means salicylic acid converts to salicyloyl chloride and rapidly reverses back to salicylic acid. Actually, salicylic acid almost converts in 5 minutes. Then, there should be the consumption of salicylic acid in another equation.

The reaction in equation 2 also represents the consumption of salicylic acid to form salicyloyl chloride. k_{back} is greater than k_{for} . This equation with k_{back} shows that salicyloyl chloride is likely to convert back to salicylic acid.

The reaction in equation 3 represents the consumption of salicyloyl chloride and salicylamide to form bis-salimide. k_{for} is greater than k_{back} . This equation with k_{for} shows that salicyloyl chloride and salicylamide are likely to form bis-salimide.

The reaction in equations 4 and 5 show the formation of benzoxazinone derivative and degradation into compound **9**, respectively. The magnitude of k_{for} in equation 4 is higher than k_{back} . But the k -value in this equation should be greater than this value in order to produce more of the desired product.

Finally, the last equation provides another by-product, tris-quaternary ammonium salt, from the reaction of triethylamine and cyanuric chloride. k_{for} is less than k_{back} . This equation seems to produce less tris-quaternary ammonium salt because k_{back} is quite larger than k_{for} .

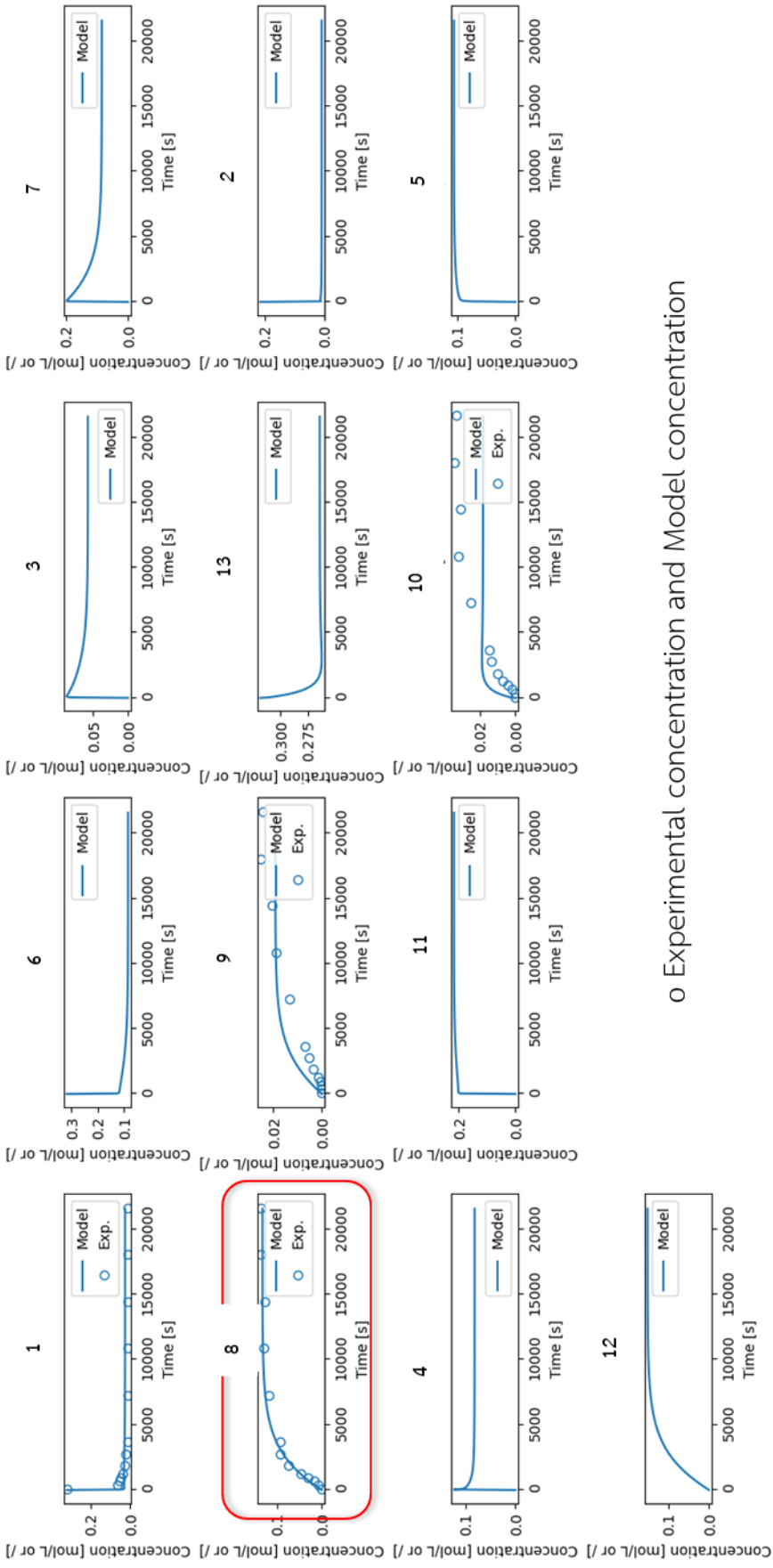
The results from the fitting are shown in Figure 22. The fitting of salicylic acid and benzoxazinone derivative from the experimental data and the model data revealed a good fit. For compound **9** and compound **10**, the fit was a little bit off from the experimental data because the adjusted parameters in the program were

specific to optimizing the benzoxazinone derivative, the main product, in order to achieve good optimization. The other components were the plot from the model concentration to predict the concentration of each component in the model.

To validate the results of model conversion/yield, the parity plot between the experimental data and computational data were plotted and shown in Figure 21. For starting material (salicylic acid), the experimental conversion (%) and model conversion (%) were plotted with 95% confidential interval band. For products (Benzoxazinone derivative or compound **(8)**, compound **(9)** and compound **(10)**, the experimental yield (%) and model yield (%) were plotted with 95% confidential interval band. The results showed that the parity plot of benzoxazinone derivative 8 was aligned with the diagonal line. The model calculation provided data that was comparable to the experimental data. Moreover, the r-square of the fitting, 0.9670, revealed the linearity of the model and experimental data. In addition, the results for salicylic acid showed that it was also on the diagonal line and had an r-square of 0.9864. Compounds 9 and 10 showed good linearity, with r-squares of 0.9851 and 0.9846, respectively, but they did not align with the diagonal line, which was in accordance with the fitting in Figure 22.

Table 10 Kinetic constant for salicylic acid:salicylamide ratio (1:1 equivalent), triethylamine (1 equivalent), and refluxing toluene (entry 3)

Equation no.	k_{for}	k_{back}
1	1.1454E+00	2.0047E+00
2	1.8703E-01	5.9475E+00
3	9.7630E-01	6.0809E-01
4	5.1550E-03	1.0770E-03
5	6.4147E-02	2.5377E-01
6	8.8097E-02	2.2158E+00



o Experimental concentration and Model concentration

Figure 21 The graphical results from fitting in entry 3

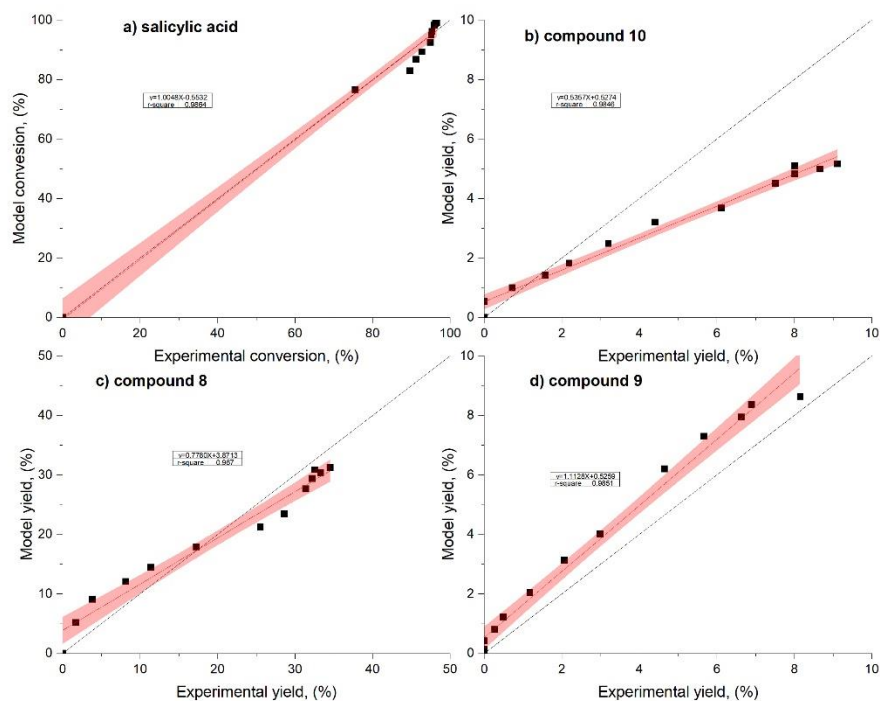


Figure 22 R^2 -value from fitted model conversion and experimental conversion (%) of salicylic acid, model yield experimental yield (%) of compound (8, 9 and 10) with 95% confidence band for salicylic acid:salicylamide:cyacuric chloride:triethylamine mole ratio of 1:1:0.67:1 at refluxing toluene.

5.2.2 the effect of triethylamine on kinetic parameter

In this study, the concentration of triethylamine was changed from the 0.1, 1.0 and 2.0 mole equivalent of salicylic acid using the same condition of 1:0.85:0.67 mole equivalent of salicylic acid, salicylamide, cyanuric chloride. In entries 4 and 5, the equilibrium constant affected the equation number 2. The k_{back} in the entry 4 and 5 were low, especially in entry 4. The equation number 2 in low triethylamine was dominated by k_{for} . (Parity plot and graphical results from fitting were shown in the appendix)

Table 11 The equilibrium constants using conditions in Table 8 from entries 2,4-5

Equation no.	Entry 2		Entry 4		Entry 5	
	k_{for}	k_{back}	k_{for}	k_{back}	k_{for}	k_{back}
1	2.41E+00	1.55E+00	5.65E-01	1.15E-01	3.30E-02	9.92E-01
2	7.49E-03	4.29E-03	4.14E-04	1.25E-08	3.60E+00	1.24E-02
3	7.19E-04	2.17E-04	1.63E-03	5.74E-01	2.61E-04	3.01E-01
4	2.33E+00	1.15E+00	3.52E+00	1.31E+00	2.43E-01	4.48E-03
5	9.00E-01	1.94E+00	3.46E+00	4.06E-01	1.80E-01	1.47E+00
6	2.61E-02	1.81E+00	5.41E-01	8.25E-01	7.33E-03	1.70E+00

k_{for}/k_{back}

0.033

289.389

0.001

54.216

0.122

0.004

5.2.3 the kinetics parameter from the effect of temperature the experiment entry 2,6-7

In this study, the effect of temperature on the equilibrium constant was studied. The experiments were conducted at the 1:1:0.67:1 mole equivalent of salicylic acid, salicylamide, cyanuric chloride and triethylamine. The temperature was changed from 80, 100, and 110 °C in entries 6, 7, and 2, respectively. (Parity plot and graphical results from fitting were shown in the appendix)

Table 12 The equilibrium constants using conditions in Table 8 from entries 2,6-7

Equation no.	Entry 6 (80 °C)			Entry 7 (100 °C)			Entry 2 (110 °C)		
	k_{for}	k_{back}	k_{for}/k_{back}	k_{for}	k_{back}	k_{for}/k_{back}	k_{for}	k_{back}	k_{for}/k_{back}
1	2.50E+00	1.51E+00	1.650	1.78E+00	2.10E+00	0.847	2.41E+00	1.55E+00	1.555
2	2.86E-02	1.26E+00	0.023	1.45E-02	1.08E-01	0.134	7.49E-03	4.29E-03	1.745
3	1.83E-04	6.51E-02	0.003	4.72E-01	1.39E+00	0.340	7.19E-04	2.17E-04	3.311
4	4.51E-02	2.37E-04	190.198	5.98E-03	2.11E-03	2.827	2.33E+00	1.15E+00	2.017
5	2.28E+00	1.82E+00	1.252	2.67E-01	1.35E+00	0.197	9.00E-01	1.94E+00	0.464
6	2.05E-02	2.80E+00	0.007	1.05E-01	3.57E+00	0.029	2.61E-02	1.81E+00	0.014

Moreover, the results showed that this chemical network in the synthesis of Benzoxazinone derivative using elemental reaction as a basis in 7 types of conditions was able to predict the amount of Benzoxazinone derivative according to the result of parity plot (in appendix), which experimental and computational data lined along with the diagonal line of the graph and R²-value represented the linearity in experiment 1, 2, 3, 5, 6, and 7. In experiment 4, the amount of triethylamine deviated from 1 equivalent of triethylamine, causing the concentration of experimental data changed due to pH of the reaction mixture. From the parity plot of experiment no. 4, it showed that in the condition of 0.1 mol equivalent of triethylamine, the regression value of salicylic acid, compounds **8**, **9**, and **10** deviated from the predicted model.

This model can predict the amount of Benzoxazinone derivative with specific conditions (in entries 1, 2, 3, 6, and 7). The change of triethylamine equivalent (0.1 mole equivalent) can deviate from the result.

5.3 The usage of kinetic parameters from optimization

The results from the optimization for kinetic parameters were the k-value (equilibrium constant) of the reaction. The usage of the k-value provided for k of the reaction. From Figure 20, the rate of the reaction could be written as:

$$\frac{d1}{dt} = -k_{1,for}[1][2] + k_{1,back}[3][4] + k_{2,for}[1][4] + k_{2,back}[3][5]$$

$$\frac{d2}{dt} = -k_{1,for}[1][2] + k_{1,back}[3][4] - k_{6,for}[2][13] + k_{6,back}[5]$$

$$\frac{d3}{dt} = k_{1,for}[1][2] + k_{1,back}[3][4] + k_{2,for}[1][4] - k_{2,back}[3][4] - k_{3,for}[3][6] + k_{4,back}[7][11]$$

$$\frac{d4}{dt} = -k_{1,for}[1][2] - k_{1,back}[3][4] - k_{2,for}[1][4] + k_{2,back}[3][5]$$

$$\frac{d4}{dt} = k_{2,for}[1][4] - k_{2,back}[3][5]$$

$$\frac{d6}{dt} = -k_{3,for}[3][6] + k_{3,back}[7][11]$$

$$\frac{d7}{dt} = k_{3,for}[3][7] - k_{3,back}[7][11] + k_{4,for}[7]$$

$$\frac{d8}{dt} = k_{4,for}[8] - k_{4,back}[8][11]$$

$$\frac{d9}{dt} = k_{5,for}[9][11] - k_{5,back}[12]$$

$$\frac{d10}{dt} = k_{6,for}[2][13]^3 + k_{6,back}[10]$$

$$\frac{d11}{dt} = k_{3,for}[3][6] - k_{3,back}[7][11] - k_{5,for}[8][11] + k_{5,back}[9]$$

$$\frac{d12}{dt} = k_{4,for}[7] - k_{4,back}[8][12]$$

$$\frac{d13}{dt} = -k_{6,for}[2][13]^3 + k_{6,back}[10]$$

whereas; 1=salicylic acid (1), 2=cyanuric chloride (2), 3=salicyloyl chloride (3), 4=2,6-dichloro-1,3,5-triazine (4), 5=2-monochloro-1,3,5-triazine (5), 6=salicylamide (6), 7=Bis-salimide (7), 8=Benzoxazinone derivative (8), 9=compound (9), 10=compound (10), 11=HCl, 12=H₂O and 13=triethylamine.

From the differential equations above, the chemicals in the solution will be predicted using the initial concentration of starting materials and solved by all equations simultaneously to provide the solution. The most important part of the k-value is to design the reactor (continuous stirred tank reactor or flow reactor) for scale-up.

The rate of reaction can be defined as

$$r_i = \frac{1}{v} \frac{dn_i}{dt} = \frac{dC_i}{dt}$$

i = specie in reaction

n_i = mole of specie i

C_i = concentration of specie i

Then,

$$r_1 = \frac{dC_1}{dt} = \frac{C_2 - C_1}{t_2 - t_1}$$

1 = salicylic acid

Table 13 The relations between conversion of salicylic acid and rate of disappear of salicylic acid in the experiment entry 3.

Time (s)	Conversion 1, (salicylic acid)	$-r_1$ ($\text{molL}^{-1}\text{min}^{-1}$)
0	0	0
5	0.80	0.0301254
10	0.83	0.0004446
15	0.84	0.0004992
20	0.88	0.0004059
30	0.91	0.0002304
45	0.94	0.0001664
60	0.96	0.0000384
120	0.96	0.0000049
180	0.96	0.0000006
240	0.96	0.0000024
300	0.96	0.0000017
360	0.97	0.0000020

The results between time and conversion were explained in the previous section. In addition, the rate of disappearance of salicylic acid ($-r_1$) rapidly decreased within five minutes, as observed in the conversion of salicylic acid in five minutes. From 10 minutes to one hour of the reaction, the rate of disappearance of salicylic acid appeared to gradually decrease. After two hours of reaction time, the rate of disappearance of salicylic acid was very low, indicating that the salicylic acid was almost fully reacted and converted to the products as shown in Table 12.

This relationship and design equation of the reactor provide a solution for the design of the reactor, for example, determining the time and volume required for the reactor.

CHAPTER VI

THE SCALE-UP OF BENZOXAZINONE DERIVATIVE SYNTHESIS

6.1 The Scale-up of Benzoxazinone derivative synthesis in a 1-L reactor

In this chapter, the synthesis conditions were chosen from section 4.5 at the ratio of 1:1, equivalent of salicylic acid and salicylamide using 1 equivalent of triethylamine, 0.67 equivalent of cyanuric chloride, and at refluxing toluene. The maximum yield of Benzoxazinone derivative from the round-bottom flask experiment was chosen in order to operate in a 1-L reactor for scaling up the experiment. The effect of mixing speed in a 1-L reactor was studied in order to provide the data for a 10-L reactor. The experiments were performed under the operating volume of a 1-L reactor, about 60% of the total volume of the reactor using 27.6 grams (0.2 mol) of salicylic acid. The duplicated experiments were performed and analyzed.

From a laboratory experiment in a round-bottom flask, the reaction time was set up to 22 hours. It was designed to observe yield increase with time. The results showed that the amount of yield of Benzoxazinone derivative slightly increased or seemed constant. It showed that after 6 to 22 hours (14 hours), yield of Benzoxazinone derivative increased by 8.8%.

For the scale-up process in a 1-10-L reactor, the reaction time was designed to operate in accordance with a 10-L reactor or 250-L reactor. Considering the operating cost (human, machine) in 14 hours (Almost 2 times the reaction time), the time required for reaction in a 1-10-L reactor was designed at 6 hours.

6.1.1 The effect of mixing speed on the %yield of Benzoxazinone derivative.

The yield of Benzoxazinone derivative profile in the 1-L reactor was performed using the mixing speed of 100, 200, 400, and 600 rpm. The comparison of yield of Benzoxazinone derivative between the mixing speed of 100, 200, 400, and 600 rpm and the round bottom flask was shown in Figure 21.

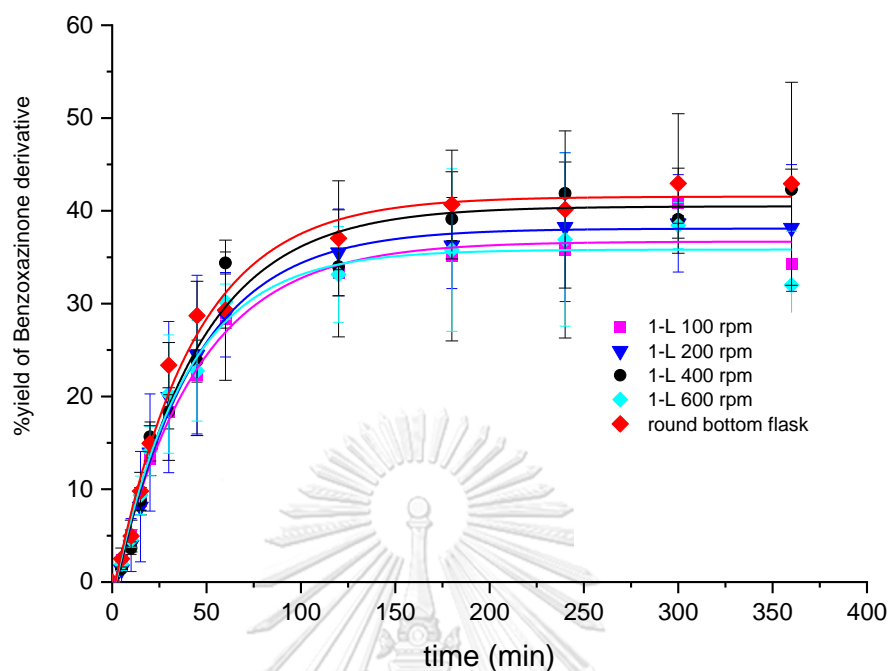


Figure 23 The effect of mixing speed on the %yield of Benzoxazinone derivative.

6.1.2 The result of the synthesis of Benzoxazinone derivative in a 1-L reactor

The results showed that yield of Benzoxazinone derivative in all experiments rapidly increased from 0 to 30 minutes, after that, slightly increased from 1 to 2 hours and seemed to be constant after 2 hours of the reaction until 6 hours. From the previous study, the laboratory scale synthesis in a round bottom flask provided the highest yield of Benzoxazinone derivative at the end of the experiment (6 hours) with 42.9 %yield. The experiments were studied from starting until 6 hours of the reaction time. Moreover, from data in chapter 4, the reaction of salicylic acid and salicylamide, the reactions of starting material were rapidly converted to salicyloyl chloride (**3**) and bis-salimide (**7**). The rate of reaction in 30 minutes was considered to be no effect on various mixing speeds. After that, at 40 minutes to 6 hours of the reaction, the effect of the mixing rate should be investigated.

The yield of Benzoxazinone derivative was more produced in ideal mixing of round bottom flask 40.3 %yield, in the experiment of 400 rpm, and 37.4 %yield at 200 rpm.

Considering the yield of Benzoxazinone derivative from 45 minutes – 6 hours of reaction time, the difference in %yield of Benzoxazinone derivative between laboratory scale (Tt) and 1-L reactor (Rt) was shown in Table 12.

Table 14 The difference in %yield of Benzoxazinone derivative between laboratory scale (round-bottom flask) and 1-L reactor

Operation	%Difference	%yield of Benzoxazinone derivative (8) at 6 hours
1-L reactor, 100 rpm	14.97	33.26±9.81
1-L reactor, 200 rpm	9.94	37.44±6.22
1-L reactor, 400 rpm	9.80	40.15±0.21
1-L reactor, 600 rpm	15.94	30.83±6.24

From the definition of %difference

$$\%Difference = \frac{100 \times \sum_{i=1}^n |Rt - Tt|}{\sum_{i=1}^n Rt}$$

Where,

Rt = %yield of Benzoxazinone derivative of Reference

Tt = %yield of Benzoxazinone derivative of Testing

N = number of sample point test

%difference is proportional to the average difference between the two profiles (Reference profile and test profile) calculated from the mean of the yield of Benzoxazinone derivative at each time point. The value of %difference is close to 1. It means the yield of Benzoxazinone derivative of the test sample is close to the

Reference. From Table 16, %difference in the interval time between 45 minutes – 6 hours provided the lowest %difference value.

The geometrical size of the reactor did not affect the chemical reaction. Apparently, in this experiment, the highest yield of Benzoxazinone derivative was yielded from the round bottom flask due to ideal mixing and good heat transfer rate. In addition, the surface area to volume ratio of the round bottom flask provided the highest order of magnitude than the jacket vessel reactor. As a result, the cooling, heating, and mixing in the round bottom flask was much higher than in the jacket vessel reactor, even in a 1-L reactor. For large-scale vessels, the effect of mixing and heat transfer rate were the pivotal parameters to study.

From the 1-L reactor experiment, the mixing speed of 400 rpm provided the highest yield among 100, 200, 400, and 600 rpm. Surprisingly, the mixing speed of 600 rpm yielded the lowest %yield of Benzoxazinone derivative due to the effect of higher vortex in the reactor at high mixing speed. The solvent volume in the 1-L reactor was used at the same volume in all four experiments. The volume level in the 1-L reactor with 600 rpm provides the highest level. This process induced the effect of a vortex. The higher the mixing speed, the more it caused an ineffective mixing in the vessel and took more extended mixing time than the vessel without vortex. Moreover, an excessive amount of air was dragged to the reaction mixture [80].

a) mixing speed at 100 rpm



Liquid level

b)

m

ixing speed at 400 rpm



Liquid level

c) mixing speed at 600 rpm



Liquid level

Figure 24 the liquid level in the benzoxazinone derivative in the 1-L reactor in the same quantity of materials a) at a mixing speed of 100 rpm, b) at a mixing speed of 400 rpm, c) at a mixing speed of 600 rpm with a high level of liquid vortex effect.

6.2 The Scale-up of Benzoxazinone derivative synthesis in a 10-L reactor

In this experiment, a 10-L reactor was performed to investigate the effect of mixing speed when the scale-up process was determined from a 1-L reactor to a 10-L reactor. The mixing speed is one of the key parameters to promote the mass transfer of reactants during the reaction. The well-mixed solution enhanced the molecule of chemical species to react and transform into the products. The mixing speed can be conducted using a variable motor speed. The optimum mixing speed was investigated in a 10-L reactor using the reaction parameters in the same condition of a 1-L reactor: 1:1 mole equivalent of salicylic acid and salicylamide (276.2 g, 2 mol) of salicylic acid: (274.2 g, 2 mol) of salicylamide), 1 mole equivalent of triethylamine (202.4 g, 2 mol), 1.34 mole equivalent of cyanuric chloride (239.2 g) and 6-L of Toluene at refluxing toluene condition. Duplicate experiments in the 10-L reactor were performed using the same sampling time of the 1-L reactor to generate yield of Benzoxazinone derivative profile.

The reaction time was set in accordance with the same time of the 1-L reactor at 6 hours to operate in a 10-L reactor.

6.2.1 The correlation between 1-L and 10-L reactor

To analyze the effect of mixing speed in a 10-L reactor, the parameters in a 10-L reactor should perform by the standard tank reactor, as shown in chapter II.

For the objective of scale-up “Equal stirrer tip speed”, the relation between standard tank reactor can be calculated from

$$N_2 = N_1 \left(\frac{D_1}{D_2} \right)^1$$

$$N_2 = 400 \text{ rpm} \left(\frac{0.05 \text{ m}}{0.12 \text{ m}} \right)^1 = 200 \text{ rpm}$$

N = stirred speed (rpm)

D = tank diameter (m)

$$D_1 = 0.06 \text{ m}, \quad D_2 = 0.12 \text{ m},$$

$$N_1 = 400 \text{ rpm}, \quad N_2 = 200 \text{ rpm},$$

For the objective of scale-up “Equal power per unit volume”, the relation between standard tank reactors can be calculated from

$$N_2 = N_1 \left(\frac{D_1}{D_2} \right)^{2/3}$$

$$N_2 = 400 \text{ rpm} \left(\frac{0.06 \text{ m}}{0.12 \text{ m}} \right)^{2/3} = 253 \text{ rpm}$$

N = stirred speed (rpm)

D = tank diameter (m)

$D_1 = 0.06 \text{ m}, \quad D_2 = 0.12 \text{ m},$

$N_1 = 400 \text{ rpm}, \quad N_2 \sim 250 \text{ rpm},$

Table 15 The relation of mixing speed between 1-L and 10-L in the standard reactor

No.	Objective	Stirred speed of 1-L reactor (rpm)	Stirred speed of 10-L reactor (rpm)	Empirical (n)
1.	Equal tip speed	400	200	1
2.	Equal power per unit volume	400	250	2/3
3.	Equal Reynold number	400	100	2
4.	Equal Froude number	400	280	1/2
5.	Equal mixing time	400	200	0
6.	Equal heat transfer coefficient per volume	400	400	-1
7.	Equal heat transfer coefficient	400	800	1/2

From **Table 3**, the stirred speed was calculated and shown in Table 13. The common objectives (equal tip speed and equal power per unit volume) were chosen from the list to conduct in a 10-L reactor. The synthesis procedure and sampling time were described in section 6.1. Additionally, the speed of 150 rpm in the 10-L reactor was conducted to compare the yield of Benzoxazinone derivative.

6.2.2 The result from the scale-up of Benzoxazinone derivative synthesis in a 10-L reactor

The yield of Benzoxazinone derivative profile was shown in Table 14. The yield of Benzoxazinone derivative in a 10-L reactor at 150, 200, and 250 rpm seem to be a similar pattern to the yield of Benzoxazinone derivative profile of the 1-L reactor. The yield of Benzoxazinone derivative rapidly increased within 30 minutes of the reaction. After that, it slightly increases from 1 – 2 hours. The yield of Benzoxazinone derivative profile after 2 hours seems to be constant production of Benzoxazinone derivative.

The yield of Benzoxazinone derivative at 6 hours of the reaction mixture in the 10-L reactor with the revolution speed of 200 rpm showed the highest yield ($43.18 \pm 2.78 \%$) in comparison with the yield of Benzoxazinone derivative of a 1-L reactor with the revolution speed of 400 rpm ($40.14 \pm 0.21\%$). Whereas the yield of Benzoxazinone derivative in a 10-L reactor with a revolution speed of 250 rpm provided the yield $40.85 \pm 4.62\%$. Meanwhile, the yield of Benzoxazinone derivative in a 10-L reactor with a revolution speed of 150 rpm provided the minimum yield ($37.39 \pm 0.93\%$) of all experiments. In this experiment, the curve of the yield of Benzoxazinone derivative was performed and plotted in Figure 23. The yield profiles of the 1-L reactor at 400 rpm and 10-L reactor at 200 rpm were similar to a 10-L reactor at 250 rpm.

The interval time for calculating the difference value was considered 45 minutes – 6 hours of the reaction time. At starting point until 30 minutes, the reactions were rapidly converted to the intermediate in the next step. Then, the

effect of mixing will be investigated after 45 minutes. Considering the difference value of Benzoxazinone derivative between the 1-L reactor and 10-L reactor in 45 minutes to 6 hours. The result showed that the 10-L reactor with 150 and 200 rpm provided the difference value in quite the same value. However, the yield of Benzoxazinone derivative in a 10-L reactor with 200 rpm provided a higher yield ($43.18 \pm 2.78 \%$) than in a 10-L reactor with 150 rpm ($37.39 \pm 0.93\%$). In this case, the difference value of Benzoxazinone derivative was calculated from the absolute value of R_t and T_t . This result implied that the higher yield of Benzoxazinone derivative (10-L reactor-200 rpm) would provide the same difference value calculated from the lower yield of Benzoxazinone derivative (10-L reactor with 150 rpm).

Moreover, the concentration of the major component at the end of the reaction was calculated and plotted in the concentration of salicylic acid, salicylamide, salicyloyl chloride, dis-salimide, and compound (7) of a 10-L reactor at 200 and 250 rpm in Figure 23. The results displayed that the Benzoxazinone derivative yielded the minimum concentration of compound (7) and unreacted starting materials when using the operation of a 10-L reactor with 200 rpm.

Table 16 The difference in yield of Benzoxazinone derivative between 1-L reactor 400 rpm (as a reference, R_t) and 10-L reactor (as Testing, T_t)

Operation	%Difference		%yield of Benzoxazinone derivative (8) at 6 hours
	400 rpm 1-L	Round bottom	
10-L reactor, 150 rpm	8.25	12.9	$37.39 \pm 0.93\%$
10-L reactor, 200 rpm	7.84	3.61	$43.18 \pm 2.78 \%$
10-L reactor, 250 rpm	8.56	8.12	$40.85 \pm 4.62 \%$

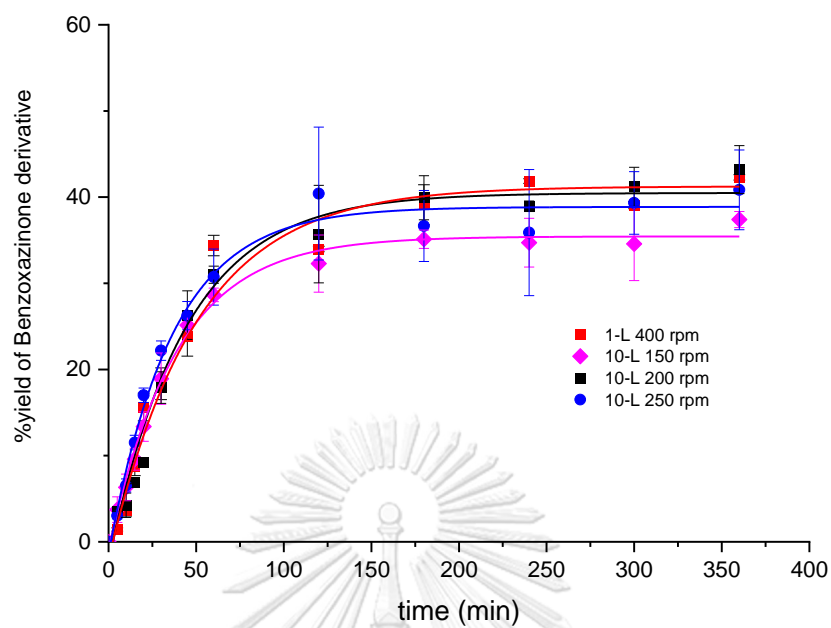


Figure 25 The comparison of %yield of Benzoxazinone derivative profile in a 10-L reactor with various speeds.

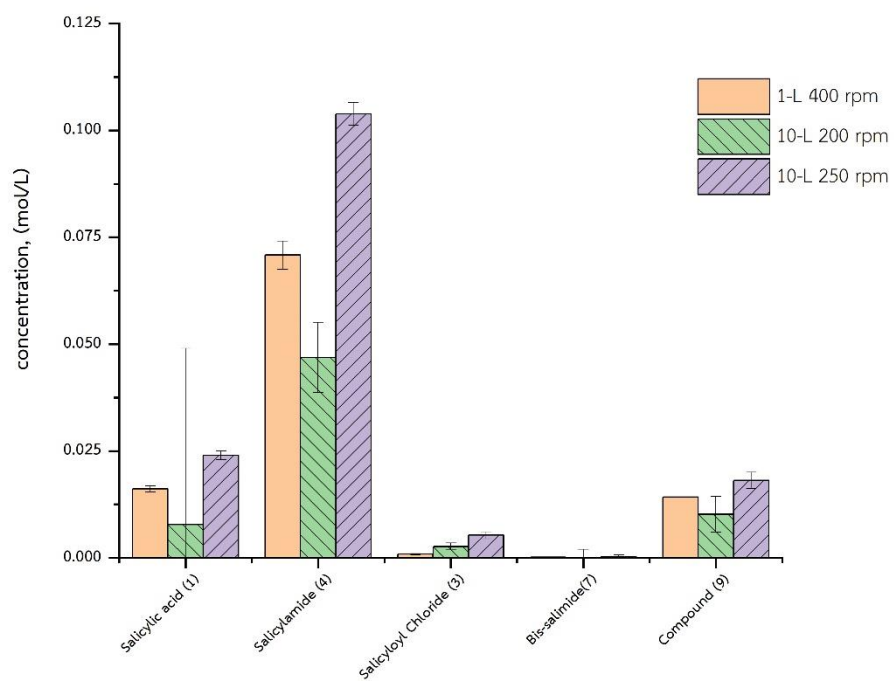


Figure 26 The components concentration of 1-L 400 rpm, 10-L 200, and 250 rpm at 6 hours of reaction time

In conclusion, it was proved that the objective of the scale-up was governed by equal tip speed. Therefore, the optimum parameters for a 10-L reactor were 1:1 equivalent of salicylic acid and salicylamide, 1 equivalent of triethylamine, 0.65 equivalent of cyanuric chloride, and refluxing toluene with a mixing speed of 200 rpm. It was found that the scale-up process involved using a constant tip speed, as the solid was formed in the reaction system. As a result, the same shear force would produce the same size of the solid. Consequently, the solid in the reaction mixture could dissolve and be transformed into the product in Figure 18.

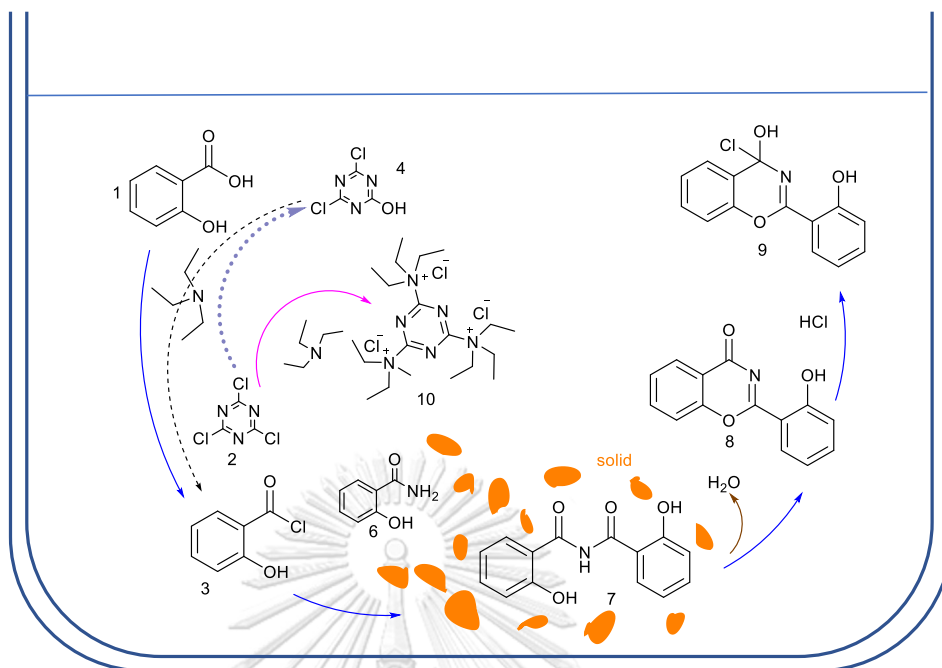


CHAPTER VII

CONCLUSION AND RECOMMENDATION

7.1 Conclusion

Benzoxazinone derivative was synthesized from a laboratory scale using a Dean-stark trap. The new compound was found during the synthesis due to the degradation of Benzoxazinone derivative in the presence of hydrochloric acid and confirmed the chemical structure *via* ^{12}C , ^1H NMR, HRMS, FT-IR, and boiling point. The route of Benzoxazinone derivative synthesis was postulated using identified compounds found in the high-performance liquid chromatography chromatogram. The reaction started with salicylic acid (1), cyanuric chloride (2) as a chlorinating agent, and triethylamine to immediately form salicyloyl chloride (3). Salicylamide (6), one of starting materials, rapidly reacted with salicyloyl chloride (3) to bis-salimide (7). The solid was found at the initial of the reaction, and it trapped the molecule of bis-salimide (7) and salicylamide (6). Dissolved bis-salimide (7) in the reaction mixture cyclized to form Benzoxazinone derivative (8). In the presence of hydrochloric acid, Benzoxazinone derivative converted to compound (9). Moreover, triethylamine reacted with cyanuric chloride to form compound 10.



Reaction picture of Benzoxazinone derivative synthesis

The synthesis parameters were investigated to yield the parameter for process scale-up. For the laboratory scale, the parameters were at the ratio of 1:1 mole equivalent ratio of salicylic acid:salicylamide, 1 mole equivalent of triethylamine, 0.67 mole equivalent of cyanuric chloride and refluxing toluene. Interestingly, higher triethylamine as a catalyst provided less compound (9) due to the basic condition. Moreover, the higher temperature in the synthesis yielded more compound (9).

The kinetic parameter was examined using CERRES (Chemical Reaction and Reactor Engineering Simulations) program. The equilibrium constant was chosen as the kinetic parameter. The model and experimental conversion and yield were plotted to validate the model. This model showed that Benzoxazinone derivative could be predictable in some conditions.

The study of process scale up was conducted using a 1-L reactor using the parameters in the laboratory scale. The mixing effect was investigated from 100, 200, 400, and 600 rpm. The results displayed that the mixing speed provided the

highest yield of Benzoxazinone derivative at 400 rpm. After the mixing speed at the 1-L reactor was investigated, the scale-up process of the 10-L reactor was performed using the geometrical similarity of the two reactors (1-L and 10-L reactor). The mixing speed of the 10-L reactor was postulated using the tip speed constant and power per volume constant. The experiment in the 10-L reactor was performed using 150, 200, and 250 rpm. The results showed that the objective of this scale-up process was tip speed constant. The mixing speed of 200 rpm in a 10-L reactor provided the highest yield of Benzoxazinone derivative in a 10-L reactor. Furthermore, the yield of Benzoxazinone derivative in the 10-L reactor was similar content in the 1-L reactor with 400 rpm and laboratory scale.

7.2 Recommendation

The scale-up process should perform in a pilot scale reactor, a 250-L reactor, using the same objective as the 10-L reactor and the geometrical similarity of 10-L and 250-L. The objective of equal tip speed was used to determine the speed of the 250-L reactor. Yield of Benzoxazinone derivative should be similar between 10-L and 250-L reactor. In addition, the components of reacted starting and compound (8) should be recorded and calculated in order to scale up in a larger reactor volume. Moreover, the heat of reaction in this reaction was highly exothermic. Therefore, the rate of triethylamine dropping into the reaction mixture should be considered to balance the heat removal of the cooling system.

REFERENCES

1. Zhang, K. and Z. Shang, *Chapter 5 - Polybenzoxazine: A smart polymer for novel environmental and catalytic applications*, in *Smart Polymer Catalysts and Tunable Catalysis*, S. Li, et al., Editors. 2019, Elsevier: Amsterdam. p. 95-114.
2. Wang, T., et al., *Synthesis of novel multi-functional fluorene-based benzoxazine resins: Polymerization behaviour, curing kinetics, and thermal properties*. *Reactive and Functional Polymers*, 2019. **143**: p. 104344.
3. Zhang, C.-X., et al., *Study on products and reaction paths for synthesis of 3,4-dihydro-2H-3-phenyl-1,3-benzoxazine from phenol, aniline and formaldehyde*. *Chinese Chemical Letters*, 2015. **26**(3): p. 348-352.
4. Huang, M.-Z., et al., *Synthesis and Herbicidal Activity of Isoindoline-1,3-dione Substituted Benzoxazinone Derivatives Containing a Carboxylic Ester Group*. *Journal of Agricultural and Food Chemistry*, 2009. **57**(20): p. 9585-9592.
5. Aibibuli, Z., et al., *Facile synthesis and herbicidal evaluation of 4H-3,1-benzoxazin-4-ones and 3H-quinazolin-4-ones with 2-phenoxyethyl substituents*. 2012(1420-3049 (Electronic)): p. 1420-3049 (Electronic).
6. M. Rashid, M.C., and A. Gupta *Benzoxazine: a biological study of benzoxazine and their derivatives*. *Heterocyclic Letters* 2018 **8**(2): p. 477-485.
7. Nadeem Siddiqui, R.A., M. Shamsheer Alam, Waquar Ahsan, *Pharmacological Profile of Benzoxazines: A Short Review*. *J. Chem. Pharm. Res.*, 2010. **2**(4): p. 309-316.
8. Rajitha, C., et al., *Synthesis and pharmacological evaluations of novel 2H-benzo[b][1,4]oxazin-3(4H)-one derivatives as a new class of anti-cancer agents*. *European Journal of Medicinal Chemistry*, 2011. **46**(10): p. 4887-4896.
9. El-Bordany, E.A. and R.S. Ali, *Synthesis of New Benzoxazinone, Quinazolinone, and Pyrazoloquinazolinone Derivatives and Evaluation of Their Cytotoxic Activity Against Human Breast Cancer Cells*. *Journal of Heterocyclic Chemistry*, 2018. **55**(5): p. 1223-1231.

10. Gao, B., et al., *Intramolecular functionalization of C(sp³)H bonds adjacent to an amide nitrogen atom: Metal-free synthesis of 2-hydroxy-benzoxazinone derivatives*. *Tetrahedron*, 2017. **73**(50): p. 7005-7010.
11. Torrens, A., et al., *Synthesis of New Benzoxazinone Derivatives as Neuropeptide Y5 Antagonists for the Treatment of Obesity*. *Journal of Medicinal Chemistry*, 2005. **48**(6): p. 2080-2092.
12. Yamada, Y., et al., *Cetilistat (ATL-962), a novel pancreatic lipase inhibitor, ameliorates body weight gain and improves lipid profiles in rats*. (0018-5043 (Print)).
13. Alper-Hayta, S., et al., *Synthesis, antimicrobial activity and QSARs of new benzoxazine-3-ones*. *European Journal of Medicinal Chemistry*, 2006. **41**(12): p. 1398-1404.
14. Lima, W.G., et al., *Synthesis and antimicrobial activity of some benzoxazinoids derivatives of 2-nitrophenol and 3-hydroxy-2-nitropyridine*. *Synthetic Communications*, 2019. **49**(2): p. 286-296.
15. Hsieh, P.-W., et al., *The evaluation of 2,8-disubstituted benzoxazinone derivatives as anti-inflammatory and anti-platelet aggregation agents*. *Bioorganic & Medicinal Chemistry Letters*, 2005. **15**(11): p. 2786-2789.
16. Madhavan, G.R., et al., *Dual PPAR-alpha and -gamma activators derived from novel benzoxazinone containing thiazolidinediones having antidiabetic and hypolipidemic potential*. (0968-0896 (Print)).
17. Da Prada M Fau - Kettler, R., et al., *Neurochemical effects in vitro and in vivo of the antidepressant Ro 11-1163, a specific and short-acting MAO-A inhibitor*. (0077-0094 (Print)).
18. Kowalski, P., et al., *The synthesis of cyclic and acyclic long-chain arylpiperazine derivatives of salicylamide as serotonin receptor ligands*. *Journal of Heterocyclic Chemistry*, 2008. **45**(1): p. 209-214.
19. El-Hashash, M.A., et al., *The Uses of 2-Ethoxy-(4H)-3,1-benzoxazin-4-one in the Synthesis of Some Quinazolinone Derivatives of Antimicrobial Activity*. (1424-8247 (Electronic)).
20. Jarussophon, S., P. Pongwan, and O. Srikun, *Benzoxazinone Intermediate for the*

- Synthesis of Deferasirox. Preparation of Deferasirox.* Organic Preparations and Procedures International, 2015. **47**(6): p. 483-489.
21. Sheth, S., *Iron chelation: an update.* Curr Opin Hematol, 2014. **21**(3): p. 179-85.
 22. Panich V, P.M., Sriroongrueng W., *The problem of thalassemia in Thailand.* Southeast Asian J Trop Med Public Health, 1992. **23**(Suppl 2): p. 1-6.
 23. Shang, X. and X. Xu, *Update in the genetics of thalassemia: What clinicians need to know.* Best Pract Res Clin Obstet Gynaecol, 2017. **39**: p. 3-15.
 24. Tanaka, C., *Clinical pharmacology of deferasirox.* Clin Pharmacokinet, 2014. **53**(8): p. 679-94.
 25. Porter, J.B. and C. Hershko, *Clinical Use of Iron Chelators, in Iron Physiology and Pathophysiology in Humans.* 2012. p. 591-627.
 26. Lindsey, W.T. and B.R. Olin, *Deferasirox for transfusion-related iron overload: a clinical review.* Clin Ther, 2007. **29**(10): p. 2154-66.
 27. Agarwal, M.B., *Deferasirox: Oral, once daily iron chelator — an expert opinion.* The Indian Journal of Pediatrics, 2010. **77**(2): p. 185-191.
 28. Freddy H. HAVALDAR, B.V.D., Ganesh Baban MULE, *Preparation of novel deferasirox analogues for antimalarial activity,* in WO2016203488A1. 2015.
 29. Tselepis, C., J.S. Fossey, and R. Byravan, *Iron complexing agent and uses thereof in the treatment and prevention of colorectal cancer,* in WO2015079244 A1 2015.
 30. Jiang, J., *Synthesis of Novel 2,4-Di(o-Hydroxyphenyl)-6-substituted Amino-1,3,5-triazine.* Asian Journal of Chemistry, 2015. **27**(5): p. 1959-1960.
 31. Kothakonda Kiran KUMARReddy, Gearu DAMODAR, and V.S. Pullela, *Process for the preparation of deferasirox,* in WO2014136062A2. 2014.
 32. Jayaraman Venkat Raman and H. Shah, *Process for the preparation of deferasirox.* WO2012069946A1, 2011.
 33. Karusala, N.R.e.a., *Crystalline form of 2-(2-hydroxy phenyl)benz[e][1,3]oxazin-4-one, process for the same and use for producing 4-(3,5-bis(2-hydroxyphenyl)-1h-1,2,4-triazol-1-yl)benzoic acid,* in WO2010023685A2. 2009.
 34. Rao, V.J., et al., *Synthesis and Characterization of Related Substances of Deferasirox, an Iron (Fe³⁺) Chelating Agent.* Synthetic Communications, 2012.

- 42(21): p. 3200-3210.
35. Miller, B., *Advanced Organic Chemistry: Reactions and Mechanisms*. 2004 Pearson Education.
 36. Howell, B.A., *Utility of kinetic analysis in the determination of reaction mechanism*. *Journal of Thermal Analysis and Calorimetry*, 2006. **85**(1): p. 165-167.
 37. Santacesaria, E., *Fundamental chemical kinetics: the first step to reaction modelling and reaction engineering*. *Catalysis Today*, 1999. **52**(2): p. 113-123.
 38. Joly, J.F., et al., *A Review of Kinetic Modeling Methodologies for Complex Processes*. *Oil & Gas Science and Technology – Revue d'IFP Energies nouvelles*, 2016. **71**(3).
 39. Westbrook, C.K., et al., *A comprehensive detailed chemical kinetic reaction mechanism for combustion of n-alkane hydrocarbons from n-octane to n-hexadecane*. *Combustion and Flame*, 2009. **156**(1): p. 181-199.
 40. Yan, B., et al., *Detailed kinetic modeling of acetylene decomposition/soot formation during quenching of coal pyrolysis in thermal plasma*. *Energy*, 2017. **121**: p. 10-20.
 41. Okoye, P.U., A.Z. Abdullah, and B.H. Hameed, *A review on recent developments and progress in the kinetics and deactivation of catalytic acetylation of glycerol—A byproduct of biodiesel*. *Renewable and Sustainable Energy Reviews*, 2017. **74**: p. 387-401.
 42. Grom, M., et al., *Modelling chemical kinetics of a complex reaction network of active pharmaceutical ingredient (API) synthesis with process optimization for benzazepine heterocyclic compound*. *Chemical Engineering Journal*, 2016. **283**: p. 703-716.
 43. Hill, C.G. and T.W. Root, *Basic Concepts in Chemical Kinetics: Molecular Interpretations of Kinetic Phenomena*, in *Introduction to Chemical Engineering Kinetics & Reactor Design*. 2014, John Wiley & sons p. 72-104.
 44. Gargurevich, I.A., *Foundations of Chemical Kinetic Modeling, Reaction Models and Reactor Scale-Up*. *Journal of Chemical Engineering & Process Technology*, 2016. **07**(02).

45. Wang, S. and H. Hofmann, *Strategies and methods for the investigation of chemical reaction kinetics*. Chemical Engineering Science, 1999. **54**(11): p. 1639-1647.
46. Fan, L.T., B. Bertók, and F. Friedler, *A graph-theoretic method to identify candidate mechanisms for deriving the rate law of a catalytic reaction*. Computers & Chemistry, 2002. **26**(3): p. 265-292.
47. Szalkai, I., *A new general algorithmic method in reaction syntheses using linear algebra*. Journal of Mathematical Chemistry, 2000. **28**(1): p. 1-34.
48. Bently, T.W., *Investigation Of Reaction Mechanisms By Product Studies*. The Investigation of Organic Reactions and Their Mechanisms. 2006: Blackwell Publishing Ltd. 18-45.
49. Vertis, C.S., N.M.C. Oliveira, and F.P.M. Bernardo, *Systematic Development of Kinetic Models for Systems Described by Linear Reaction Schemes*, in *12th International Symposium on Process Systems Engineering and 25th European Symposium on Computer Aided Process Engineering*. 2015. p. 647-652.
50. Blackmond, D.G., *Reaction Progress Kinetic Analysis: A Powerful Methodology for Mechanistic Studies of Complex Catalytic Reactions*. Angewandte Chemie International Edition, 2005. **44**(28): p. 4302-4320.
51. Fishtik, I., A. Alexander, and R. Datta, *Enumeration and discrimination of mechanisms in heterogeneous catalysis based on response reactions and unity bond index–quadratic exponential potential (UBI–QEP) method*. Surface Science, 1999. **430**(1): p. 1-17.
52. Toch, K., J.W. Thybaut, and G.B. Marin, *A systematic methodology for kinetic modeling of chemical reactions applied to n-hexane hydroisomerization*. AIChE Journal, 2015. **61**(3): p. 880-892.
53. Tirronen, E. and T. Salmi, *Process development in the fine chemical industry*. Chemical Engineering Journal, 2003. **91**(2): p. 103-114.
54. Seo, H., et al., *Graph-theoretical identification of pathways for biochemical reactions*. Biotechnology Letters, 2001. **23**(19): p. 1551-1557.
55. Flores-Sánchez, A., A. Flores-Tlacuahuac, and L.L. Pedraza-Segura, *Model-Based Experimental Design to Estimate Kinetic Parameters of the Enzymatic Hydrolysis*

- of Lignocellulose*. Industrial & Engineering Chemistry Research, 2013. **52**(13): p. 4834-4850.
56. Grénman, H., et al., *Modelling the Kinetics of a Reaction Involving a Sodium Salt of 1,2,4-Triazole and a Complex Substituted Aliphatic Halide*. Organic Process Research & Development, 2003. **7**(6): p. 942-950.
57. Jin, X., et al., *Kinetic modeling of carboxylation of propylene oxide to propylene carbonate using ion-exchange resin catalyst in a semi-batch slurry reactor*. Chemical Engineering Science, 2017. **168**: p. 189-203.
58. Blackmond, D.G., *Reaction progress kinetic analysis: a powerful methodology for mechanistic studies of complex catalytic reactions*. Angew Chem Int Ed Engl, 2005. **44**(28): p. 4302-20.
59. Susnow, R.G., et al., *Rate-Based Construction of Kinetic Models for Complex Systems*. The Journal of Physical Chemistry A, 1997. **101**(20): p. 3731-3740.
60. Goldsmith, C.F. and R.H. West, *Automatic Generation of Microkinetic Mechanisms for Heterogeneous Catalysis*. The Journal of Physical Chemistry C, 2017. **121**(18): p. 9970-9981.
61. Katare, S., et al., *An Intelligent System for Reaction Kinetic Modeling and Catalyst Design*. Industrial & Engineering Chemistry Research, 2004. **43**(14): p. 3484-3512.
62. Singh, U.K., et al., *REACTION KINETICS AND CHARACTERIZATION*. Chemical Engineering in the Pharmaceutical Industry, 2019: p. 151-190.
63. Fogler, H.S., *Collection and analysis of rate data, in Elements of Chemical Reaction*. 1992, Prentice Hall. p. 190-240.
64. Goršek, D.P.a.A., *Kinetic Parameters Determination Using Reaction Calorimetry: Study of Sodium Benzoate Synthesis*. J. Chem. Chem. Eng., 2011. **5**: p. 89-94.
65. e Silva, C.F.P.M. and J.F.C. da Silva, *Evaluation of Kinetic Parameters from the Synthesis of Triaryl Phosphates Using Reaction Calorimetry*. Organic Process Research & Development, 2002. **6**(6): p. 829-832.
66. Zogg, A., et al., *Isothermal reaction calorimetry as a tool for kinetic analysis*. Thermochimica Acta, 2004. **419**(1): p. 1-17.
67. Crevatin, A., et al., *Kinetic Investigations of a Ketonization Reaction Using*

- Reaction Calorimetry*. Industrial & Engineering Chemistry Research, 1999. **38**(12): p. 4629-4633.
68. Kartnaller, V., et al., *Evaluating the kinetics of the esterification of oleic acid with homo and heterogeneous catalysts using in-line real-time infrared spectroscopy and partial least squares calibration*. Journal of Molecular Catalysis B: Enzymatic, 2016. **123**: p. 41-46.
69. Ehly, M., et al., *Scale-up of batch kinetic models*. Anal Chim Acta, 2007. **595**(1-2): p. 80-8.
70. Saeki, Y. and T. Emura, *Technical progresses for PVC production*. Progress in Polymer Science, 2002. **27**(10): p. 2055-2131.
71. Monsalve-Bravo, G.M., H.M. Moscoso-Vasquez, and H. Alvarez, *Scaleup of Batch Reactors Using Phenomenological-Based Models*. Industrial & Engineering Chemistry Research, 2014. **53**(22): p. 9439-9453.
72. Hugh Stitt, H.Simmons, and M.J.H., *Scale-Up of Chemical Reactions*, in *Process Understanding: For Scale-Up and Manufacture of Active Ingredients*, I. Houson, Editor. 2011, Wiley-VCH Verlag GmbH & Co. p. 115-197.
73. Hemrajani, R.R. and G.B. Tatterson, *Mechanically stirred vessels*, in *Handbook of Industrial Mixing: Science and Practice*. 2004: John Wiley&Sons, Inc.
74. Hannon, J., *Characterization and First Principles Prediction of API Reaction Systems*, in *Chemical Engineering In the pharmaceutical Industry: R&D to Manufacturing*, D.J.A. Ende, Editor. 2011, John Wiley & sons p. 113.
75. Atherton, J., I. Houson, and M. Talford, *Understanding the reaction*, in *Process Understanding: For Scale-Up and Manufacture of Active Ingredients*, I. Houson, Editor. 2011, WILEY-VCH Verlag & Co. KGaA. p. 87-125.
76. Bourne, J.R., *Mixing and the Selectivity of Chemical Reactions*. Organic Process Research & Development, 2003. **7**(4): p. 471-508.
77. Keng, P.S., et al., *Scale-up synthesis of lipase-catalyzed palm esters in stirred-tank reactor*. Bioresource Technology, 2008. **99**(14): p. 6097-6104.
78. Imamoglu, E. and F.V. Sukan, *Scale-up and kinetic modeling for bioethanol production*. Bioresource Technology, 2013. **144**: p. 311-320.
79. Gholap, S. and N. Gunjal, *2,4,6-Trichloro-1,3,5-triazine (TCT) mediated one pot*

direct synthesis of N-benzoylthioureas from carboxylic acids. Arabian Journal of Chemistry, 2017. **10**: p. S2750-S2753.

80. Munshi, D.R.A.K.B., *Numerical Study of Vortex Formation inside a Stirred Tank.* International Scholarly and Scientific Research & Innovation 2014. **8(12)**



Appendix

1 HPLC calculation

1.1 concentration calculation

The components concentration in the solution can be determined using the High-performance liquid chromatography (HPLC) to evaluate the signal compared to the standard. The equation is shown below.

$$C_i = \frac{A_{sam} - b}{a} \times \frac{\text{dilution factor}}{\text{response factor}} \times \frac{1}{MW}$$

Whereas

C_i = Concentration of component i

A_{sam} = Area of component i from HPLC

a,b from the standard calibration curve with a linear plot

$Y = aX + b$

MW = Molecular weight of component i

1.2 %conversion of salicylic acid/salicylamide calculation

$$\%conversion\ of\ X_i = \frac{\text{Initial Concentration of i} - \text{Concentration of i (mol/l)} \times 100}{\text{mole of salicylic acid at starting}}$$

1.3 %yield of Benzoxazinone derivative/compound (7) calculation

$$\%yield\ of\ y_j = \frac{\text{Concentration of j (mol/l)}}{\text{Initial Concentration salicylic acid (mol/l)}}$$

Table 17 Molecular weight of selected components

Component name	Chemical structure	Molecular Weight
Salicylic acid (1)	$C_7H_6O_3$	138.12
Salicylamide (6)	$C_7H_7NO_2$	137.14
Salicyloyl chloride (3)	$C_7H_5ClO_2$	156.56
Bis-salimide (7)	$C_{14}H_{11}NO_4$	257.24
Benzoxazinone derivative (8)	$C_{14}H_9NO_3$	239.23
Compound (10)	$C_{21}H_{45}N_6Cl_3$	487.89

The example of calculation of Benzoxazinone derivative in the experiment “4.5.1 The effect of the ratio of salicylic acid and salicylamide with 1:0.85 salicylic acid : salicylamide ratio”.

Table 18 the concentration and area of Benzoxazinone derivative working standard for the calibration curve.

Entry	Concentration (mg/ml)	Area
1	0.00020356	1.9573
2	0.00203557	24.3120
3	0.00814227	95.2923
4	0.02035568	237.6562
5	0.50889200	5860.7373

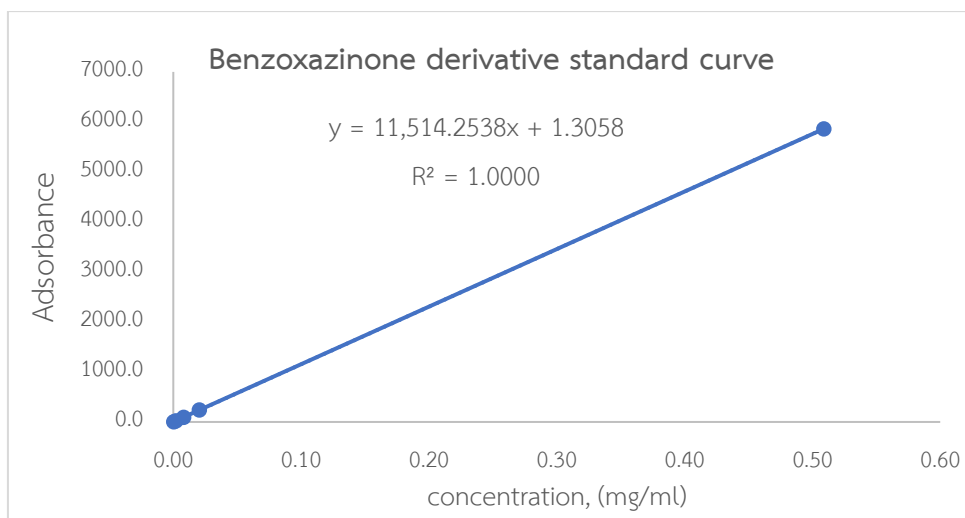


Figure 27 Calibration curve of Benzoxazinone derivative in the experiment of “The effect of the ratio of salicylic acid and salicylamide with 1:0.85 salicylic acid : salicylamide ratio”

Calculation of Benzoxazinone derivative at 10 minutes

- The triplicate sample was performed in this section.
- Three samples at 10 minutes from 3 experiments were examined using HPLC.
- The initial weight of salicylic acid was 13.8 g (0.1mol)

From

$$C_i = \frac{A_{sam} - b}{a} \times \frac{\text{dilution factor}}{\text{response factor}} \times \frac{1}{MW}$$

$$Weight_{sam} = \frac{24.1811 - 1.3058}{11,514.2538} = \frac{314000}{1} = 0.6238 \text{ g}$$

$$Conc_{.sam} = \frac{weight_{sam}}{MW \times vol.} = \frac{0.92 \text{ g}}{239.23 \left(\frac{\text{g}}{\text{mol}}\right) \times 0.314 \text{ L}} = 0.0123 \text{ mol/L}$$

$$\% \text{yield of Benzoxazinone derivative} = \frac{0.0123 \text{ mol/L} \times 0.314 \times 100}{0.1 \text{ mol}} = 3.86 \%$$

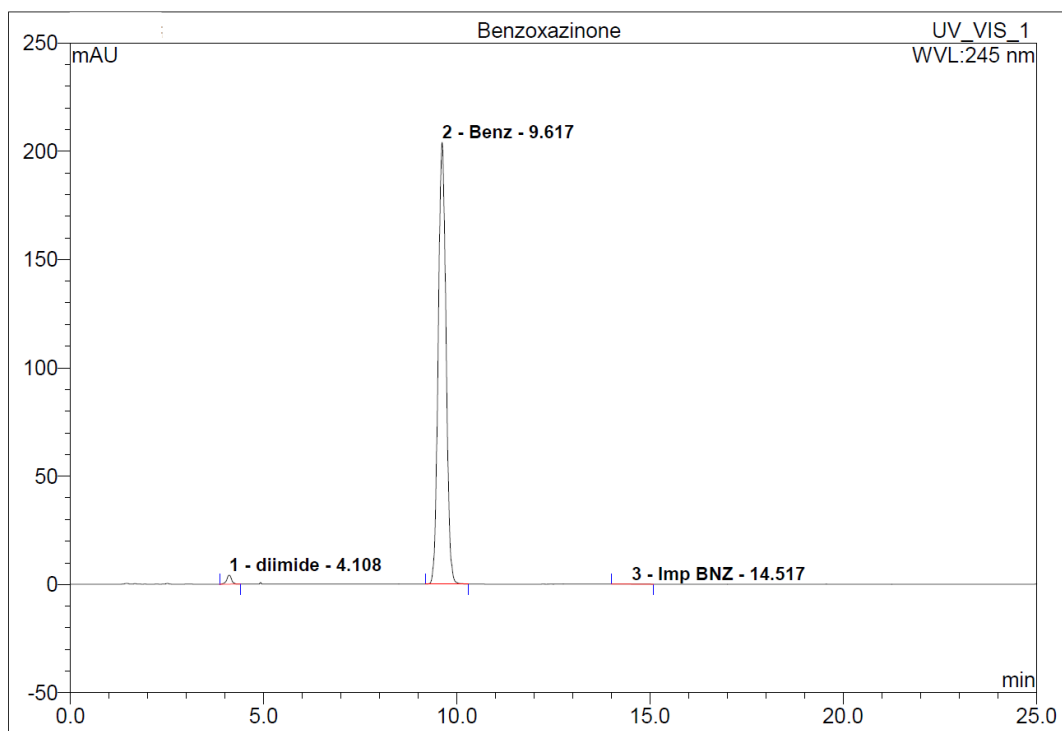
Table 19 The example calculation of Benzoxazinone derivative in the section “The effect of the ratio of salicylic acid and salicylamide with 1:0.85 salicylic acid : salicylamide ratio”

reaction time (min)	Sam. No. (min)	area sam.	Conc. Sam.	dilution (10 ³ 300*1000/10)	benzoxazinone (g) (RF=1)	benzoxazinone (g)	SD	Benzoxazinone (mol/L)	SD
0	0-1	0.0000	0.000000	314000	0.00	0.00	0.00	0.0000	0.0000
	0-2	0.0000	0.000000	314000	0.00				
	0-3	0.0000	0.000000	314000	0.00				
5	5-1	10.5073	0.000799	314000	0.25	0.40	0.13	0.0054	0.0018
	5-2	18.8492	0.001524	314000	0.48				
	5-3	18.9369	0.001531	314000	0.48				
10	10-1	24.18115	0.001987	314000	0.62	0.92	0.26	0.0123	0.0034
	10-2	40.73269	0.003424	314000	1.08				
	10-3	40.25478	0.003383	314000	1.06				
15	15-1	59.72465	0.005074	314000	1.59	1.95	0.31	0.0259	0.0041
	15-2	79.71481	0.006810	314000	2.14				
	15-3	78.56536	0.006710	314000	2.11				
20	20-1	76.23747	0.006508	314000	2.04	2.72	0.59	0.0363	0.0078
	20-2	113.2534	0.009723	314000	3.05				
	20-3	113.99821	0.009787	314000	3.07				
30	30-1	117.80282	0.010118	314000	3.18	4.13	0.82	0.0549	0.0110
	30-2	171.58989	0.014789	314000	4.64				
	30-3	168.59116	0.014529	314000	4.56				
45	45-1	192.24969	0.016583	314000	5.21	6.10	1.03	0.0813	0.0137
	45-2	216.7981	0.018715	314000	5.88				
	45-3	266.34573	0.023018	314000	7.23				
60	62-1	241.89915	0.020895	314000	6.56	6.84	0.34	0.0911	0.0046
	60-2	248.52264	0.021471	314000	6.74				
	60-3	266.34573	0.023018	314000	7.23				

1.4 The purity of Benzoxazinone derivative using the parameters in entry 3

The mole ratios of salicylic acid (1), cyanuric chloride (2), salicylamide (6), and triethylamine at 1:0.67:1:1 with 110 °C (Reflux) was conducted in laboratory scale.

After the reaction was complete, the reaction mixture was cooled down to 80 °C and filtrated to remove the solid. The solvent was removed under reduced pressure. After that the ethanol was poured into the flask containing yellow solid and cooled down to 0 °C. after that the mixture was filtrated. The solid was dry in vacuum oven at 60 °C for 5 hours. The analysis was conducted using HPLC and the results showed the purity (area %) was more than 98.64%.



No.	Ret.Time min	Peak Name	Height mAU	Area mAU*min	Rel.Area %	Amount	Type
1	4.11	diimide	4.139	0.602	1.25	n.a.	BMB
2	9.62	Benz	204.007	47.644	98.64	n.a.	BMB
3	14.52	Imp BNZ	0.097	0.054	0.11	n.a.	BMB
Total:			208.242	48.300	100.00	0.000	

Figure 28 The HPLC chromatogram show the peak of Benzoxazinone derivative

2 kinetic parameters experiment

2.1 program for kinetic study

Fitting parameters in this experiment were calculated using CERRES (Chemical Reaction and Reactor Engineering Simulations). The program was designed for the simulation of various types of chemical reactors under different operating conditions with user-supplied chemistry, allowing for complex bulk and surface reaction (micro) kinetics. In addition, the operation mode in the program consists of the operation, such as the comparison of the model results to experimentally measured values and reaction rate parameter optimization (fitting). Dr. Damjan Lašič Jurković, the programmer, provided this program in order to compute with efficiency,

ease of use, and wide functionality. He worked at the Department of Catalysis and Chemical Reaction Engineering at the National Institute of Chemistry in Ljubljana, Slovenia.

The main advantage of this program

1. Efficient computation

This software prioritizes efficient computation, enabling rapid simulations of even large systems with demanding numerical characteristics. It accomplishes this through a robust C-language backend featuring advanced BDF solvers, multi-threading, the automatic creation of Jacobian matrices for differential equations, and the compilation of essential code segments.

2. Relevant examples from literature

In this program, the multiple relevant examples from literature references can be used as a baseline for other models.

3. Model-experiment compare, parameter optimization, sensitivity analysis

In addition to plain reactor simulations, this software includes several other modes of operation. User can use it to compare model results to experimental data and perform parameter optimization to enhance the model's predictive accuracy. It also allows user to conduct sensitivity analysis to determine the most influential reactions in the model network

4. Complex user-defined chemistry

This program features highly customizable chemical reaction systems, allowing user to create complex networks involving hundreds of surface and bulk reactions between various species. Additionally, user can provide user-defined reaction rate expressions for each of the reactions.

The functional window of the program was shown in Figure 26. The users should prepare the 3 sets of data.

1. Experimental data in Figure 27
2. Chemistry data in Figure 28
3. Operation mode in Figure 29

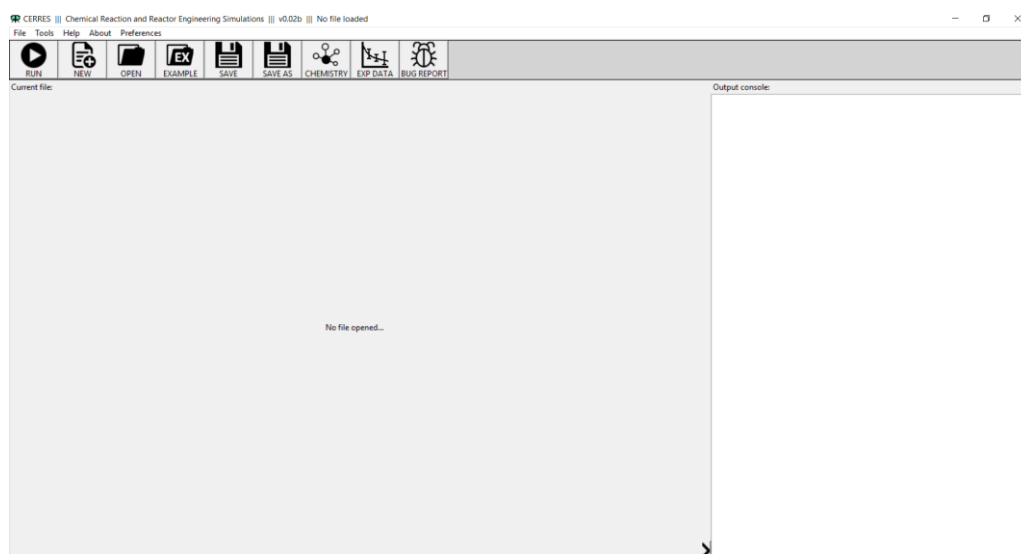


Figure 29 The first page of CERRES (Chemical Reaction and Reactor Engineering Simulations).

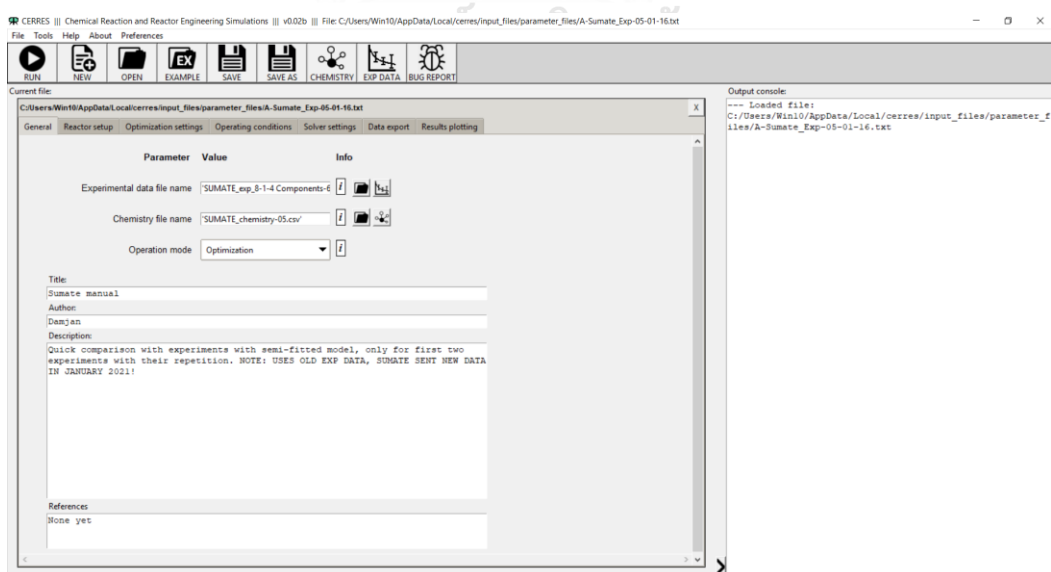


Figure 30 The 3 parameters of Experimental data, Chemistry data, and mode of Operation.

In chemistry data, the rate of the reaction was assigned as defined below

$$R = k_{for} C_{reacg,1}^{order_{reacg,1}} C_{reacg,2}^{order_{reacg,2}} \dots - k_{back} C_{prod,1}^{order_{prod,1}} C_{prod,2}^{order_{prod,2}} \dots$$

Where k_{for} and k_{back} are the rate constants of the forward and backward reaction, $C_{reag,i}$ and $C_{prod,i}$ are the concentrations of reagent, i and product, i , and $order_{reacg,i}$, and $order_{prod,i}$ are the orders for each species, which by default equals the stoichiometric amount of species i in the reaction. For the liquid phase species, the C is concentrations (mol/L).

The screenshot shows the CHESS Chemistry Editor interface. The top menu bar includes File, Edit, View, and Help. Below the menu bar, there are icons for New, Open, Example, Save, Save As, File Info, and Check. The main window is divided into several sections:

- Species lists:** Contains sections for Gas species, Liquid species, Adsorbed/surface species, Catalyst sites, and User defined variables. The Liquid species section is expanded, showing a list of species: SAcid, SAamide, SChlor, BisSAamide, BProd, BImp, TEA, CyCl, CyClOH, HCl, CyEt, CyClOEt, and H2O.
- List of reactions and constants:** A table with columns for #, Reagents, Products, k forward, k backward, Reversible y/n, User defined rate y/n, and User defined rate expression. The table contains six reactions:

#	Reagents	Products	k forward	k backward	Reversible y/n	User defined rate y/n	User defined rate expression
1	SAcid-CyCl-TEA	SChlor-CyClOH+	2.678530e-02	0.000000e+00	<input checked="" type="checkbox"/>	<input type="checkbox"/>	
2	SAcid-CyClOH+	SChlor+TEA+CyCl	6.552880e-02	0.000000e+00	<input checked="" type="checkbox"/>	<input type="checkbox"/>	
3	SChlor + SAamide	BisSAamide + HCl	1.000000e+00	2.000000e+00	<input checked="" type="checkbox"/>	<input type="checkbox"/>	
4	BisSAamide	BProd+H2O	3.000000e-03	4.000000e-05	<input checked="" type="checkbox"/>	<input type="checkbox"/>	
5	BProd+HCl	BImp	1.000000e-04	5.000000e-05	<input checked="" type="checkbox"/>	<input type="checkbox"/>	
6	TEA+CyCl	CyEt	1.000000e+03	1.600000e+01	<input checked="" type="checkbox"/>	<input type="checkbox"/>	

Figure 31 Chemical species in the synthesis.

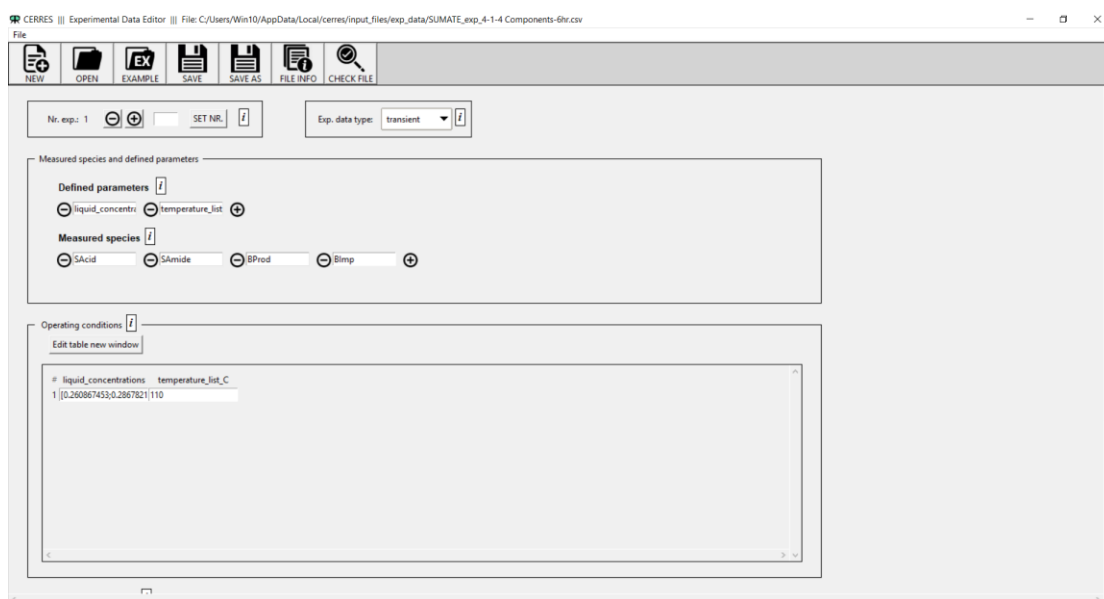


Figure 32 The experimental data set.

The example of fitted calculation in “The effect of the ratio of salicylic acid and salicylamide with 1:0.85 salicylic acid : salicylamide ratio” was shown in Table 18 using 6 hours of the synthesis process.

Four sets of chemical species were assigned to perform process optimization. The concentration of salicylic, Benzoxazinone derivative (compound **8**), and compound **9**, **10** were calculated from the experiment using HPLC to monitor the reaction progression. Model concentration was the concentration (mol/L) calculated from the optimization of fitted kinetic constant using CERRES (Chemical Reaction and Reactor Engineering Simulations). After that, conversion and yield (%) were calculated and plotted in a parity plot.

Table 20 The example for conversion/yield (%) of 4 species in the experiment and model calculation from program optimization in entry 2.

Experimental data				Computational data			
conversion, (%)	yield, (%)	yield, (%)	yield, (%)	conversion, (%)	yield, (%)	yield, (%)	yield, (%)
salicylic acid	compound 10	compound 8	compound 9	salicylic acid	compound 10	compound 8	compound 9
0.00	0.00	0.00	0.00	0.00	0.00	0.00	0.00
75.52	0.00	1.69	0.00	67.83	39.99	1.32	0.00
89.56	0.72	3.86	0.00	89.43	54.78	4.12	0.02
91.17	1.57	8.13	0.26	96.39	59.74	7.21	0.06
92.66	2.19	11.38	0.49	98.75	61.46	10.21	0.13
94.89	3.20	17.25	1.17	99.85	62.27	15.59	0.35
95.13	4.41	25.51	2.07	99.99	62.38	22.02	0.80
95.29	6.12	28.61	2.99	100.00	62.38	26.82	1.38
95.93	7.51	31.36	4.65	100.00	62.38	36.06	4.11
96.23	8.01	32.20	5.67	100.00	62.38	37.84	6.73
96.33	8.66	33.28	6.63	100.00	62.38	37.34	8.87
96.49	8.01	32.52	6.89	100.00	62.38	36.30	10.53
96.54	9.11	34.51	8.15	100.00	62.38	35.29	11.79

2.2 The results from program optimization

Table 21 Kinetic constant for salicylic acid:salicylamide ratio (1:0.75 equivalent), triethylamine (1 equivalent), and refluxing toluene (entry 1)

Equation no.	k_{for}	k_{back}
1	1.5727E+00	8.1789E-01
2	8.5813E-01	1.3151E+00
3	4.1639E-04	1.3821E+00
4	2.2648E+00	1.1916E-03
5	1.4194E+00	1.8643E+00
6	2.3282E-02	6.2524E-01

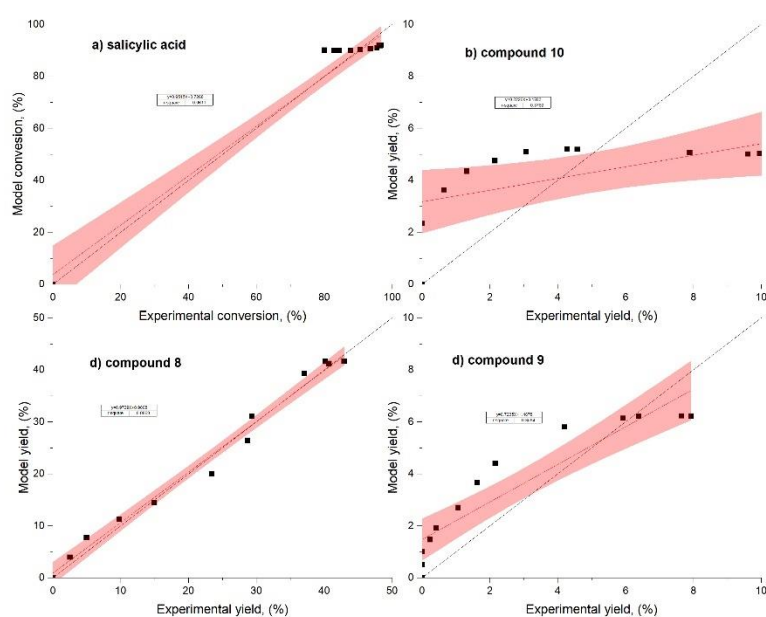


Figure 33 R^2 -value from fitted model conversion and experimental conversion (%) of salicylic acid, model yield experimental yield (%) of compound (8, 9 and 10) with 95% confidential band for salicylic acid:salicylamide ratio (1:0.75 equivalent), triethylamine (1 equivalent), and refluxing toluene.

The abbreviation in graphical results from model and experiment fitting

Abbreviation

SAcid : salicylic acid
 SAmid : salicylamide
 Schlor : salicyloyl chloride
 BisSAmide : Bis-salimide
 BProd : Benzoxazinone
 derivative, compound
 (8)
 Bimp : compound (9)
 TEA : triethylamine

Abbreviation

CyCl : cyanuric chloride
 CyClOH : Compound (4),
 HCl : Hydrochloric acid
 CyEt : compound (10),
 CyClOH2 : compound (5)
 H2O : water

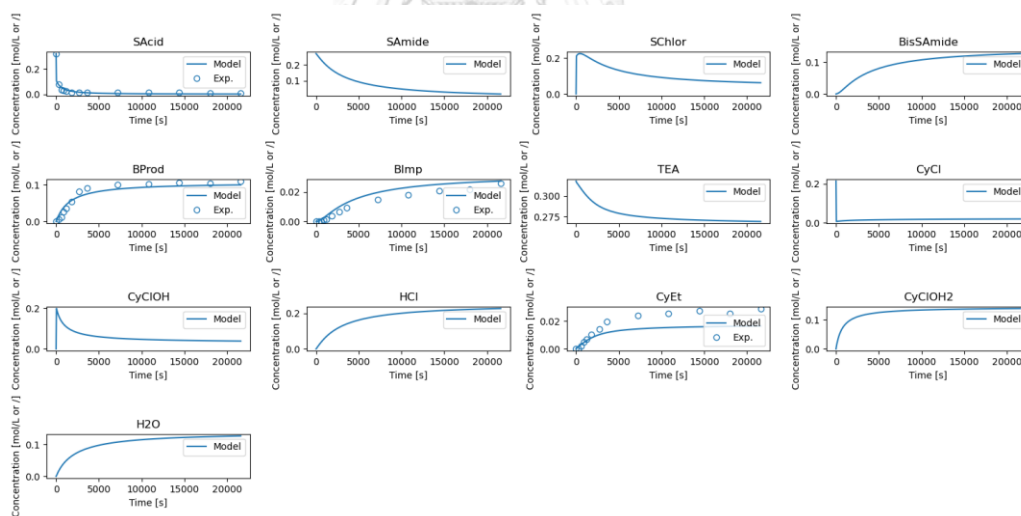


Figure 34 The graphical results from fitting in entry 1

Table 22 Kinetic constant for salicylic acid:salicylamide ratio (1:0.85 equivalent), triethylamine (1 equivalent), and refluxing toluene (entry 2)

Equation no.	k_{for}	k_{back}
1	2.4142E+00	1.5529E+00
2	7.4888E-03	4.2922E-03
3	7.1889E-04	2.1710E-04
4	2.3284E+00	1.1546E+00
5	8.9995E-01	1.9405E+00
6	2.6080E-02	1.8064E+00

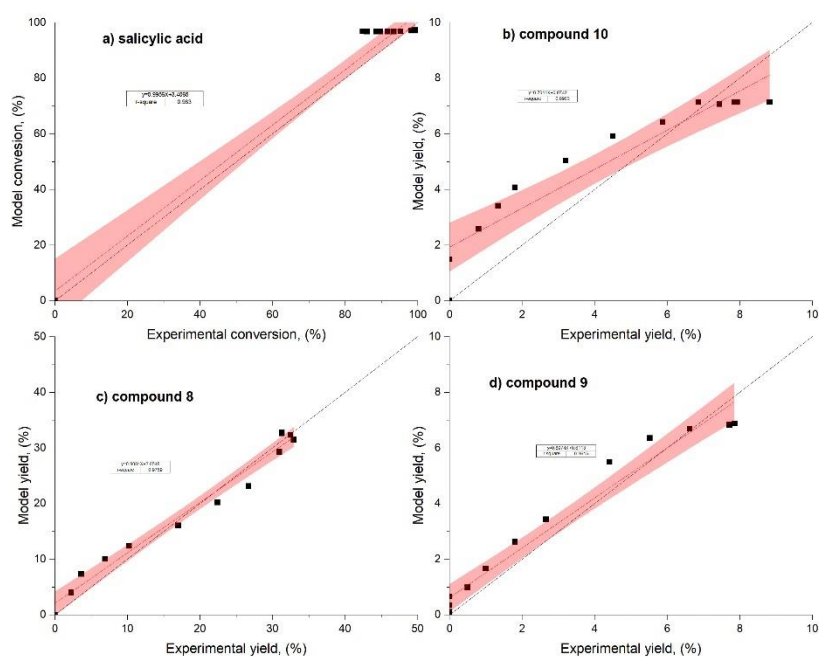


Figure 35 R^2 -value from fitted model conversion and experimental conversion (%) of salicylic acid, model yield experimental yield (%) of compound (8, 9 and 10) with 95% confidential band for salicylic acid:salicylamide ratio (1:0.85 equivalent), triethylamine (1 equivalent), and refluxing toluene.

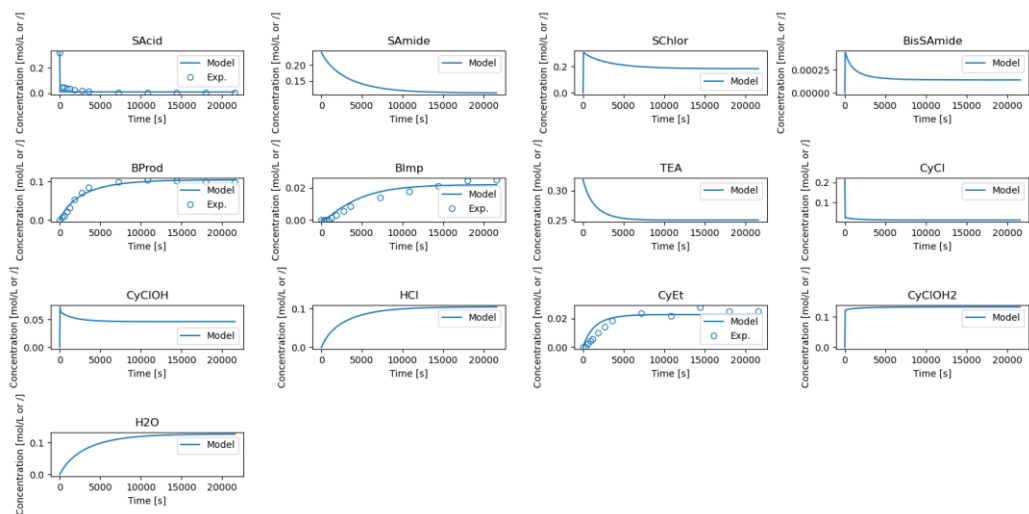


Figure 36 The graphical results from fitting in entry 2



Table 23 Kinetic constant for salicylic acid:salicylamide ratio (1:0.85 equivalent), triethylamine (0.1 equivalent), and refluxing toluene (entry 4)

Equation no.	k_{for}	k_{back}
1	5.6527E-01	1.1541E-01
2	4.1379E-04	1.2461E-08
3	1.6315E-03	5.7429E-01
4	3.5156E+00	1.3094E+00
5	3.4589E+00	4.0649E-01
6	5.4109E-01	8.2534E-01

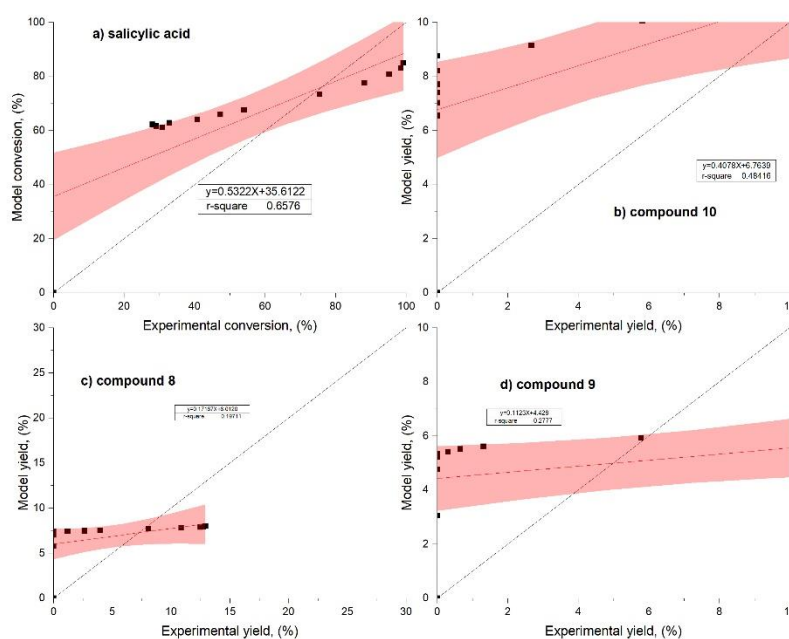


Figure 37 R^2 -value from fitted model conversion and experimental conversion (%) of salicylic acid, model yield experimental yield (%) of compound (8, 9 and 10) with 95% confidential band salicylic acid:salicylamide ratio (1:0.85 equivalent), triethylamine (0.1 equivalent), and refluxing toluene

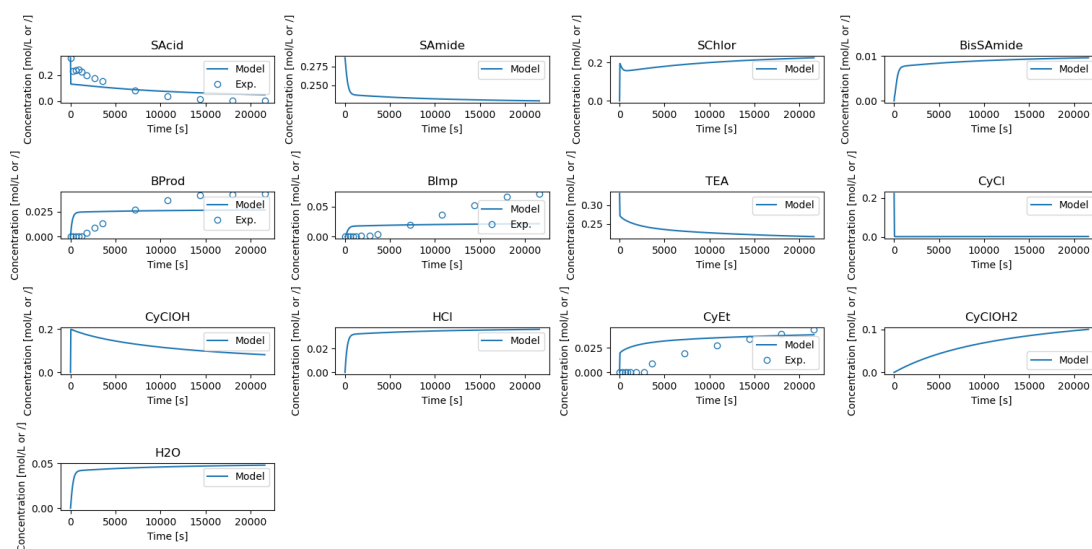


Figure 38 The graphical results from fitting in entry 4



Table 24 Kinetic constant for salicylic acid:salicylamide ratio (1:0.85 equivalent), triethylamine (2 equivalent), and refluxing toluene (entry 5)

Equation no.	k_{for}	k_{back}
1	3.3047E-02	9.9202E-01
2	3.5983E+00	1.2434E-02
3	2.6116E-04	3.0112E-01
4	2.4281E-01	4.4785E-03
5	1.7975E-01	1.4682E+00
6	7.3319E-03	1.7036E+00

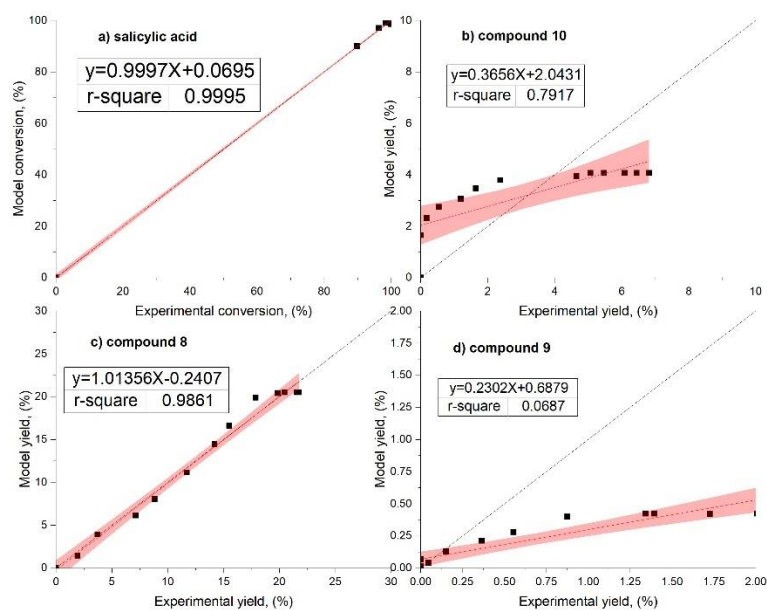


Figure 39 R^2 -value from fitted model conversion and experimental conversion (%) of salicylic acid, model yield experimental yield (%) of compound (**8**, **9** and **10**) with 95% confidential band salicylic acid:salicylamide ratio (1:0.85 equivalent), triethylamine (2 equivalent), and refluxing toluene

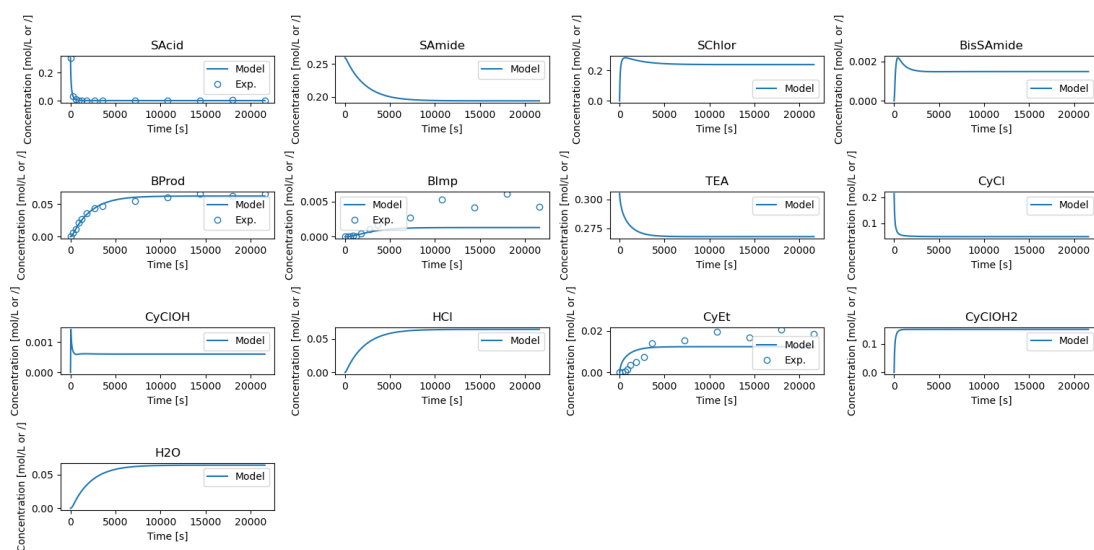


Figure 40 The graphical results from fitting in entry 5



Table 25 Kinetic constant for salicylic acid:salicylamide ratio (1:0.85 equivalent), triethylamine (1 equivalent), and 80 °C reaction temperature (entry 6)

Equation no.	k_{for}	k_{back}
1	2.4957E+00	1.5125E+00
2	2.8603E-02	1.2635E+00
3	1.8296E-04	6.5075E-02
4	4.5143E-02	2.3735E-04
5	2.2774E+00	1.8187E+00
6	2.0519E-02	2.8035E+00

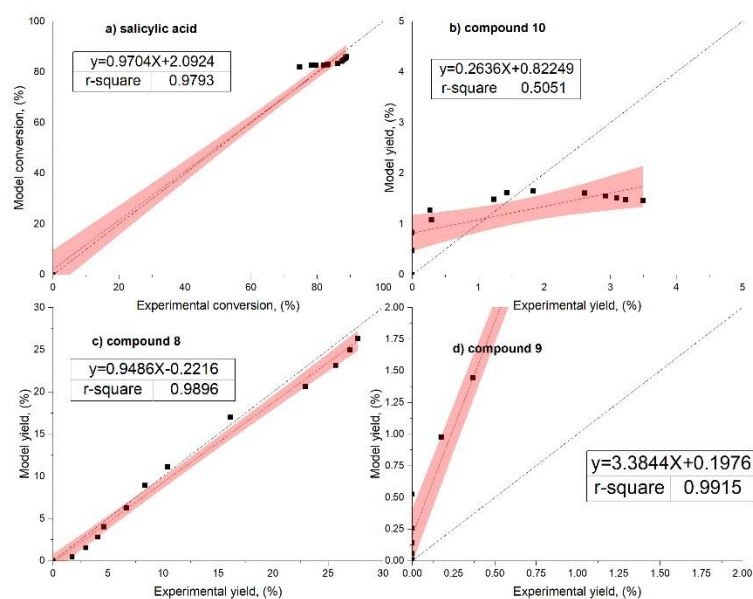


Figure 41 R^2 -value from fitted model conversion and experimental conversion (%) of salicylic acid, model yield experimental yield (%) of compound (8, 9 and 10) with 95% confidential band salicylic acid:salicylamide ratio (1:0.85 equivalent), triethylamine (1 equivalent), and 80 °C reaction temperature.

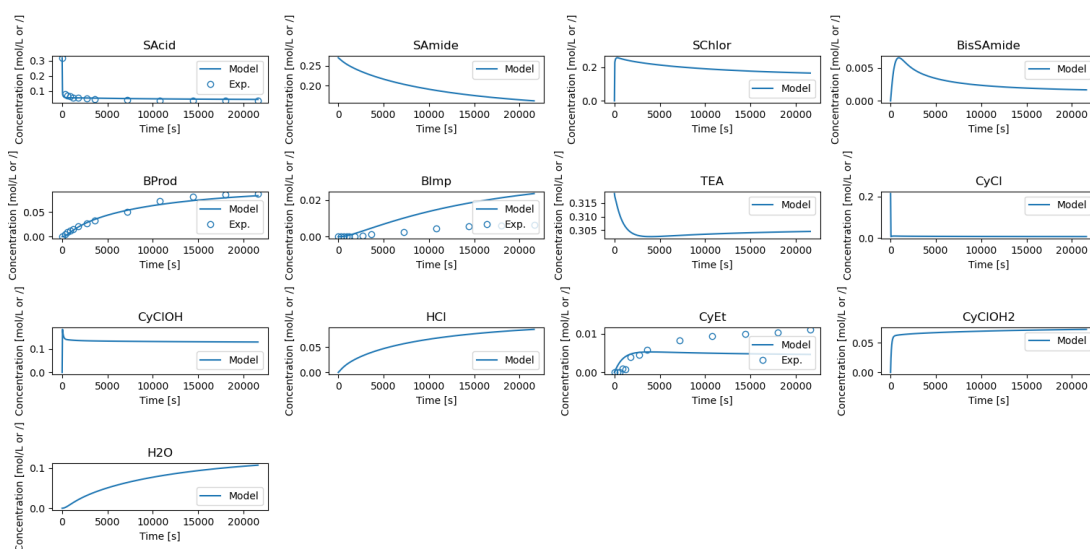


Figure 42 The graphical results from fitting in entry 6



Table 26 Kinetic constant for salicylic acid:salicylamide ratio (1:0.85 equivalent), triethylamine (1 equivalent), and 100 °C reaction temperature (entry 7)

Equation no.	k_{for}	k_{back}
1	1.7792E+00	2.1015E+00
2	1.4531E-02	1.0805E-01
3	4.7168E-01	1.3889E+00
4	5.9764E-03	2.1137E-03
5	2.6656E-01	1.3542E+00
6	1.0463E-01	3.5686E+00

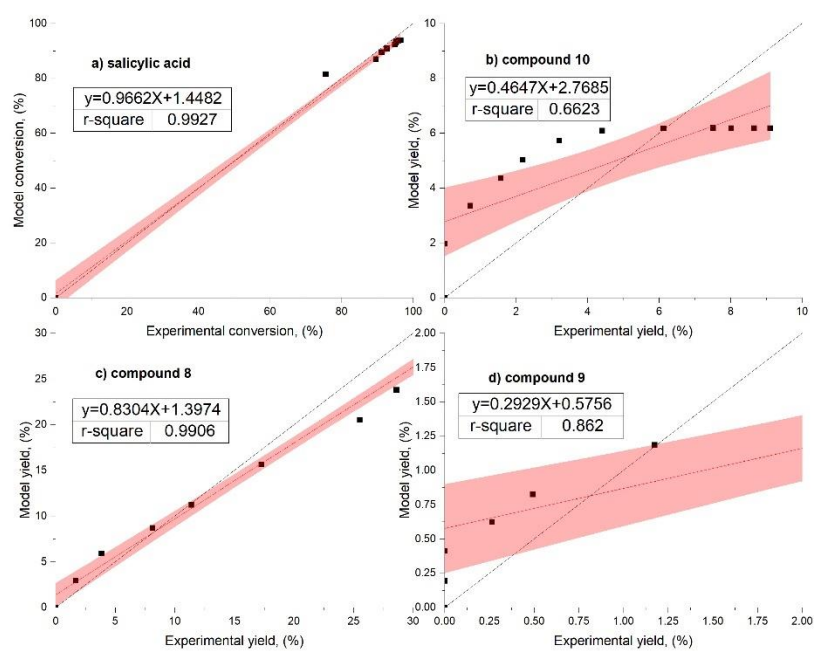


Figure 43 R^2 -value from fitted model conversion and experimental conversion (%) of salicylic acid, model yield experimental yield (%) of compound (8, 9 and 10) with 95% confidential band salicylic acid:salicylamide ratio (1:0.85 equivalent), triethylamine (1 equivalent), and 100 °C reaction temperature.

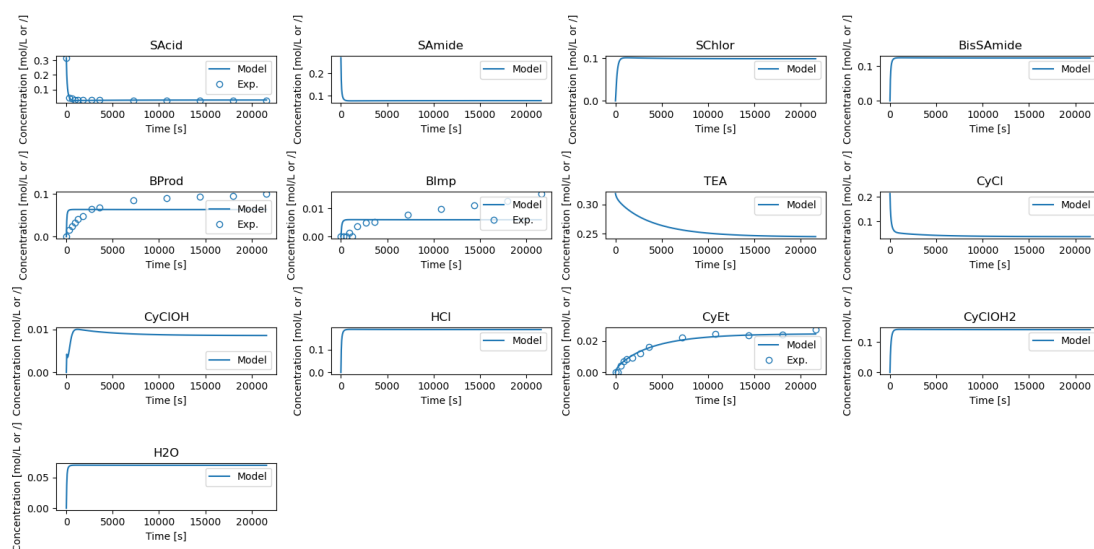


Figure 44 The graphical results from fitting in entry 6



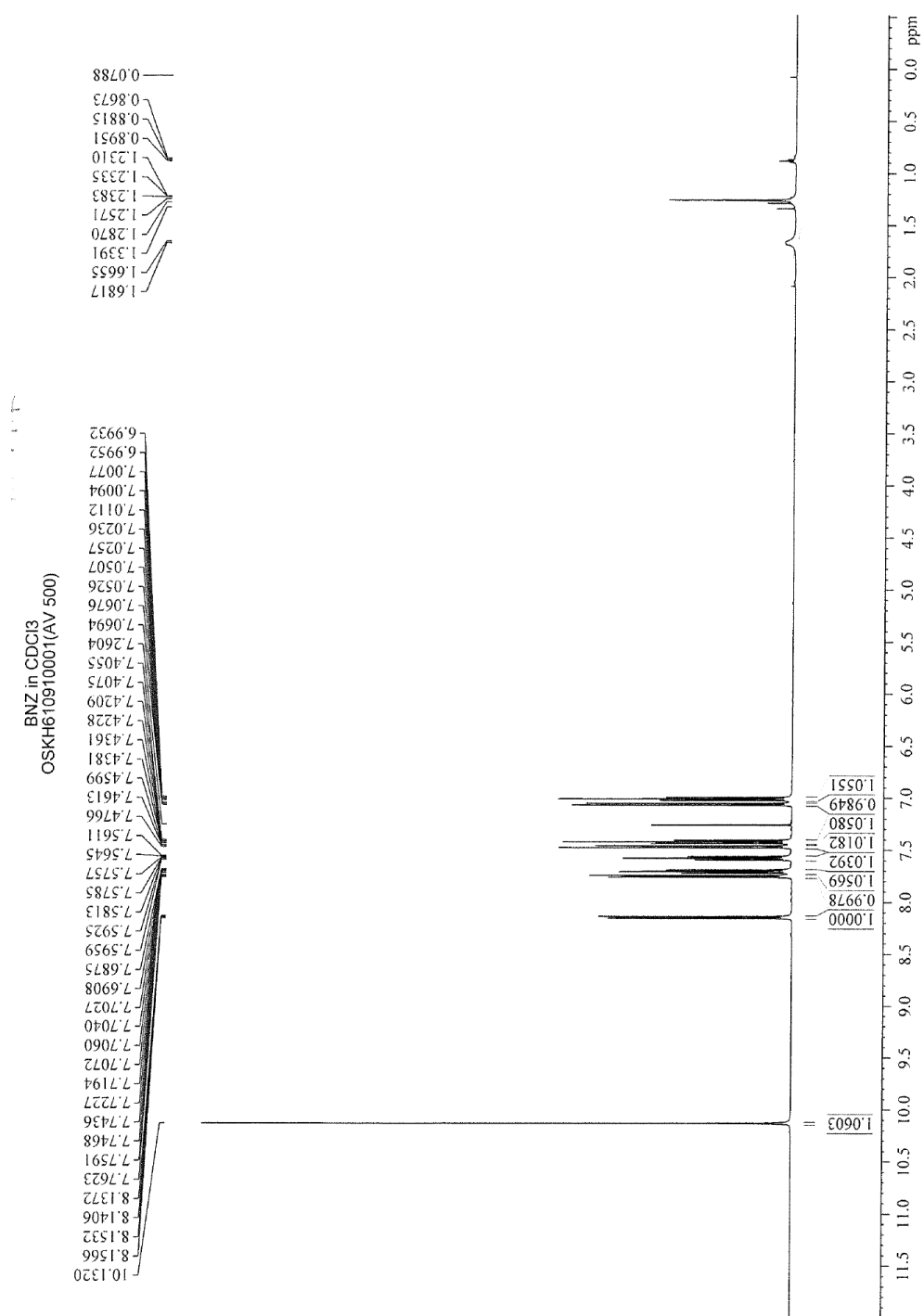


Figure 45 ^1H NMR spectrum of 4-chloro-2-(2-hydroxyphenyl)-4*H*-benzo[e][1,3]oxazine-4-ol, compound (**9**) in CDCl_3

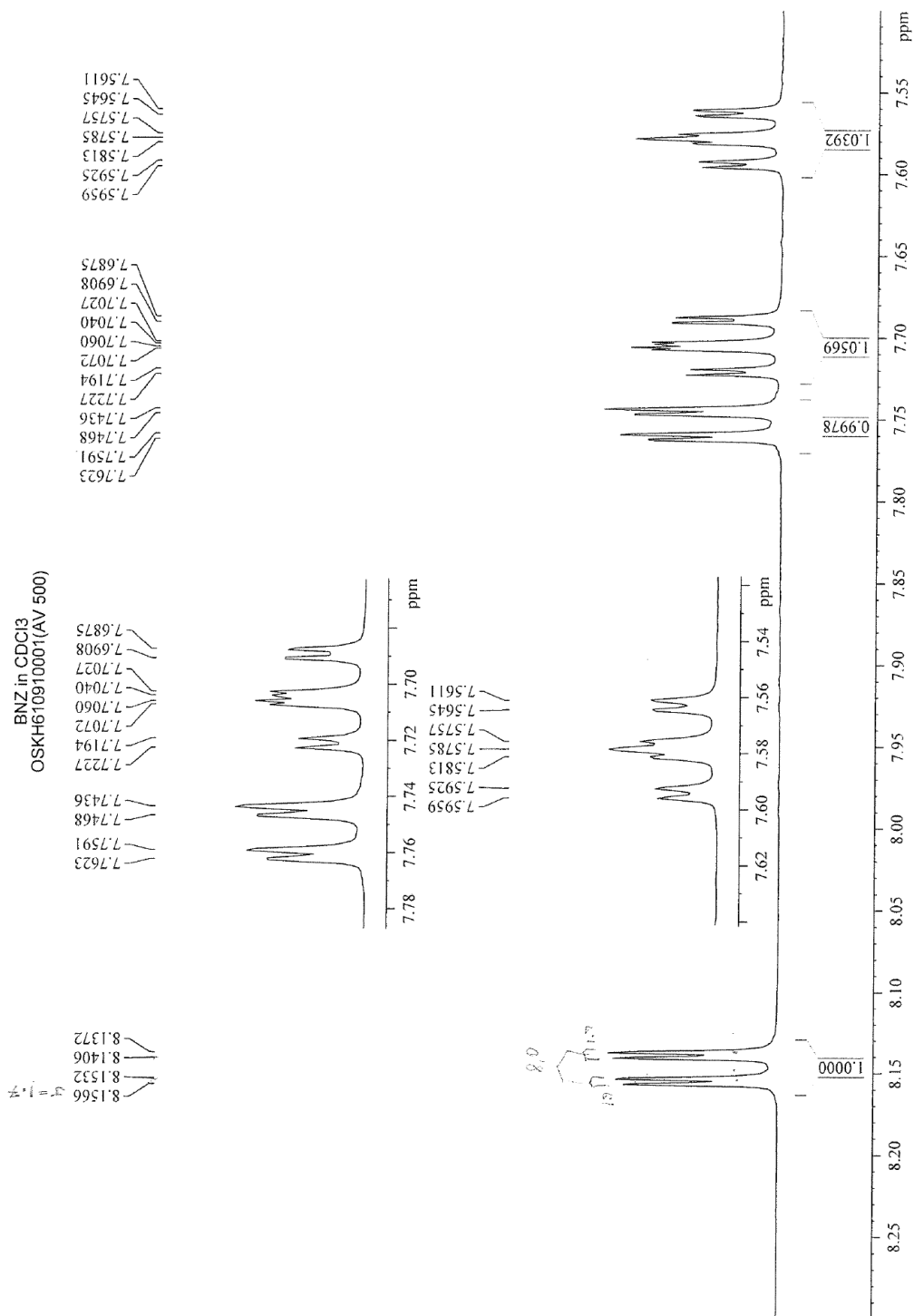


Figure 46 ^1H NMR spectrum of 4-chloro-2-(2-hydroxyphenyl)-4*H*-benzo[e][1,3]oxazine-4-ol, compound (**9**) in CDCl_3

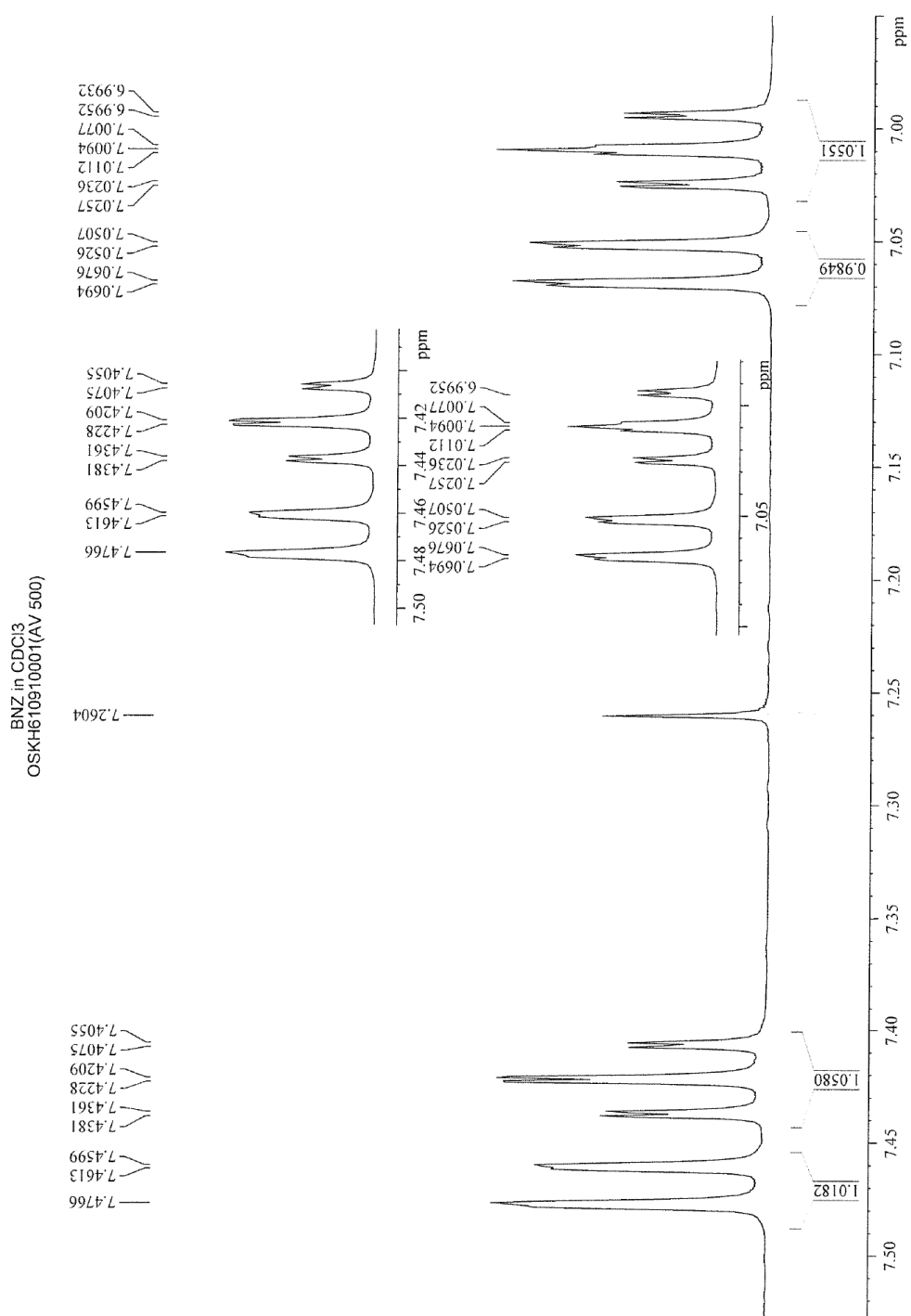


Figure 47 ¹H NMR spectrum of 4-chloro-2-(2-hydroxyphenyl)-4H-benzo[e][1,3]oxazine-4-ol, compound (**9**) in CDCl₃

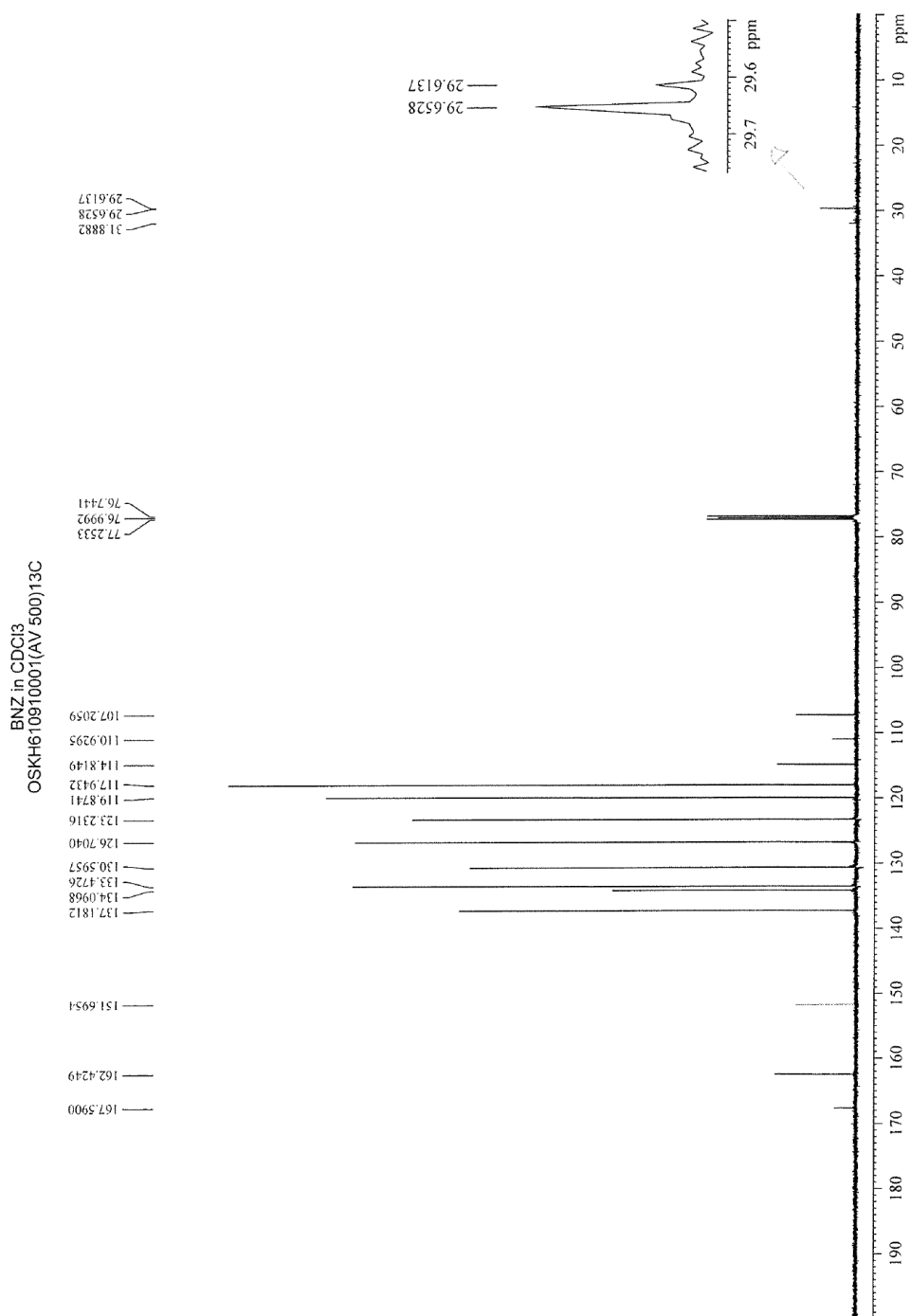


Figure 48 ^{13}C NMR spectrum of 4-chloro-2-(2-hydroxyphenyl)-4H-benzo[e][1,3]oxazine-4-ol, compound (**9**) in CDCl_3

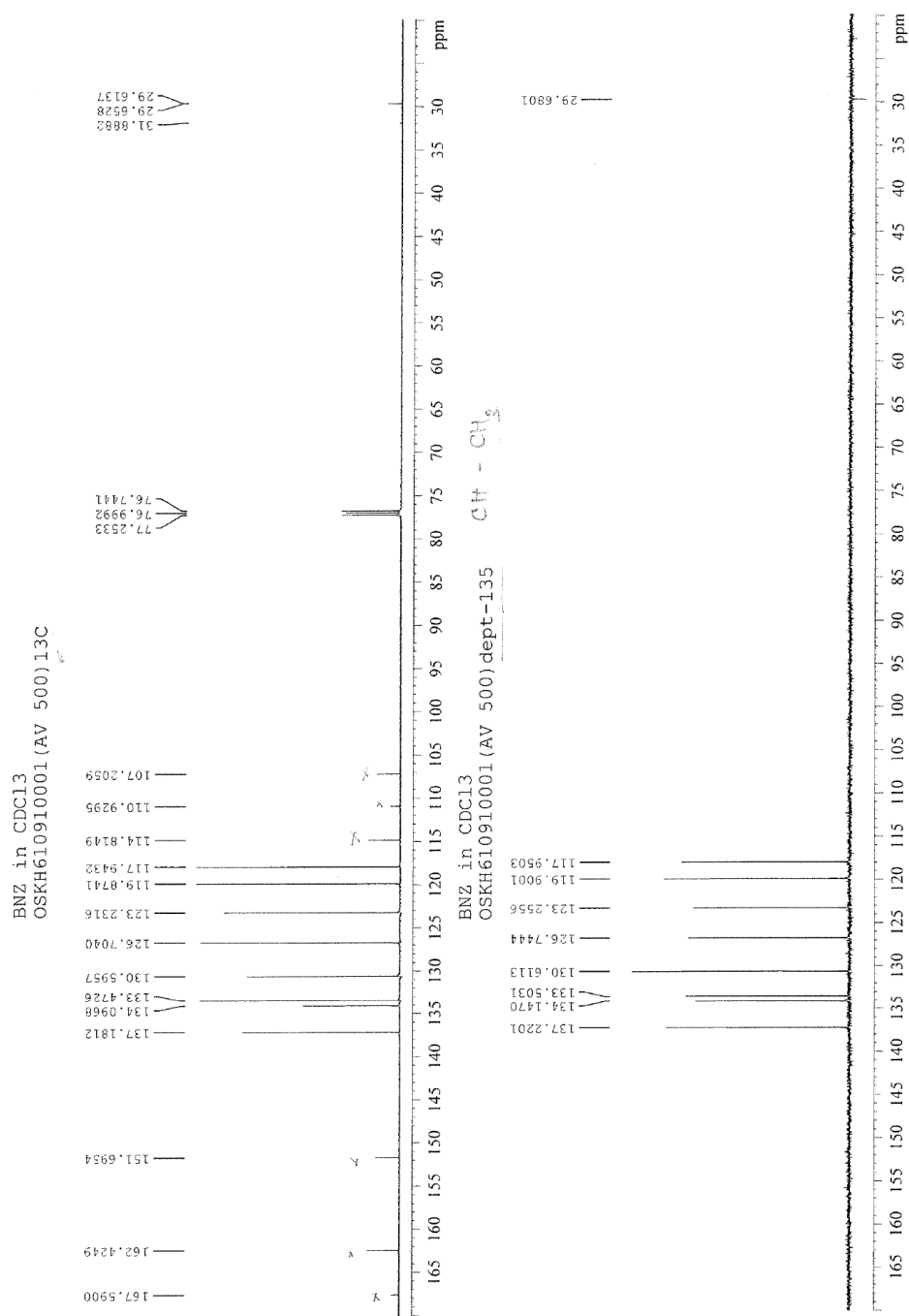


Figure 49 ^{13}C NMR (Dept-135) spectrum of 4-chloro-2-(2-hydroxyphenyl)-4H-benzo[e][1,3]oxazine-4-ol, compound (9) in CDCl_3

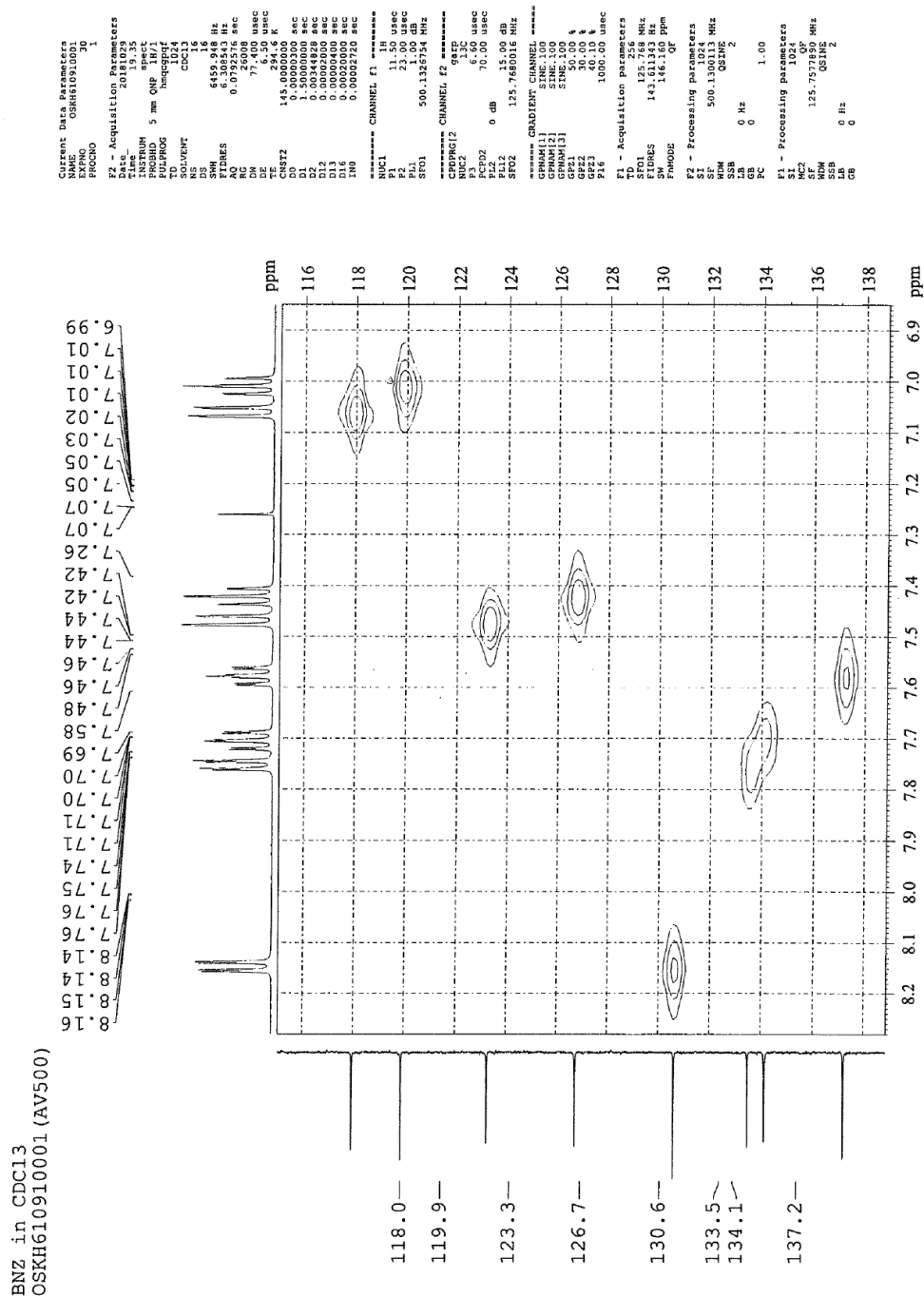


Figure 51 ¹³C NMR HMQC spectrum of 4-chloro-2-(2-hydroxyphenyl)-4H-benzo[e][1,3]oxazine-4-ol, compound (9) in CDCl₃

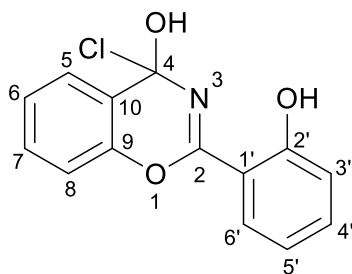


Figure 52 The position in structure of 4-chloro-2-(2-hydroxyphenyl)-4H-benzo[e] [1,3] oxazine-4-ol

Table 27 $^1\text{H-NMR}$ and $^{13}\text{C-NMR}$ spectroscopic data of 4-chloro-2-(2-hydroxyphenyl)-4H-benzo[e] [1,3] oxazine-4-ol, compound (**9**) in CDCl_3

position	δ_c (ppm)	δ_H (ppm)
1	162.4	
2		
3		
4	107.2	
5	123.2	7.47
6	134.1	7.71
7	126.7	7.42
8	133.5	7.75
9	151.7	
10	114.8	
1'	110.9	
2'	167.6	10.13
3'	117.9	7.06
4'	130.6	8.15
5'	119.9	7.01
6'	137.2	7.58

Table 28 ^{13}C -NMR and DEPT spectroscopic data of 4-chloro-2-(2-hydroxyphenyl)-4H-benzo[e] [1,3] oxazine-4-ol, compound (**9**) in CDCl_3

δ (ppm)	DEPT-135
169.59	
162.42	
151.69	
137.18	137.22
134.09	134.14
133.47	133.50
130.59	130.61
126.70	126.74
123.23	123.25
119.87	119.90
117.94	117.95
114.81	
110.92	
107.20	

Table 29 ^1H -detected heteronuclear multiple quantum correlations (HMQC) spectroscopic data of 4-chloro-2-(2-hydroxyphenyl)-4H-benzo[e] [1,3] oxazine-4-ol, compound (**9**) in CDCl_3

δ_{H} (ppm)	δ_{C} (ppm)	assignment
10.13		C-2'
8.15	130.6	C-4'
7.75	133.5	C-8
7.68 – 7.73	134.1	C-6
7.56 – 7.60	137.2	C-6'
7.47	130.6	C-5
7.40 – 7.44	126.7	C-7
7.06	117.9	C-3'
6.95 – 7.03	119.9	CH-5'

Table 30 ^1H -detected heteronuclear multiple bond correlations (HMBC) spectroscopic data of 4-chloro-2-(2-hydroxyphenyl)-4H-benzo[e] [1,3] oxazine-4-ol, compound (**9**) in CDCl_3

δ_{H} (ppm)	Carbon correlated with δ_{H}
10.13	110.9 (C-1'), 117.9 (C-3'), 137.2 (C-6'), 162.4 (C-2)
8.15	117.9 (C-3'), 137.2 (C-6'), 162.4 (C-2), 167.6 (C-2')
7.75	114.8 (C-10), 123.2 (C-2), 134.1 (C-2), 151.7 (C-9)
7.68 – 7.73	107.2 (C-4), 123.2 (C-2), 133.5 (C-8), 151.7 (C-9)
7.56 – 7.60	126.7 (C-7), 130.6 (C-4'), 133.5 (C-8), 162.4 (C-2)
7.47	107.2 (C-4), 114.2 (C-10), 126.7 (C-7), 133.5 (C-8), 151.7 (C-9)
7.40 – 7.44	107.2 (C-4), 114.8 (C-10), 123.2 (C-2), 133.5 (C-8), 137.2 (C-6), 151.7 (C-9)
7.06	110.9 (C-1'), 119.9 (C-5'), 130.6 (C-5), 162.4 (C-2), 167.6 (C-2')
6.95 – 7.03	110.9 (C-1'), 117.4 (C-3'), 130.6 (C-5), 137.2 (C-6'), 162.4 (C-2)

Mass Spectrum List Report

Analysis Info

Analysis Name	OSGPO20180614001.d	Acquisition Date	6/14/2018 9:39:52 AM
Method	Tune_low_90_04092017.m	Operator	Administrator
Sample Name	SOLID	Instrument	micrOTOF 72

Acquisition Parameter

Source Type	ESI	Ion Polarity	Positive	Set Corrector Fill	50 V
Scan Range	n/a	Capillary Exit	60.0 V	Set Pulsar Pull	337 V
Scan Begin	50 m/z	Hexapole RF	90.0 V	Set Pulsar Push	337 V
Scan End	3000 m/z	Skimmer 1	70.0 V	Set Reflector	1300 V
		Hexapole 1	25.0 V	Set Flight Tube	9000 V
				Set Detector TOF	2295 V

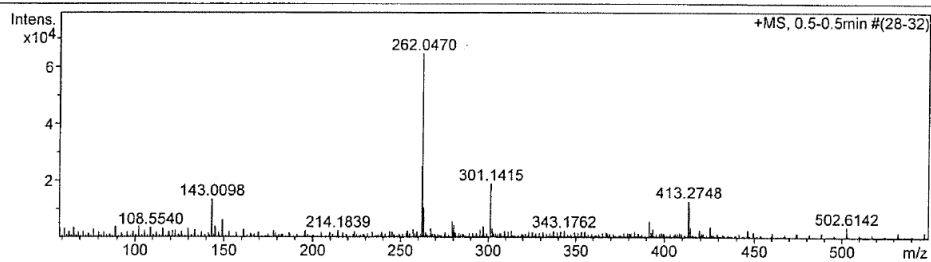
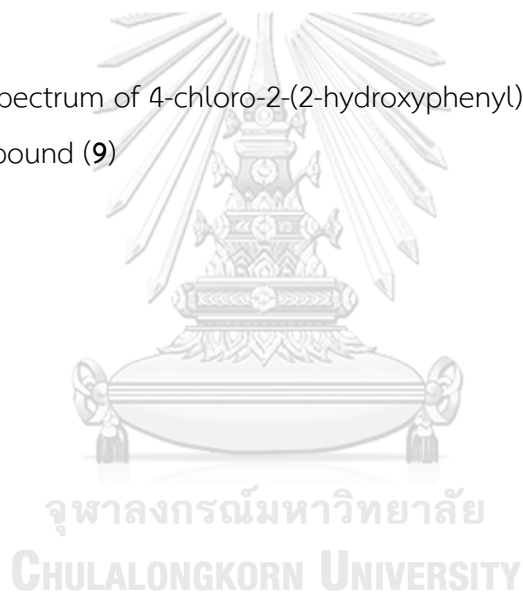


Figure 53 HSMS spectrum of 4-chloro-2-(2-hydroxyphenyl)-4*H*-benzo[e][1,3]oxazine-4-ol, compound (9)



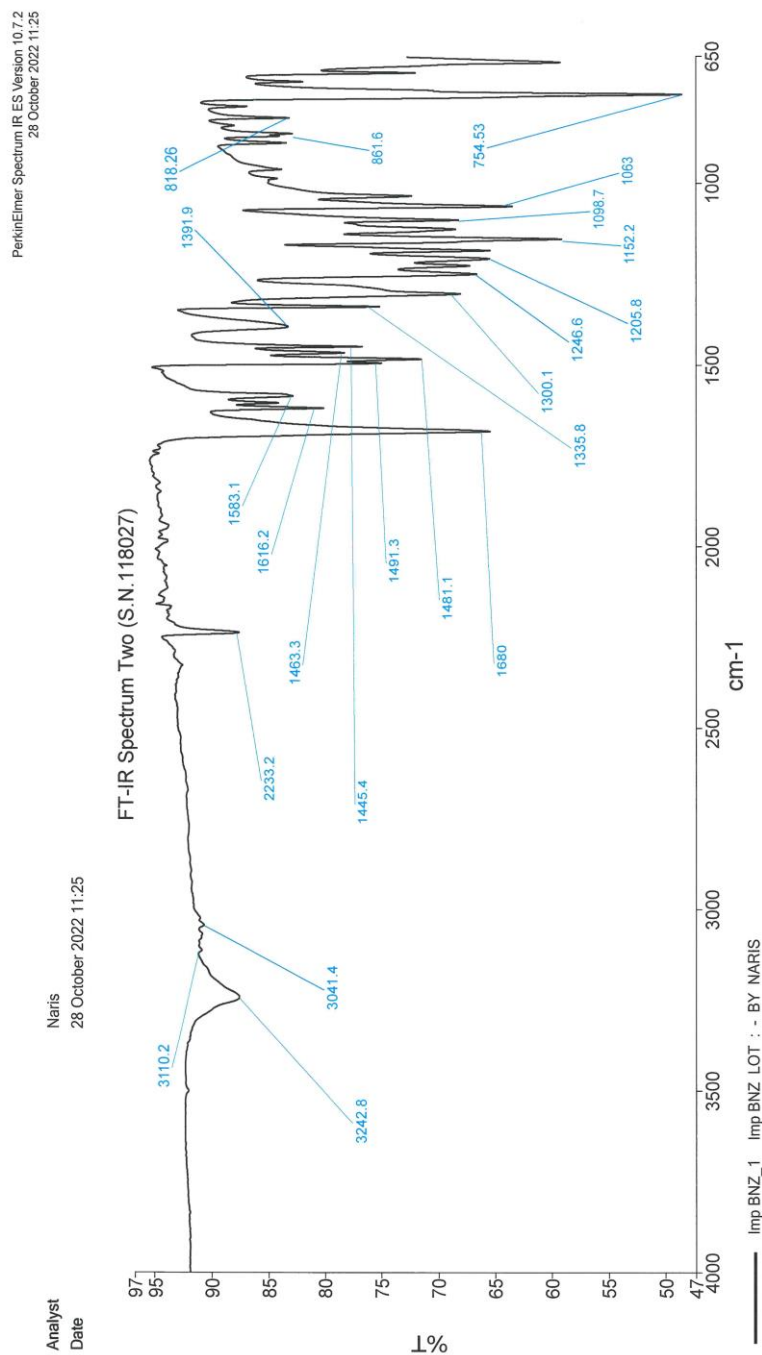
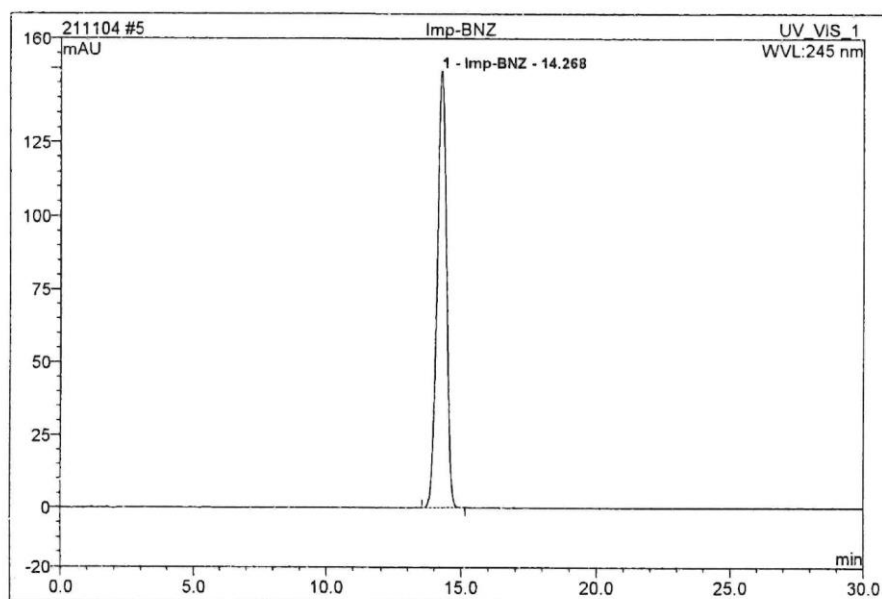


Figure 54 FT-IR spectrum of 4-chloro-2-(2-hydroxyphenyl)-4H-benzo[e][1,3]oxazine-4-ol, compound (9)

5 Imp-BNZ			
12.5mg/vol.25			
Sample Name:	Imp-BNZ	Injection Volume:	20.0
Vial Number:	RA5	Channel:	UV_VIS_1
Sample Type:	unknown	Wavelength:	245
Control Program:	Assay	Bandwidth:	2
Quantif. Method:	Benzoxazinone	Dilution Factor:	1.0000
Recording Time:	11/5/2021 12:25	Sample Weight:	1.0000
Run Time (min):	30.00	Sample Amount:	1.0000



No.	Ret.Time min	Peak Name	Height mAU	Area mAU*min	Rel.Area %	Amount	Type
1	14.27	Imp-BNZ	149.072	60.829	100.00	4.884	BMB
Total:			149.072	60.829	100.00	4.884	

Figure 55 HPLC chromatogram of 4-chloro-2-(2-hydroxyphenyl)-4H-benzo[e] [1,3] oxazine-4-ol, compound (9)

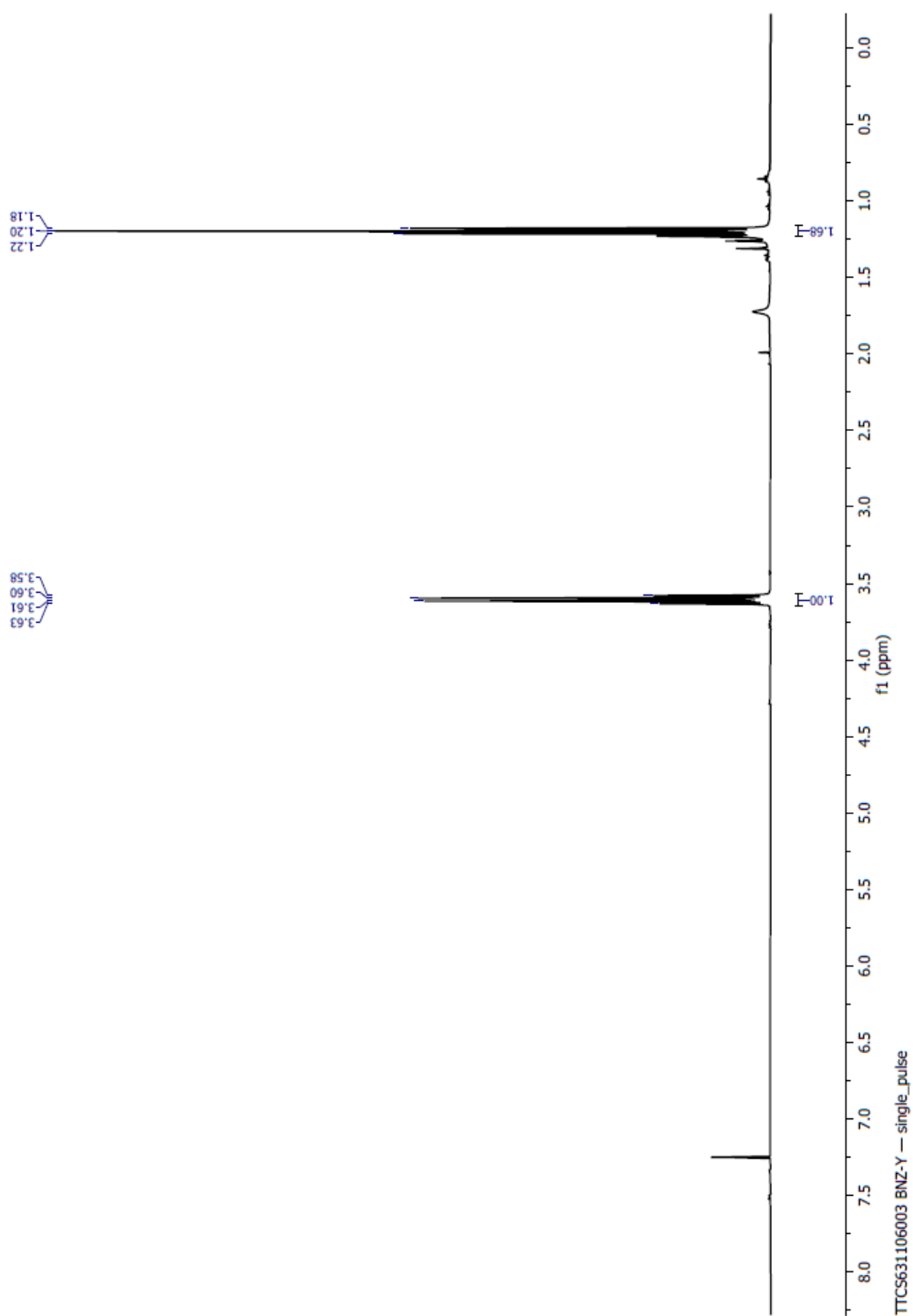
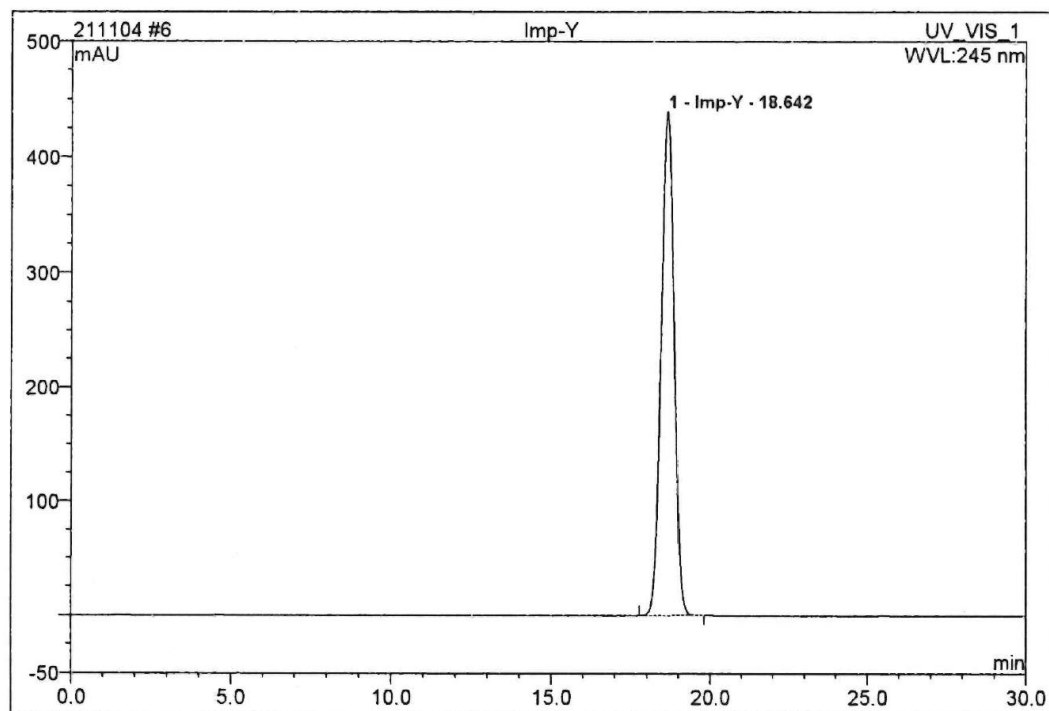


Figure 56 ^1H NMR spectrum of Tri-quaternary salt (compound **10**) in DMSO- d_6

6 Imp-Y			
5mg/vol.5			
Sample Name:	Imp-Y	Injection Volume:	20.0
Vial Number:	RA6	Channel:	UV_VIS_1
Sample Type:	unknown	Wavelength:	245
Control Program:	Assay	Bandwidth:	2
Quantif. Method:	Benzoxazinone	Dilution Factor:	1.0000
Recording Time:	11/5/2021 12:55	Sample Weight:	1.0000
Run Time (min):	30.00	Sample Amount:	1.0000



No.	Ret.Time min	Peak Name	Height mAU	Area mAU*min	Rel.Area %	Amount	Type
1	18.64	Imp-Y	439.289	210.426	100.00	5.150	BMB
Total:			439.289	210.426	100.00	5.150	

Figure 57 HPLC chromatogram of Tri-quaternary salt compound 10.

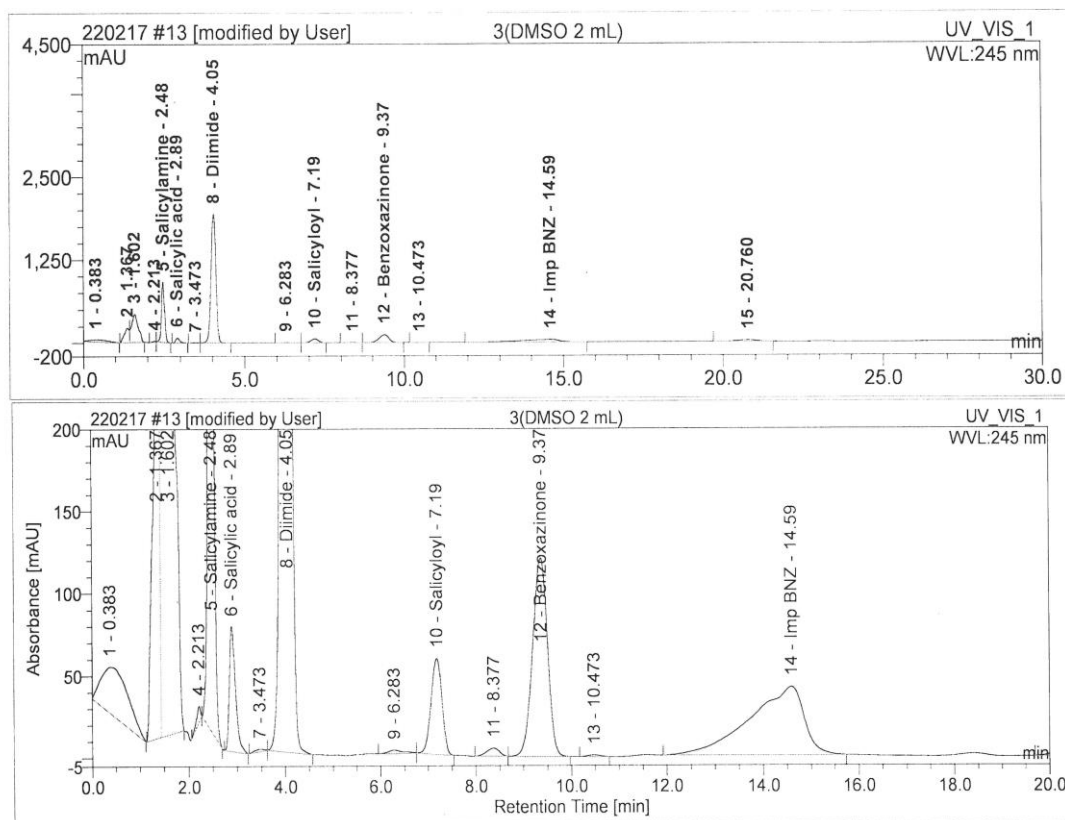


Figure 58 HPLC chromatogram of solid compositions after 6 hours of Benzoxazinone synthesis using 20%DMSO/Acetonitrile as dilution medium.

VITA

NAME Sumate Boonkird

DATE OF BIRTH 25 August 1977

PLACE OF BIRTH Bangkok

INSTITUTIONS ATTENDED Chulalongkorn University,
Suranaree University of Technology

HOME ADDRESS 33 soi 22 Sukhapiban 5 Rd. Taraeng, Bangkhen, Bangkok,
Thailand, 10220

PUBLICATION Ultrasound-assisted extraction of capsaicinoids from
Capsicum frutescens on a lab- and pilot-plant scale,
Ultrasonics Sonochemistry, Volume 15, Issue 6, September
2008, Pages 1075-1079.